Ph.D. Thesis

Seismic and energy renovation of RC framed buildings with cross-laminated timber panels equipped with innovative friction dampers

Carola Tardo

Supervisors:

Prof. Eng. Giuseppe Margani
Prof. Eng. Edoardo Michele Marino

Co-supervisors:

Prof. Eng. Gianpiero Evola
Dr. Alberto Moretti (Adveco srl - industrial partner)
Prof. Eng. Roberto Tomasi (NMBU - academic partner)

University of Catania
Department of Civil Engineering and Architecture
Ph.D. Course in Evaluation and Mitigation of Urban and Land Risks - XXXIV cycle
A.Y. 2018/2021

Ph.D. Thesis

SEISMIC AND ENERGY RENOVATION OF RC FRAMED BUILDINGS WITH CROSS-LAMINATED TIMBER PANELS EQUIPPED WITH INNOVATIVE FRICTION DAMPERS

Carola Tardo

UNIVERSITÀ degli STUDI di CATANIA

DIPARTIMENTO **I**NGEGNERIA **C**IVILE E **AR**CHITETTURA

Norwegian University of Life Sciences

La borsa di dottorato è stata cofinanziata con risorse del
Programma Operativo Nazionale Ricerca e Innovazione 2014-2020 (CCI 2014IT16M2OP005),
Fondo Sociale Europeo, Azione I.1 "Dottorati Innovativi con caratterizzazione Industriale"

UNIONE EUROPEA
Fondo Sociale Europeo

Ministero dell'Università e della Ricerca

PON RICERCA E INNOVAZIONE 2014 - 2020

ABSTRACT

In the European seismic countries, most of the building stock is highly energy-intensive and earthquake-prone since it was built before the enforcement of effective energy and seismic codes. In these countries, renovation actions that synergically integrate both energy-efficient and anti-seismic interventions are strongly needed, looking at the resilience of buildings against earthquakes as one of the main values of a sustainable city. However, the implementation of such interventions is currently limited by barriers that are mostly related to the excessive costs and the high invasiveness of traditional seismic retrofit actions.

To overcome these barriers, a new holistic design approach to the building renovation is required, which should result in innovative and integrated retrofit interventions able to specifically meet the needs of cost-effectiveness, quick installation, reduced users' disturbance, and low environmental impact.

In this framework, this Ph.D. thesis aims at analysing the potential of a novel integrated retrofit technology for RC framed buildings. The proposed retrofit system consists in cladding the existing building envelope with a new prefabricated timber-based external shell that acts as seismic-resistant and energy-efficient skin, contributing also to renovate the architectural image of the building. The new skin combines structural Cross-Laminated Timber (CLT) panels – connected to the existing RC frame through innovative friction dampers – with non-structural panels that integrate high-performing windows.

The potential of the proposed technology is analysed in terms of seismic and energy performance, and technical feasibility.

Pushover analyses on a case study RC frame preliminarily demonstrate the high potential impact of the proposed seismic retrofit system (CLT panels equipped with novel friction dampers) on the response of existing buildings to be upgraded. Hence, different prototypes of the friction damper are tested under cyclic loading, identifying the most promising in terms of structural efficiency. Dynamic thermal simulations on multi-story buildings, at pre- and post-intervention state, show the relevant energy efficiency of the system, especially in the winter. Moreover, proper technical solutions are investigated to ensure the technical feasibility and versatility of the proposed retrofit technology.

Keywords: seismic and energy renovation; RC framed buildings; Cross Laminated Timber; friction damper; prefabricated panels.

Table of contents

1

Introduction

The *environmental issue* is still a main point of the worldwide community and needs to play a key role in the governments' agenda as well as in public opinion.
Referring to the building sector, the high environmental impact of the existing building stock is now widely recognized. In Europe, residential and non-residential buildings are currently responsible for 40% of the final energy demand and for approximately 36% of greenhouse gas (GHG) emissions [1], thus contributing to climate changes and related natural hazards (e.g. floods, hurricanes, torrential rainfalls, windstorms, landslides). In 2017, just the residential sector accounted for 27.2% of the final energy consumption [2]. The highly building energy demand is mostly related to the poor thermal performance of the building envelopes, as well as the low efficiency of cooling and heating systems. This is mainly due to the fact that 75% of the EU buildings and more than 80% of the residential ones were built before 1990, i.e. before the enforcement of most EU energy regulations for buildings [3-4].
In this context, in 2018 the Energy Performance of Buildings Directive (EPBD) stated that each Member State shall establish a long-term strategy for the renovation of the national building stock, in order to facilitate the cost-effective transformation of existing buildings into nearly zero-energy buildings. In particular, the States are committed to define a roadmap leading to the goal of reducing, by 2050, the GHG emissions in the EU by 80-95% compared to 1990 [5]. Other medium-term commitments, set by the Energy Union and the Energy and Climate Policy Framework for 2030, aspire to reducing GHG emissions by at least 40% by 2030 (from 1990 levels) [6], and to reaching the energy savings target of at least 32.5% by 2030 [7].
In recent years, the sustainability in the building sector, commonly related to the environmental and energy issue, has been extended to the issue of structural safety, incorporating the concept of resilient cities into that of sustainable cities [8]. In particular, the resilience of buildings against earthquakes, which affects a relevant part of the European territory, has been recognized as the main value of a sustainable city.
However, in most European earthquake-prone countries – such as Italy, Turkey, Romania and the whole Balkan peninsula [9] – the building stock designed without anti-seismic criteria or according to old seismic standards is extremely wide, including mainly Unreinforced Masonry (URM) or Reinforced Concrete (RC) framed buildings [10] .

For instance, in Italy, around 66% of the existing residential buildings was built before 1974 [11], when the first code for earthquake-resistant buildings (Law 64/1974 [12]) was not in force and only gravity loads were considered at the design stage. These buildings are over 50 years old, which means that they have also reached their nominal service life, exhibiting structural deficiencies mainly due to the naturally decay of the materials originally used. Moreover, the seismic classification map of the Italian national territory has been gradually updated and enlarged based on both the intensity and frequency of past earthquakes. Consequently, many buildings erected after the 1974 according to the seismic laws of the construction time do not comply with the current seismic regulations.

The strong earthquakes occurred in Europe in the last decades demonstrated the high level of seismic vulnerability of mostly existing buildings and the catastrophic consequences that the buildings damage or collapse can entail in terms of human losses, economic harm, and environmental impact. Only in the last 50 years, in Europe earthquakes have caused more of 35000 deaths and over €300 billion monetary losses [13]. In the same period, in Italy earthquakes caused around 5000 death and over €180 billion monetary losses, destroyed a considerable part of the Italian building stock, whose value is hardly quantifiable [14]. As a result of the recent devastating earthquakes in Italy (i.e. L'Aquila 2009, Emilia 2012, Amatrice-Norcia-Visso 2016), several buildings previously subjected to energy efficiency interventions have been seriously damaged (Figure 1.1), frustrating these interventions and the related economic investment.

The environmental issue related to buildings' seismic vulnerability has been also highlighted, in consideration of the environmental impact in terms of carbon footprint associated to buildings repair or reconstruction after a seismic event [16]. Specifically, the expected annual embodied equivalent CO_2 associated to seismic risk has been estimated equal to 87% of the annual operational CO_2 after only energy retrofitting interventions.

(a)

(b)

Figure 1.1. Collapse of buildings retrofitted only in terms of energy efficiency after recent earthquakes in Italy: (a) Emilia Romagna 2012; (b) Marche 2016 [15].

The framework depicted above evidences that in earthquake-prone countries energy-efficient and anti-seismic renovation interventions must be synergically combined in order to: (i) prevent human and economic losses caused by seismic events; (ii) prevent buildings damage in the event of seismic events, avoiding the environmental impact associated to their potential repair or reconstruction; (iii) prevent earthquake damages that may frustrate any energy-efficient intervention alone; (iv) avoid the doubling of several costs in case of implementation of the two retrofit intervention in distinct periods (e.g. for building-site setup, demolition works, scaffolding, renders and finishings, etc.)[17-19]; (v) increase the users' living comfort and safety, as well as the building value. Retrofit interventions should also be preferred to demolition-and-reconstruction practice, if the latter is not necessary, since entail lower embodied energy, global warming potential, economic impact, and waste production [20-22].

Local governments are moving in the direction of buildings renovation, by introducing policies to promote it on large-scale.

In Italy, in recent years significant tax incentives have been issued to promote the seismic upgrading and the energy efficiency of the building stock. Tax deductions from 50% to 85% (namely SISMA-BONUS) of the renovation cost have been provided for interventions aimed at improving the seismic risk class of existing buildings, while deductions from 50% to 75% (namely ECO-BONUS) have been provided for interventions aimed at improving the buildings energy efficiency. In May 2020, the Italian Government also issued an urgent legislation [23] to promote the recovery of the Italian economy, following the crisis caused by the COVID-19 pandemic, by introducing a new financial incentive (namely SUPER-BONUS) for energy and structural renovation of the building stock. This incentive increased the tax deduction rate up to 110%, also introducing other relevant financial methods, like the tax credit transfer that has reduced or even avoided the economic burden for the building owners.

Despite the regulations and financial incentives promoted in the last years by both EU and local governments, many barriers currently hinder the seismic and energy retrofit of existing buildings. Most of these barriers are related to the seismic retrofit actions.

On one hand, there is a lack of attractive, cost-effective, and low-disruptive technical solutions. For instance, in Italy anti-seismic interventions on apartment blocks built between the 1950s and 1980s provide the major contribution to the total renovation

costs, ranging from 200 to 500 €/m^2, compared to the contribution of the energy-efficiency interventions that range from 100 to 250 €/m^2 [24]. The current tax incentives in Italy ensure the economic return on the initial investment, but at present they have a limited duration since are valid until 2022. Furthermore, most of the current seismic retrofit interventions are highly invasive, requiring long time for implementation and the occupants' relocation during the works - often for several months -, resulting in the building operativity interruption.

On the other hand, the buildings renovation is hindered by social and cultural barriers, mainly due to the insufficient spread of a culture of both seismic risk and environmental protection. In particular, the lack or partial knowledge of seismic risk on a given territory often determines its low perception by the building owners, who not consider as priority the adoption of anti-seismic interventions. The low public perception of the seismic risk is also due to its being an "invisible risk", which tends to be removed from the individual memory if not occurred repeatedly [25].

In order to overcome the main technical and economic barriers, new holistic approaches to the building renovation have been recently investigated.

Different studies have been examined evaluation methodologies to combine structural and energy retrofit techniques [26-28] or define incremental retrofit strategies by considering benefits such as cost-effectiveness, resource optimization, timesaving and disruption reduction, in order to select the most-effective and compatible solution for a given set of performance targets [29].

Other studies have been focused on the development of potential novel seismic and energy retrofit solutions which can be able to meet the current needs of cost-effectiveness, quick installation, and reduced users' disturbance. In this framework, wood has shown great potential as sustainable and renewable retrofitting material to upgrade the seismic and thermal performance of existing buildings, thanks to the recent advancement of engineered timber products, such as cross laminated timber (CLT), as well as wood-based insulating materials.

This doctoral/PhD thesis places in this latter research line, by focusing on existing RC framed buildings, which represents a large portion of the EU building stock that is highly energy-intensive and extremely vulnerable to earthquakes. Typically, these buildings are multi-storey and have infill walls made of brittle hollow clay bricks. RC frames are often oriented along one-direction and poor structural details usually characterize members and joints, resulting in low strength, stiffness, and deformation capacity of the structure in relation to lateral actions. Furthermore, the

thermal resistance of the buildings envelope is generally very low due to the high thermal transmittance (U) of the envelope components. Specifically, the U-value of the opaque envelope components (i.e. external walls, roof and flooring) usually range between 1.0 W/m^2 K and 2.0 W/m^2 K, while the U-value of transparent envelope components (i.e. windows) usually range between 2.5 W/m^2 K and 5.7 W/m^2 K [29].

In this framework, the present PhD thesis aims at analysing the potential of a novel seismic and energy retrofit technology, which is based on the use of prefabricated CLT-based panels placed over the exterior walls and connected to the RC structure by means of innovative devices for seismic energy dissipation (dampers). Specifically, this solution is here analysed in terms of seismic performance, energy efficiency, and technical feasibility.

The work is organized in 8 chapters (Figure 1.2) as follow: Chapter 2 reviews the state-of-the-art on traditional and innovative seismic ad energy retrofitting technologies for RC framed buildings, focusing on recent research on the topic of timber-based renovation interventions; Chapter 3 highlights the main goals and methodology of this work; Chapters 4-7, the core of the research, illustrate and analyse the proposed retrofit technology in terms of impact on the seismic response of RC structures (Chapter 4), structural efficiency of the damper (Chapter 5), energy efficiency (Chapter 6) and technical feasibility (Chapter 7); Chapter 8 presents the overall conclusions and possible future works.

This PhD thesis has been carried out through the funding of PhD scholarship in the National Operational Course for Research and Innovation 2014-2020, European Social Fund, Action I.1 "Innovative PhDs with industrial characterization".

A first release of the damper conceived within this work has been covered by Italian patent under priority number No. 102019000012402 [30].

This thesis has contributed to the main concept of the Horizon 2020 innovation project, called e-SAFE (energy and Seismic AFfordable rEnovation solutions), funded by the European Commission under grant agreement No 893135 [31] .

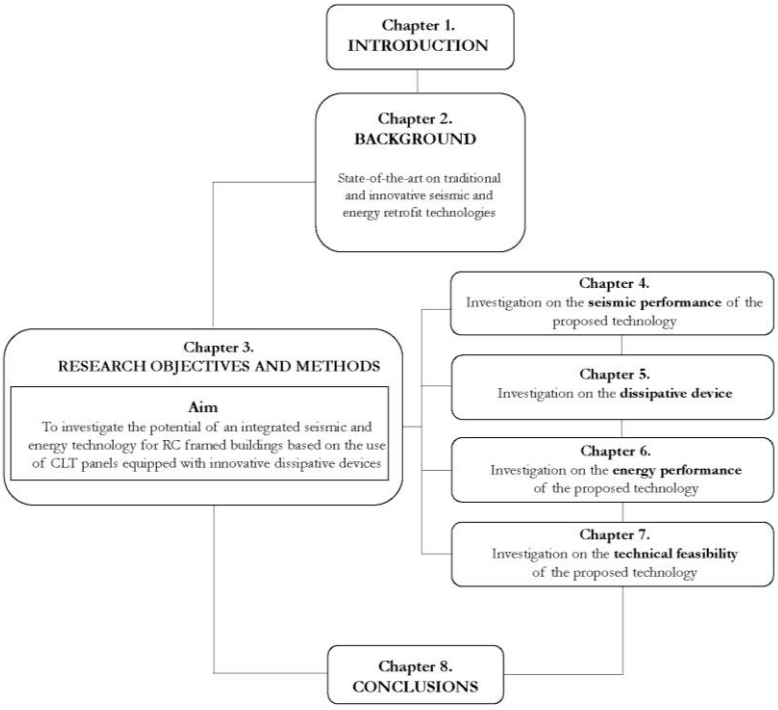

Figure 1.2. Flow-chart of thesis structure

References

[1] N. Sajn. Energy efficiency of buildings: A nearly zero-energy future?; European Parliamentary Research Service: European Union, 2016.

[2] Eurostat. Energy consumption in households. Available online: https://ec.europa.eu/eurostat/statisticsexplained/index.php/Energy_consumption_in_households#Energyproducts_used_in_the_residential_sector.

[3] BPIE (Buildings Performance Institute Europe). Available online: http://bpie.eu/wp-content/uploads/2017/12/State-of-the-building-stock-briefing_Dic6.pdf

[4] Economidou, M.; Laustsen, J.; Ruyssevelt, P.; Staniaszek, D. Europe's buildings under the microscope; BPIE: Brussels, Belgium, 2011; ISBN: 9789491143014.

[5] Directive (EU) 2018/844 of the European parliament and of the Council of 30 May 2018 amending Directive 2010/31/EU on the energy performance of buildings and Directive 2012/27/EU on Energy Efficiency.

[6] Conclusions of the European Council, EUCO 169/14, CO EUR 13, CONCL 5, Brussels, 24 October 2014.

[7] Conclusions of the European Parliament and of the Council of 11 December 2018 amending Directive 2012/27/EU on energy efficiency, EUCO 169/14, CO EUR 13, CONCL 5, Brussels, 24 October 2014.

[8] Bellini, O.E.; Marini, A. Passoni, C. Sistemi a esoscheletro adattivo per la resilienza dell'ambiente costruito - Adaptive exoskeleton systems for the resilience of the built environment. In TECHNE, 2018. 15, 71-80.

[9] Seismic Hazard Harmonization in Europe (SHARE). European seismic hazard map. Available online: http://www.share-eu.org/sites/default/files/SHARE_Brochure_public.web_.pdf

[10] Ozcebe S, Crowley H, Baker H, Spence R, Foulser-Piggott R (2014). D7.5 Census data collection and harmonization for Europe. NERA project deliverable.

[11] Italian National Statistical Institute 2011. Population Housing Census. Available online: http://daticensimentopopolazione.istat.it/Index.aspx?lang=en&SubSessionId=f51c0068-9a7d-42c5-abe4-9c3ef54656a0&themetreeid=-200

[12] Cruciani, C. Law 64/1974. In Provvedimenti per le Costruzioni con Particolari Prescrizioni per le Zone Sismiche; Gazzetta Ufficiale della Repubblica Italiana n. 76 del 2.2.1974: Rome, Italy, 2011. (In Italian)

[13] EM-DAT. The International Disaster Database. Available online: https://www.emdat.be/.

[14] Presidency of the Council of Ministers Italian Civil Protection Department. National risk assessment. Overview of the potential major disasters in Italy:

seismic, volcanic, tsunami, hydro-geological/hydraulic and extreme weather, droughts and forest fire risks, 2018.
[15] Images available online: https://www.ilsettempedano.it/2016/11/06/attivita-produttive-mercoledi-un-incontro-a-taccoli/ https://www.archistruttura.it/portfolio-item/mirandola-capannone/
[16] Belleri, A.; Marini, A. Does seismic risk affect the environmental impact of existing buildings? *Energ. Buildings* 2016, 110, 149-158.
[17] Federico, M.; Zuccaro, G. Seismic and energy retrofitting of residential buildings: A simulation- Based approach. UPLanD 2016, 1, 11–25.
[18] La Greca, P.; Margani, G. Seismic and Energy Renovation Measures for Sustainable Cities: A Critical Analysis of the Italian Scenario. *Sustainability* 2018, 10(1), 254.
[19] Mastroberti, M; Bournas, D.; Vona, M.; Manganelli, B.; Palermo, V. Combined seismic plus energy retrofitting for the existing RC buildings: economic feasibility. *16th European Conference on Earthquake Engineering*. Thessaloniki, 18-21 June 2018.
[20] Power, A. Housing and sustainability: Demolition or refurbishment? *Proc. ICE Urban Des. Plan.* 2010, *163*, 205-216.
[21] Alshamrani, O.S.; Galal, K.; Alkass, S. Integrated LCA-LEED sustainability assessment model for structure and envelope systems of school buildings. *Build. Environ.* 2014, 80, 61-70.
[22] Alba-Rodríguez, M. D.; Martínez-Rocamora, A.; González-Vallejo, P.; Ferreira-Sánchez, A.; Marrero, M. Building rehabilitation versus demolition and new construction: Economic and environmental assessment. *Environ. Impact Assess. Rev.* 2017, 66, 115-126.
[23] Decreto-legge 19 maggio 2020, n. 34. Misure urgenti in materia di salute, sostegno al lavoro e all'economia, nonche' di politiche sociali connesse all'emergenza epidemiologica da COVID-19.
[24] D'Agata, G.; Margani, G.; Pettinato,W. Cost evaluation of seismic and energy retrofit for apartment blocks in southern Italy. In Demolition or Reconstruction? Proceedings of the Colloqui.AT.e 2017, Ancona, Italy, 28–29.
[25] Irrera A. (2016) Quando la terra trema. Percezione del rischio sismico e cultura della prevenzione nella città di Catania. M.S. Thesis. University of Catania.
[26] D'Angola, A.; Manfredi, V.; Masi, A.; Mecca, M. Energy and seismic rehabilitation of RC buildings through an integrated approach: an application case study. *Green Energy Adv.*, 2019.
[27] Caverzan, A.; Lamperti Tornaghi, M.; Negro, P. A roadmap for the improvement of earthquake resistance and eco-efficiency of existing buildings and cities, in: Proc. SAFESUST Work., JRC science hub, JRC, Ispra, 2015, pp. 1–136.

[28] Passoni, C.; Guo, J.; Christopoulos, C.; Marini, A.; Riva, P. Design of dissipative and elastic high-strength exoskeleton solutions for sustainable seismic upgrades of existing RC buildings, *Eng. Struct.* 2020, 221.

[29] Menna, C.; Del Vecchio, C.; Di Ludovico, M.; Mauro, G.M.; Ascione, F.; Prota, A. Conceptual design of integrated seismic and energy retrofit interventions. *Journal of Building Engineering*. 2021, 38, 102190.

[30] Margani, G.; Marino, E.M.; Tardo, C. (inventors); University of Catania (assignee). Dispositivo di connessione dissipativa per pannelli in legno a strati incrociati. Italian Patent No 102019000012402. Ufficio Italiano Brevetti e Marchi. July 05, 2021. https://www.uibm.gov.it/bancadati/Number_search/type_url?type=wpn

[31] e-SAFE project (energy and Seismic AFfordable rEnovation solutions) http://esafe-buildings.eu/en/project/.

2

State of the art on traditional and innovative retrofit technologies for RC framed buildings

Summary

This chapter presents a review of the state-of-the-art on traditional and innovative seismic ad energy retrofitting technologies for RC framed buildings, distinguishing between most common solutions to be combined in an additive way and newly integrated solutions based on a holistic approach to building renovation. The main features, advantages and disadvantages, costs and disruption level are analysed for each retrofit technology, with a special focus on recent research on the topic of CLT-based renovation solutions.

2.1 Overview of combined and integrated seismic and energy retrofit technologies

2.1.1 Combined retrofit technologies

Currently, the seismic and energy upgrading of the existing building stock can be achieved mainly by combining the relative retrofit techniques in an additive way. The result is the superposition of two different interventions, which are generally implemented separately, in distinct periods.
A review of the main combined retrofit technologies for RC framed buildings is following presented.

2.1.1.1 Seismic retrofit technologies

The main current seismic retrofit interventions for RC framed buildings are reported in Figure 2.1, classifying them according to the strategy used to increase seismic resistance.

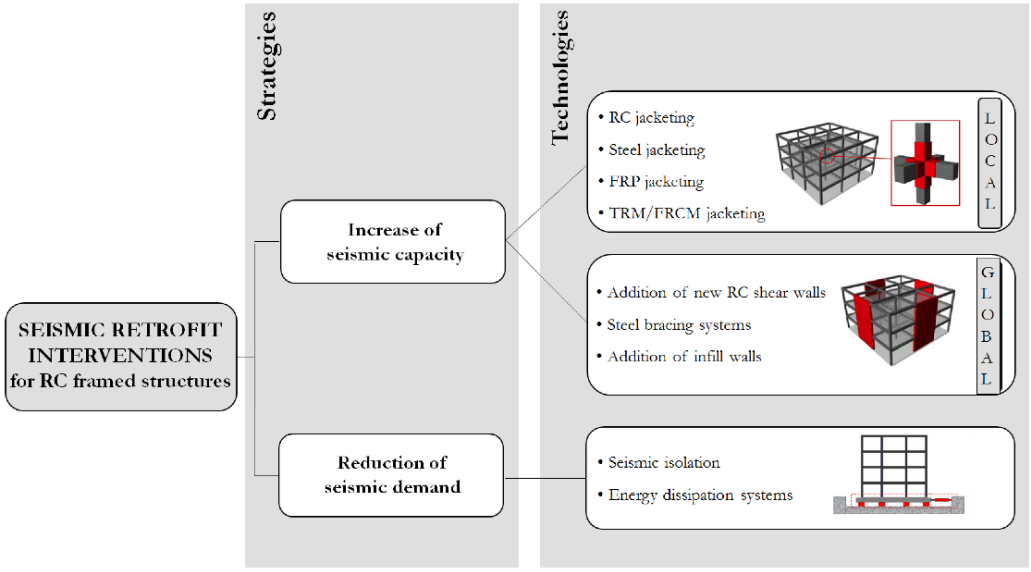

Figure 2.1. Main seismic retrofit interventions for RC framed buildings (images from [2])

These strategies consist in: i) increasing the strength and/or ductility capacity of the structure; ii) reducing the structure seismic demand.
The first one can be achieved by means of strengthening interventions at local or global level of the structure, or a combination of the two ones (hybrid solutions). Local interventions include several jacketing techniques to reinforce the individual structural members (columns and beams), while maintaining the original building frame system. The RC or steel jacketing (Figures 2.2a-b) are the most traditional techniques, which consist in wrapping the individual frame member by a RC layer or by steel angles and battens, respectively. These interventions allow the increase of the flexural and shear strength of RC members, also improving their ductility capacity through the confinement of concrete. In fact, the jacket prevents the concrete from dilating, forcing it in lateral compression and increasing its compressive strength and ductility [3]. However, RC and steel jacketing involves the increase of the cross-section of resisting members, thus requiring intensive labour, accurate detailing, high implementation time and relevant quantities of materials, which means higher embodied CO_2 emissions and more energy during manufacturing [4].
The fibre-reinforced polymer (FRP) jacketing (Figure 2.2c) is a more recent solution based on the use of innovative composite materials. Composites are made of synthetic or organic high strength fibres (e.g. boron, carbon, aramid, fiberglass, etc.) in the form of strips or sheets, which are bonded onto the RC members surface by means of high-performing epoxy adhesives. The result is a significant strength and ductility increase of the RC members, without considerably changing their geometry. FRP jacketing is corrosion-resistant, low-maintenance and considerably lighter compared to traditional jacketing techniques, not requiring heavy construction equipments, and thus reducing implementation time [5]. However, it entails high costs, skilled labour, hazardous handling, bad fire behaviour and cannot be applied at low temperature or wet surfaces, mainly due to the use of the organic resins [6-7].
To go beyond the FRP limits, researchers have recently introduced the textile-reinforced mortar (TRM) (Figure 2.2d), which combines textile fibre reinforcement having open-mesh configuration with inorganic matrices, such as cement-based mortars. TRM is a more affordable and worker-friendly material. It resists at high temperature and can be applied at low temperature or on wet surfaces, thanks to the use of organic resins [8-9].

(a) (b) (c) (d)

Figure 2.2. Jacketing techniques: (a) RC, (b) steel, (c) FRP and (d) TRM jacketing.

Regardless of the type of jacketing techniques, local interventions require the temporary downtime of the building and considerable demolitions and reconstruction actions, which affect up to 70-75% of the total construction costs in a new building [10]. In fact, the RC members should be isolated and relevant portions of infill walls, cladding layers and - in some cases - mechanical systems must be demolished and reconstructed.

Otherwise, the interventions at global level consist in creating a new seismic-resistant system that is connected to the existing building structure to draw part of the seismic force. The addition of new RC shear walls (Figure 2.3) is one of the most common techniques. The new walls may be added inside (Figure 2.3a) or outside (Figure 2.3b) the existing framed structure**.** The first option entails higher occupants' disturbance and more intensive supplemental interventions, such as the demolition of the existing infill walls. The second option is less invasive but require space outside the existing building, which might not be available. Overall, this technique can increase both the global strength and stiffness of the structure, reducing the storey drifts and thus the damage in frame members, as well as the effects of in-plan and vertical irregularities of the building [12]. More recently, the use of RC rocking walls has been proposed. RC rocking walls are equipped with vertical post-tensioned tendons that are base-anchored and cause the walls self-centering in the event of earthquakes. The self-centering effect allows rocking walls to suffer minimum damage compared to monolithic fixed-base RC walls. On the other hand, the rocking walls distribute the development of plastic hinges in the whole structure [13], thus exploiting its energy dissipation capacity.

School "A. Baggi" in Sassuolo (Modena, Northern Italy)

(a) (b)

Figure 2.3. Addition of new RC shear walls (a) along the perimeter and (b) outside the existing building (image 2.3a from [11])

Another technique to strength RC framed buildings at global level consists in the addition of steel bracing systems, inside (Figure 2.4a) or outside (Figure 2.4b) the existing building. Different types of bracing systems can be designed according to the building performance requirements, i.e. eccentric, concentric, buckling-restrained and post-tensioned bracings. Compared to RC shear walls, steel bracing systems enable the openings accommodation, add minor mass to the existing structure and reduce implementation time thanks to the dry installation [16].

Overall, both the addition of new RC shear walls or steel bracing systems allow the improvement of the global response of the existing buildings in terms of stiffness, strength, and displacement demand. However, as a major drawback these systems require relevant enlargement and reinforcement of the existing foundations or the built of new ones.

The addition of masonry infills, FRP- and TRM-strengthened infills or precast concrete panels onto the RC framed structure is also used to improve the global seismic performance of existing RC framed buildings, by achieving different performance levels in terms of strength and stiffness increase [12].

School "Cappuccini" in Ramacca [14] (Catania, Sourthern Italy)

School "Vito Capialbi" in Vibo Valentia [15] (Sourthern Italy)

(a) (b)

Figure 2.4. Addition of (a) steel buckling restrained brace (BRBs) and (b) hysteretic dissipative steel brace

An alternative seismic upgrading strategy is based on the reduction of the seismic demand of the structure by means of base isolation techniques or energy dissipation systems. Base isolation consists in inserting seismic isolation devices at the bottom or at the top of columns at the ground floor to decouple the building structure or part of it from foundations (Figure 2.5) [17]. This solution is very effective since it enlarges the fundamental period of the structure and in turn reduces the seismic forces it experiences. However, it entails high implementation costs since it requires to cut the existing columns and results also less effective for high-rise buildings.
Seismic demand can also be reduced by means of supplementary dampers that allow the dissipation of part of the seismic energy provided by earthquakes, thus reducing the displacement demand of the structure [19-20]. Currently, the building market offers several types of seismic dampers (viscous, friction, yielding, magnetic etc.), that can be embedded in the structure or integrated in new external seismic-resistant systems (Figure 2.4).

Figure 2.5. Retrofit intervention by means of seismic insulation technique in a residential building located in the city of L'Aquila (Central Italy) [18]

2.1.1.2 Energy retrofit technologies

The current retrofit technologies for enhancing the energy efficiency of existing buildings are aimed at: i) reducing the building energy demand for heating and cooling; ii) promoting the energy production on-site from renewable sources; iii) improving Heating, Ventilating and Air Conditioning (HVAC) equipment (Figure 2.6).

The first strategy is applied by increasing the thermal resistance of the building envelope, which generally results very low in buildings built between the 1960s and the 1990s. Accordingly, the main solutions to reduce the building energy demand consist in the application of insulation materials on the opaque envelope components, as well as the replacement of the existing windows with high-performing ones (multiple glazing with inert-gas filling, thermal-break frames, low-emission coatings, etc.).

To implement the first solution, many types of thermal insulation materials are currently available on the market, which are divided into conventional insulation material, e.g. mineral wool, polyurethane (PUR), cellulose, expanded polystyrene (EPS), extruded polystyrene (XPS), and advanced ones, such as Vacuum Insulation Panels (VIP), aerogels, Gas-filled Panels (GRP), Transparent Insulation Materials

(TIM) (Table 2.1) [21-22]. The thickness of the insulation material depends on the U-value to be achieved, according to the specific climate zone.
A further solution for the energy demand reduction includes the adoption of passive measures to exploit natural energy resources – such as solar radiation, evaporative cooling, and natural ventilation – as well as to ensure an adequate sun shading.

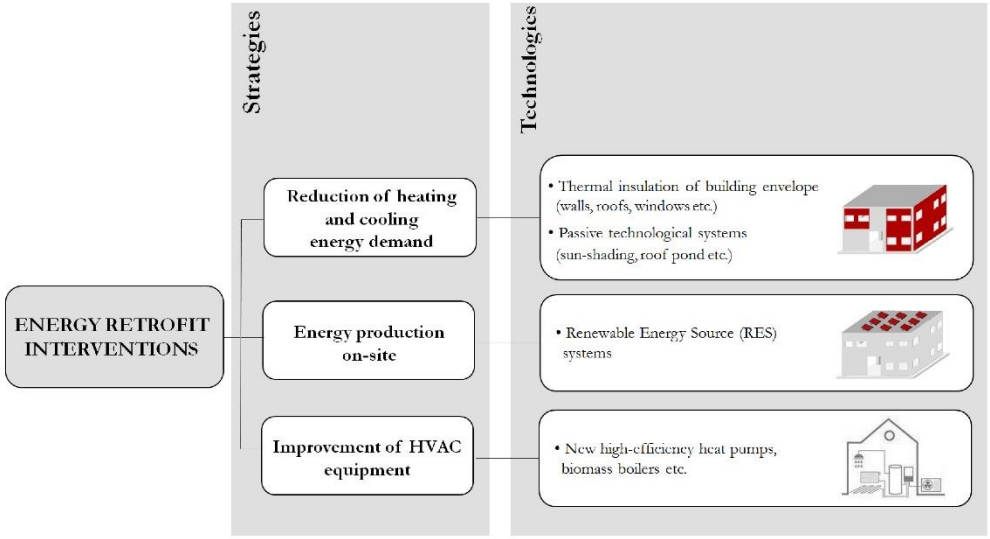

Figure 2.6. Classification of the main energy retrofit interventions.

The second energy-efficiency strategy involves the installation of Renewable Energy Source (RES) systems – such as photovoltaic (PV) panels, solar thermal (ST) collectors and wind power micro-turbines – to produce energy on-site from solar and wind power, thus replacing fossil energy sources, i.e. natural gas, oil, coal. In particular, solar collectors and PV panels – usually made of mono- or poly-crystalline silicon – are one of the most cost-effective solutions especially in southern and central Europe, where sun-based RES system turn out to be quite efficient [23].
Finally, the third strategy includes the improvement or replacement of the existing heating and cooling systems with high-efficient ones. Traditional gas boilers or district heating network of first generation for space heating and domestic hot water (DHW) generally have low efficiency and require high primary energy consumption. Possible solutions are the replacement of the boilers with condensing ones with efficient electric heat pumps that today are widely used for space heating purposes

thanks to their high efficiency and for the possibility to be fed also from renewable energy sources.

Material	Thermal conductivity (mW/mK)	Resistance fire, water and chemicals	Cost per thermal resistance	Environmental impact of production and use
Mineral wool	30-40	Low	Low	Low
Expanded polystyrene (EPS)	30-40	Low	Low	High
Extruded polystyrene (XPS)	30-35	Moderate	High	High
Cellulose	40-50	Low	Low	Low
Polyurethane (PUR)	20-30	Moderate	High	High
Vacuum insulation panels (VIP)	4-8	Low	High	Moderate
Gas-filled panels (GRP)	10-40	Low	High	Moderate
Aerogels	13-14	Moderate	High	Moderate
Nano insulation material (NIM)	<4	Moderate	High	Moderate

Table 2.1. Properties of main thermal insulation materials (data from [22])

2.1.2. Integrated retrofit technologies

Recently, new and innovative retrofit solutions aimed at combining seismic and energy renovations actions in an integrate way, instead of an additive way, have been investigated, in view of a holistic approach to building renovation. These solutions are primarily based on the installation from the buildings outside, in order to avoid occupants' relocation during works and, consequently, minimize disruption. The external installation also allows to avoid supplemental demolition interventions, thus reducing implementation time and costs and minimizing waste production.
The integrated retrofit solutions that have been recently investigated are mainly based on the use of:

i) engineered steel exoskeletons;

ii) wet envelope technologies;

iii) timber-based envelope technologies.

A review of them is following presented.

2.1.2.1 Engineered steel exoskeletons

The concept of a multi-skin exoskeleton aimed at improving both the seismic and thermal performance of existing RC framed buildings has been introduced by Takeuchi et al. [25-26]. It was firstly applied to the Midorigaoka-1st building at Tokyo Institute of Technology (Figure 2.7), which was designed in 1966 before the revision of the Japanese Building Code in 1971. The authors proposed to apply on the building envelope a steel-framed façade, which is equipped with BRBs and covered by an outer skin of glass and/or louvers. The BRBs allow the dissipation of seismic energy in the event of earthquakes, reducing the drifts demand of the structure and consequently its damage. Instead, the double glass façade system with integrated oriented louvers mitigates the inner temperature both in winter and summer, thus reducing the heating and cooling energy demand, respectively. The solution proposed by Takeuchi et al. also aimed at renovating the original building appearance, undermining the traditional view of the exoskeleton as a mere structural system. This integrated retrofit solution resulted highly effective to increase the

seismic and thermal performance of the Midorigaoka-1st building, allowing the continuous tenants occupancy during the retrofit works.

The research on the potential use of engineered steel exoskeletons as holistic renovation strategy has been recently revived and expanded, looking at the system's features of adaptability, easy maintenance, and reparability, as well as materials recyclability related to the dry installation. These features much comply with the main principles of environmental sustainability, in a Life Cycle perspective of building renovation [27]. Different shear walls and shell solutions to be coupled with energy-efficiency ones in the design of sustainable multi-skin exoskeletons have been examined [28], and a procedure for their design has been proposed to define interventions leading to equivalent seismic performances of the retrofitted buildings [29].

D'Urso and Cicero [30] also underlined the considerable potentiality of architectural renovation of steel exoskeletons, proposing the use of parametric design to generate multiple integrated retrofitting solutions for building façade, in order to choose that which better interprets the aesthetic canons selected by the designer (Figure 2.8).

Moreover, the H2020 Pro-GET-onE innovation project [31-32] is currently developing several retrofit solutions based on the addition of multi-skin exoskeletons. The aim of the project is to investigate the use of external steel bracings both as a new seismic-resistant system as well as structural support for a newly energy-performing envelope made of pre-assembled components, that also create additional and customized living spaces, thus increasing the building global value and the users' living comfort (Figure 2.9).

Overall, steel exoskeletons may result in highly improvement of the seismic and energy-efficiency performance of the existing building stock, allowing the maintenance of the building operativity and complying with the main objectives of the design for environmental sustainability.

However, as main drawbacks, the availability of space around the building perimeter as well as the built of a new foundation system are mandatory requirements for the exoskeleton installation. Furthermore, the implementation costs are quite high, ranging from 250 to 700 euro/mq, based on the exoskeleton type [33-34].

Figure 2.7. Engineered steel exoskeleton in the Midorigaoka-1st building [25]

Figure 2.8. Study on the potential of architectural renovation of engineered steel exoskeletons [30] .

Figure 2.9. Case study of the Pro-GET-onE research project [32]

2.1.2.2 Wet envelope technologies

One of the most recent technology for the concurrent seismic and energy renovation of RC framed buildings is the insulating RC coating system. This system consists in cladding the building envelope with a new earthquake-resistant and thermal-insulating skin made up of a thin RC slab, which is casted in situ and cladded with insulation and cladding materials. This innovative technology has been developed to give a structural role to traditional external thermal insulation composite systems (ETICS), allowing the improvement of the strength and stiffness capacity of the existing structure by operating only on the outer envelope, without changing the building geometry. Currently, various insulating RC coating solutions are available in the Italian building market. For instance, Ecosism S.r.l. has recently introduced the system called "Geniale cappotto sismico" (Figure 2.10)[35].

(a) (b)

Figure 2.10. "Geniale cappotto sismico" system: (a) components and (b) application to a residential building located in Treviso (Northern Italy) [35]

Specifically, this system is realized by means of disposable galvanized steel formworks that are equipped with two customizable insulation layers with a thin RC slab in between (Figure 2.10a). The two insulation layers are pre-assembled in the steel formworks off-site, while the RC slab is casted on-site after arranging the steel rebars, and anchored to the existing structure both at foundations and floors level. Additional vertical and horizontal ribs can also be provided to improve the bending behavior of the RC slabs and to reduce the risk of out-of-plane instability. A plaster finishing layer is then applied on-site. Today, different applications of the "Geniale

cappotto sismico" system have been implemented in Italy (Figure 2.10b), demonstrating its effectiveness in terms of time saving.
Similarly, Ferry S.r.l. proposes the "Sismacoat" system [36], where the RC slab is casted on-site between cold-formed profiles, while Paver S.p.A proposes to cast it into expanded clay blocks, which act as disposable formworks and have insulation materials inside [37].
Currently, the integration of the advanced TRM jacketing technique with different energy retrofitting technologies is under validation as potential new retrofit solution [38]. Specifically, this solution provides the strengthening of masonry-infilled RC frames with TRM and then the application of different thermal insulation materials (e.g. TRM+PUR, TRM+XPS, TRM+Aerogels, TRM+NIM) or thermal systems (e.g. capillary tube heating systems) afterward, while the inorganic cement-based mortar for the TRM bonding is still in a fresh state and can act as support system (Figure 2.11). This intervention allows the increase of the global lateral response of the existing structure without the need to work on the foundations. Furthermore, it is easily applicable also on URM buildings and reduces the building down-time, if carried out from the outside.

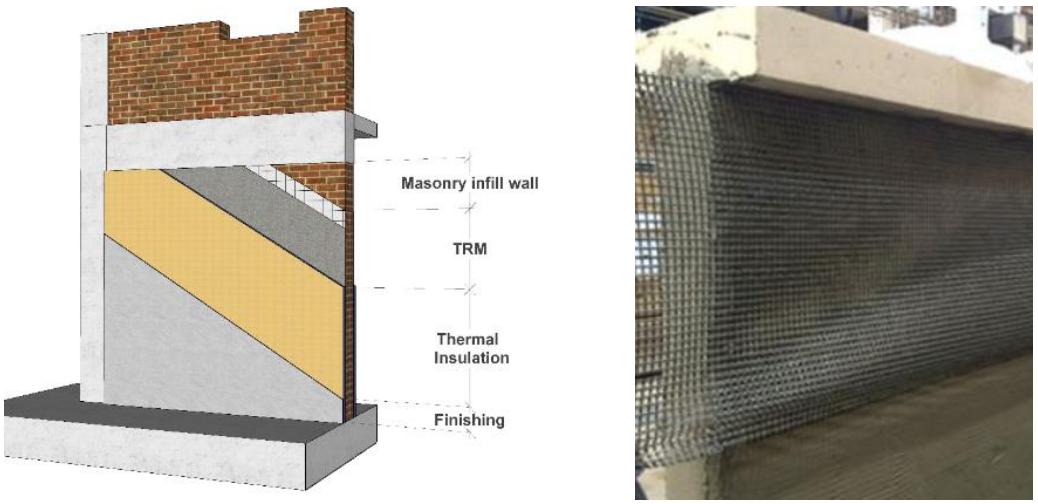

Figure 2.11. Combined seismic and energy retrofitting with TRM and thermal insulation [38].

The improvement of both seismic and thermal performance of RC framed buildings without the need of new foundations can be achieved also by replacing the existing infills with better performing ones, such as reinforced masonry (RM) or infills made of autoclaved aerated concrete (ACC) blocks [39-40]. However, the interventions based on the infills-replacement cause considerable amount of waste, that is not always recyclable, and require the occupants' relocation. Furthermore, a full seismic upgrade of the building is unlikely to be achieved in high seismicity areas [40].

2.1.2.3 Timber-based technologies

The current needs of cost-effectiveness, quick installation, and lower users' disturbance, as well as more environmentally friendly approaches to the building renovation have led the research community to investigate other prospective construction materials against traditional concrete and steel. In fact, concrete and steel manufacture is highly energy intensive, contributing to a significant portion of global carbon emissions [41].

In this framework, timber has showed great potential as sustainable retrofitting material to upgrade the seismic and thermal performance of the existing RC framed buildings, thanks to the recent advancement of engineered timber products, such as Cross-Laminated Timber (CLT). Timber is one of the most environmentally friendly materials, being highly recyclable and a natural carbon sink. The high level of prefabrication of CLT also makes it much attractive to retrofitting uses, making the industrialization of the building renovation sector as one of the main future challenges.

In accordance with the aim of the thesis, the main features of CLT and the recent literature on the topic are detailed in next Section.

2.2 The potential use of cross-laminated timber for the integrated seismic and energy building renovation

2.2.1 Cross-laminated timber: main features and challenges

Cross-laminated timber has been conceived for structural purpose in the 1980s in Central Europe and today is widely spread around the world for buildings applications.

CLT is a plate-like engineered timber product commonly composed of an uneven number of timber board layers (usually ranging from three to five, but even more), which are arranged crosswise to each other at an angle of 90° and connected by adhesive bonding (Figure 2.12a-b). The result is a rigid composite element having high mechanical performance. In fact, the crosswise build-up provides the CLT panel high capacity of bearing loads both in-plane and out-of-plane, allowing its application as a full-size wall and floor element (Figure 2.12c). Occasionally, the CLT element is also realized with the most outer two layers parallel each other, in order to provide it with greater strength and stiffness capacity along one load direction. The engineered CLT configuration also minimizes swelling and shrinkage rate, providing the panel high dimensional stability in-plane, while in thickness direction both swelling and shrinkage effects are equal to solid timber ones [42]. All these features enable the construction of more robust and complex larger-span structures compared to traditional lightweight framed systems.

The strength class of timber boards in homogeneous CLT sections is commonly C24 according to EN 338 [43], using mainly softwood species such as Norway spruce. Timber strength class C26/18 is also allowed for the transverse layers in case of combined CLT sections.

Regarding the physical properties, CLT is a bad heat conductor, thanks to its low thermal conductivity (0.10 ÷ 0.13 W m^{-2} K^{-1}), with good thermal insulation and thermal inertia properties [44].

Dimensionally, CLT panel can reach 30 m in length (l_{CLT}) and 4.80 m in width (w_{CLT}), while the overall thickness (t_{CLT}) limit is equal to 500 mm (Figure 2.12a). Generally, standard thicknesses of individual CLT layers are t_l = 20, 30, 40 mm and CLT producers avoid to glue the adjacent timber boards within the same layer, minimizing the width of gaps (w_{gap}), in consideration of the most common joining

techniques based on the use of dowel-type fasteners such as nails, screws or dowels [45]. Regardless, the width of gaps between adjacent boards is allowed up to 6 mm, according to the European product standard EN 16351 [46].

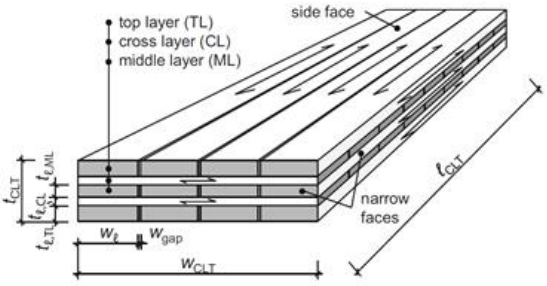

(a)

(b)

(c)

Figure 2.12. (a) Specifications of CLT element (image from [45]);
(b) CLT elements with 3 and 5 layers; (C) box-like structure of a typical CLT building.

The CLT manufacture is characterized by a high level of prefabrication that makes the buildings construction process faster and easier, involving only the assembly and connection of the individual panels. Specifically, the manufacturing process includes the typical steps of glulam production (Figure 2.13). Basically, kiln dried timber boards are strength and stiffness graded, cut out of local imperfections and finger-jointed in the side or narrow face. Therefore, timber boards are close to create the longitudinal and transverse layers of CLT. Optionally, adjacent timber boards may

be edge bonded, getting single-layer panels. Without narrow face bonding, gaps between the boards may occur. Then, timber boards or single-layer panels are assembled by adhesive bonding on the side face and pressed. Adhesive bonding is normally carried out mechanically and contactless (i) on single boards in a continuous through-feed device or (ii) on CLT layers already pre-positioned in a positioning or press bed [47].

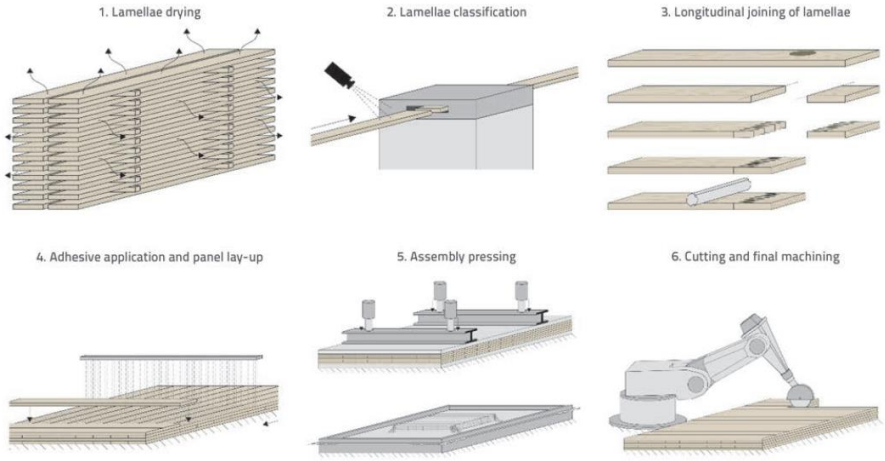

Figure 2.13. CLT manufacturing process [47].

The high mechanical and physical performance, the natural and environmental properties as well as the high level of prefabrication of the CLT product have promoted its rising spread in recent years, as attested by the growing number of residential and office buildings erected worldwide, with production capacities growth rates of 15÷20% per year [48].

The recent development of innovative structural connection systems and hybrid CLT-based construction systems have also enabled the construction of mid-rise and high-rise buildings, showing the great potential of timber-based constructions, to which is expected that building industry will be addressed in the coming decades (Figure 2.14).

CLT buildings resulted potential also as lateral force-resisting systems in earthquake-prone areas. Specifically, comprehensive research activities carried out on this topic over the past 20 years highlighted that the behaviour of CLT buildings under seismic

loading primarily depends on the ductility of the connection systems between CLT panels (e.g. hold-downs and steel brackets), while the panels act almost as rigid bodies with local damage at the connections [49]. CLT-steel hybrid systems have been also proven as earthquake-resistant structural systems [50-54].

(a) (b) (c)

Figure 2.14. (a) Brock Commons Project in Vancouver [51];
(b) Daston Lane Project in London [52]; (c)Housing block in Sweden [53].

2.2.2 Cross-laminated timber as retrofit solution: state-of-the-art review

The increasing attention to the environmental sustainability has led the research community to investigate the building renovation sector as a further CLT application field. In particular, recent studies investigated the use of CLT panels as strengthening elements to increase the seismic performance of both the existing URM buildings [55-59] and RC framed ones [59-62]. Among the advantages of such potential use are the low building mass increase compared to other seismic upgrading techniques, thanks to the low mass of CLT (CLT weight= 470 kg/m^3), as well as the benefits of dry interventions, such as quick and easy installation and materials reversibility and recyclability.

Referring to RC framed buildings, different strengthening interventions by the application of CLT panels to the building envelope have been investigated.

First extensive works on the topic have been carried out by Sustersic and Duijc [59-60], who proposed a low invasive retrofit solution consisting in applying a new outer CLT-shell on the existing building envelope (Figure 2.15a). The intervention is

compatible with an integrated retrofitting approach aimed also at increasing the energy efficiency of the building. The idea was indeed to exploit the insulating properties of CLT material in combination with other insulation layers to improve also the thermal performance of the building. The authors proposed to connect the panels and the existing structure through special dissipative devices (Figure 2.15b). In detail, the proposed device is made of ductile steel brackets that allow seismic energy dissipation in the event of earthquakes. On the one side, the steel brackets are connected to the CLT panels by means of a U-shaped steel profile, which is attached to the panels through special timber connectors and self-tapping screws. On the other side, brackets are connected to the existing structure through a steel tie, that is anchored on the perimeter beams of the building by means of steel-threaded rods. Conversely, both the CLT-steel and RC-steel connection are conceived to be oversized.

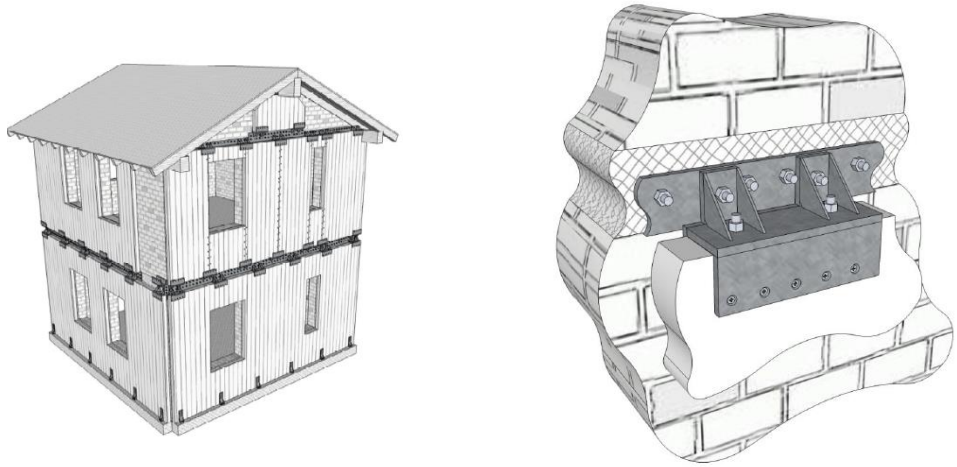

(a) (b)

Figure 2.15. (a) CLT-based retrofit solution and (b) dissipative connection device proposed by Sustersic and Dujic [60]

The performance of the above-described technique has been assessed by means of dynamic shaking table tests on a two-storey, one-bay RC frame. Both the bare and masonry infilled configuration were analysed (Figures 2.16-2.17). In particular, tests on the bare frame with and without the application of CLT panels at the ground

floor (Figure 2.16a) have been performed in elastic state, by using the original Petrovac earthquake with a peak ground acceleration of 0.5 g and the modified Landers accelerogram. The comparison of the structure natural period resulted from sweep tests at pre- and post- intervention state showed a notable increase of the lateral stiffness of the RC frame after the application of CLT panels, since the 1st vibration frequency of the frame changed from 2 to 3.7 Hz (Figure 2.16b).

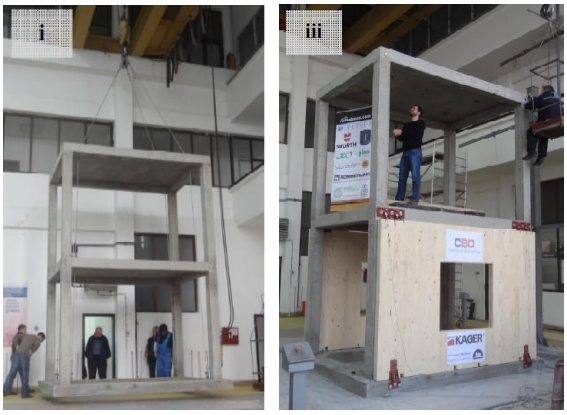

(a)

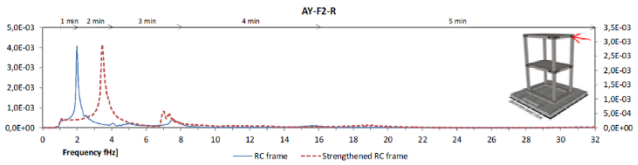

(b)

Figure 2.16. (a) Seismic shaking table testing on the bare RC frame at pre-and post-intervention state and (b) sweep test power spectral analyses carried out by Sustersic and Dujic [60].

Then, masonry infills have been added in the same RC frame (Figure 2.17a) and the structure natural periods have been measured for both the strengthened and un-strengthened frame configurations. At post-intervention state, the increase of the lateral stiffness of the frame was not as prominent as without infill, and local damage have been observed in one of the infills (Figure 2.17b).
The un-strengthened infilled structure has been then tested by using the modified Landers earthquake scaled to 0.75 until the infills cracked and fell out. CLT panels

have been later applied to the damaged structure. The strengthened structure was able to withstand the 0.75 g Landers earthquake two times without further damage and an additional Petrovac earthquake. The maximum story drifts experienced by the strengthened structure was 30% smaller than the un-strengthened counterpart. These results showed the potential of CLT shell-solution to prevent the collapse of RC framed buildings.

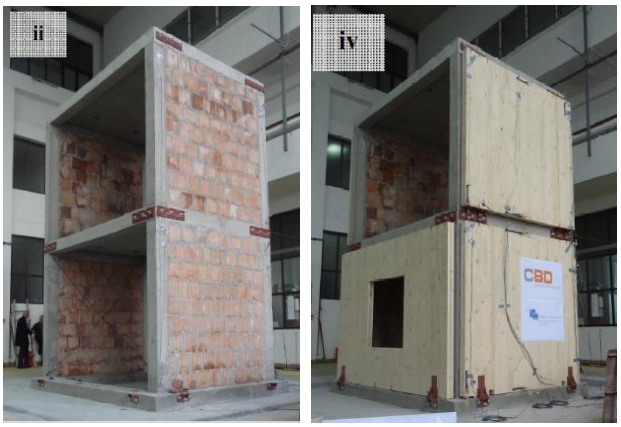

(a)

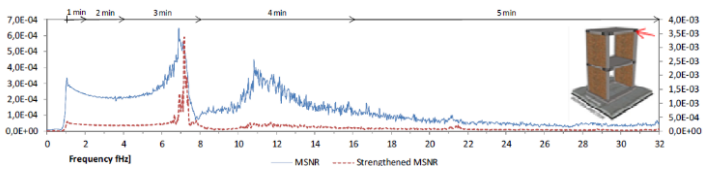

(b)

Figure 2.17. (a) Seismic shaking table testing on the masonry infilled RC frame at pre-and post- intervention state and (b) sweep test power spectral analyses carried out by Sustersic and Dujic [60].

The application on the existing buildings envelope of a new CLT-based skin acting as stiffening against seismic actions as well as thermal insulation system has been recently investigated within the AdESA project [61-62], resulting in a real application on a pilot building. The AdESA system consists of CLT panels connected to the existing RC structure and a new foundation system. Hence, the new CLT envelope is cladded on-site with insulation and finishing materials.

The system includes the use of dissipative panel-to-panel connections, which are made of rows of metal slats having out-of-plane bending capacity (Figure 2.18a-b) in order to develop plastic deformations in the event of earthquakes, thus limiting the seismic force transferred to foundations and keeping CLT panels in elastic range. Instead, the connections of CLT panels both to the new foundation and the existing structure are made with oversized traditional steel pins.
The system has been applied on a two-storey gym built in 1981 in Brescia (Northern Italy) and characterized by a precast concrete structure (Figure 2.18c). The intervention included the use of 10-cm thick CLT panels, cladded on-site with 8-cm thick EPS insulation panels and a finishing plaster. Additional structural interventions have been also required to adapt the investigated retrofit system to the specific pilot building, such as ribbon windows and precast RC walls. As result, the overall retrofit system allowed the seismic upgrading of the building, as well as the reduction of the building energy consumptions by 50%. Although the selected pilot shows different features in comparison to most common residential buildings, the results obtained from the first application of the AdESA system demonstrated its potentiality as integrated and low invasive seismic and energy retrofit intervention.

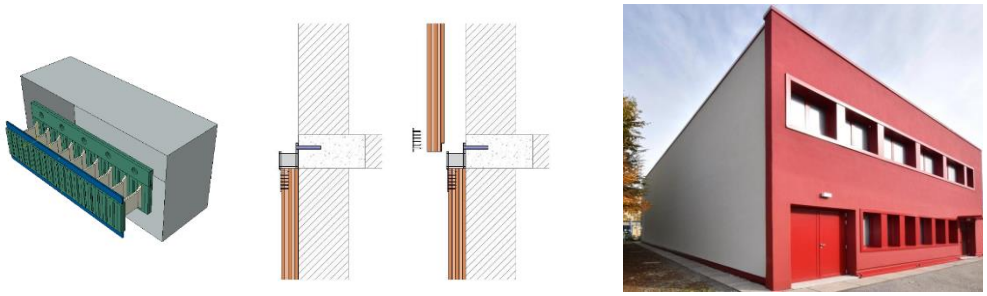

(a) (b) (c)

Figure 2.18. The AdESA system: (a) dissipative panel-to-panel connection; (b) installation process of CLT panels [63]; (c) case study after the intervention [62].

The same integrated and low-disruptive CLT shell-based retrofit solution has been proposed also by the Italian company Wood Beton S.p.A., which has recently introduced the "Rhinoceros-wood" system in the building market [64] (Figure 2.19).

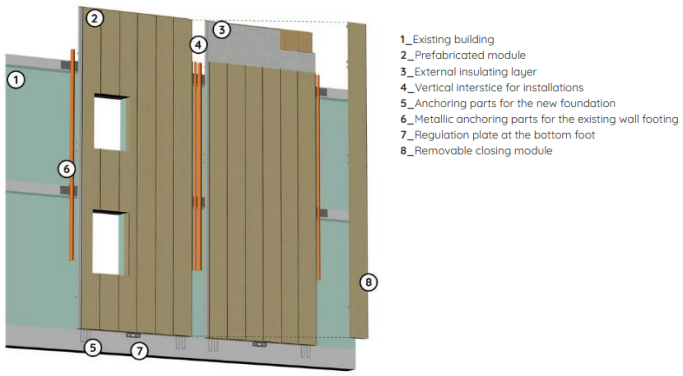

Figure 2.19. The "Rhinoceros-wood" system [64].

This system has been conceived to be totally prefabricated in order to reduce costs and time for implementation, thus promoting the industrialization of the building sector. Accordingly, the strengthening components to be applied to the outer walls consist of prefabricated CLT-based panels that integrate insulation and finishing layers. Specifically, as shown in Figure 2.20, the connection between the prefabricated panels and the existing structure is provided at slab level, by mutually connecting steel plates, which are previously arranged both on the existing slab and on the backside of the CLT panel. The vertical gap between the adjacent panels is then used to place a new plant system that integrates or replaces the existing one. Prefabricated CLT panels could integrate also new windows in replacement of the existing ones. Moreover, in presence of balconies on the building facades the system provides for their demolition and replacement with new prefabricated ones.
The "Rhinoceros-wood" system has been applied to a RC framed building built in the 1960s in Costa Volpino (Bergamo, Northern Italy), allowing to demonstrate the improvement of the building seismic performance and the technical-feasibility of the system. However, its application is currently limited to buildings up to a maximum of 3 storeys that require a low stiffness increase, since the improvement of the buildings seismic performance is provided only by the strengthening actions of the CLT panels.

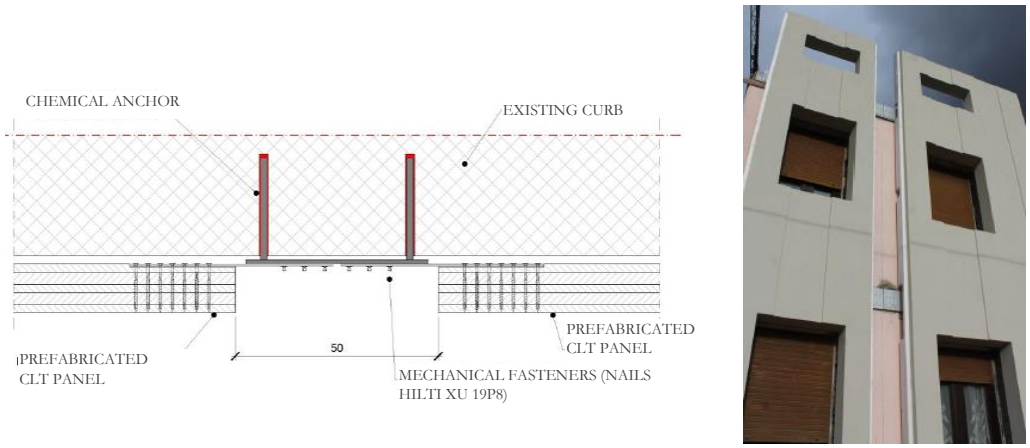

Figure 2.20. Construction detail of the CLT-structure connection provided by the "Rhinoceros-wood" system.

In addition to the CLT shell-retrofit solution, other CLT applications have been investigated as potential seismic retrofit methods for RC framed buildings. Among them, the use of CLT panels as infill shear walls has been proposed by Haba et al. [65-66] and Stazi et al. [67].

Specifically, Haba et al. [65-66] investigated shear walls composed of narrow CLT elements bonded to each other and onto the RC frame with epoxy resin. The intervention provides increase of stiffness, strength and ductility capacity as demonstrated by the experimental activities conducted by the authors. In particular, cyclic loading tests were performed on RC frames in 1/3 scale (1800-mm wide and 970-mm height) infilled with couples of 3-ply Japanese cedar CLT elements that have been adhesive bonded on-site (Figure 2.21). The cyclic response of the specimens has been investigated by varying both the number of CLT elements within the RC frames and the fibre orientation of CLT layers. Specifically, specimens with seven (types T, X, X-S in Figure 2.21a) and four pairs of CLT elements (type T-O in Figure 2.21a) have been analysed. In specimens X and X-S, the fibres of the external layers of infilled CLT elements have been oriented of 30° with respect to the direction of the applied lateral load, while in the other specimens have been oriented of 90°. Moreover, in specimen X-S, CLT elements have been connected to the RC frame by means of T-shaped steel connections.

By comparing the load-drift angle curves resulted from each test (Figure 2.21b), every reinforced specimen resulted stiffer, stronger, and more ductile than the bare

one. In particular, the best performance of the proposed retrofit method has been obtained when the fibre orientation of the external layers of the CLT elements is 30 degrees inclined. A small drop of strength at the end of elastic region has been observed in each specimen, due to the failure of the bonding connection between concrete and panels. Then, the curves of each specimen are immediately followed by secondary linear part, caused by the compression of the part of panels, the friction and shear key resistance between concrete and panels.

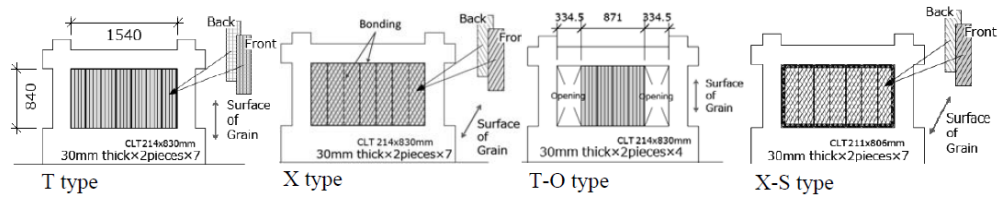

(a)

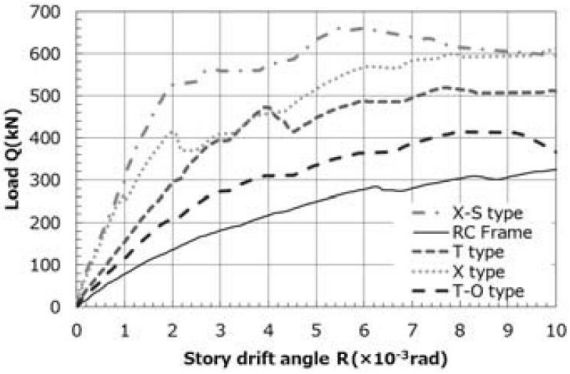

(b) (c)

Figure 2.21. Experimental campaign carried out by Haba et al. [66]:
(a) specimens; (b) load-drift angle relation (in tension); (c) CLT panels setting.

Experimental and numerical investigations on the potentiality of infilled CLT shear walls for seismic retrofit of RC frames were carried out also by Stazi et al. [67]. The authors performed experimental and numerical monotonic diagonal compression tests on 3-ply CLT specimens to investigate their elastic and post-elastic in-plane shear behaviour when subject to a combined stress state (Figure 2.22a). The

experimental tests have been conducted with and without metal shoes on the lateral side of the panel, which intent to reproduce a direct load transmission from the RC frame to the CLT infill. A brittle linear behaviour has been observed in all CLT specimens, with higher stiffness and strength values in case of panels equipped with metal shoes. However, by comparing the results in terms of shear strength with that of masonry infill panels, CLT infills showed higher strength capacity, thus resulting effective to strengthen RC framed structures. These results were confirmed by monotonic numerical analyses on a one story one-bay RC frame, that were aimed at investigating the change in the in-plane lateral response of the RC frame due to the insertion of 3-ply CLT infill panel, by simulating a perfect bonding between panel and structure to reproduce the presence of strong connections. The numerical results proved that the CLT infill allows the RC frame to reach a higher lateral stiffness and peak force value compared to common infills, i.e. made of regular masonry or Autoclaved Aerated Concrete (AAC) blocks (Figure 2.22b). In particular, the global lateral stiffness of the CLT infilled frame resulted 7 times higher than the stiffness obtained in case of the other above-mentioned infills. Similarly, the shear strength resulted 4 times higher than the infilled configuration of the stronger AAC masonry infill.

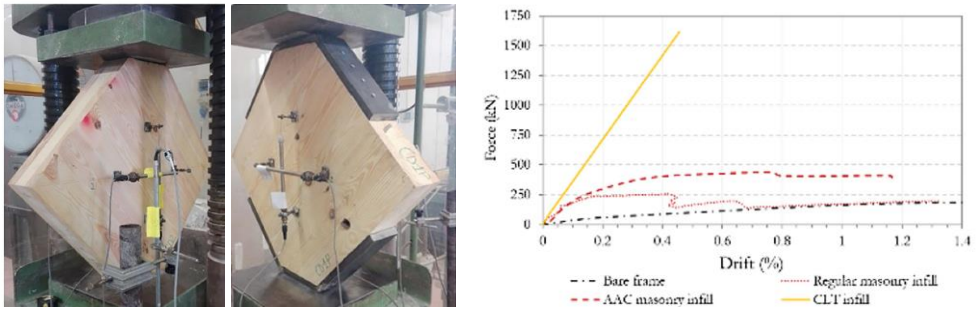

(a) (b)

Figure 2.22. (a) Diagonal compression tests on CLT specimens and (b) results of numerical pushover analyses on a RC frame carried out by Stazi et al. [67]

An alternative low-damage and low-invasiveness retrofit intervention has been recently investigated by Sandoli et al. [68], who proposed the use of post-tensioned, re-centering and dissipative rocking CLT walls (named Pres-Lam technology) in the external perimeter of the existing buildings. Pres-Lam structural timber walls are

hybrid system characterized by vertical post-tensioned tendons in a centrally located duct to anchor the timber walls to the foundation (Figure 2.23). During seismic motion, the presence of the post-tensioned tendons causes a re-centering effect in the structural walls. This effect is related to the building seismic displacements and allows to minimize residual deformations in the walls, thus avoiding their damage. The re-centering effect of the rocking CLT walls during seismic motion together with their quick and external installation make the Pres-Lam wall system more attractive compared to common RC shear walls that, on the contrary, are subjected to permanent damage due to the development of plastic hinges.
Preliminary numerical investigation performed by the authors on a case study building designed for gravity load only showed the considerable potential effectiveness of the proposed solution in terms of improvement of seismic capacity.

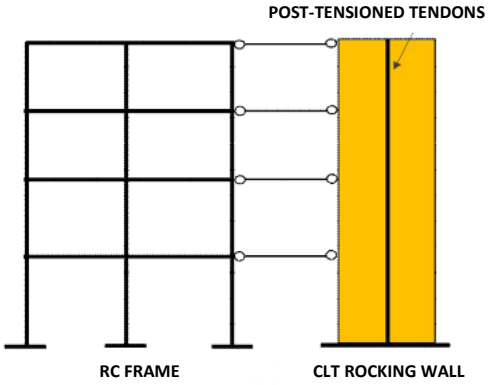

Figure 2.23. System RC frame-CLT rocking wall [68].

2.3 Conclusions and comments

Currently, the main barriers which hinder the combined use of most common seismic and energy retrofit techniques for RC framed buildings are mostly related to the excessive costs and the high invasiveness of seismic retrofit actions. In fact, the common anti-seismic interventions that need to be implemented inside the building require the occupants' relocation during the works - often for several months -, resulting in additional costs for temporary alternative accommodation and relevant disruption related to the interruption of everyday routines. Conversely, interventions from the outside of the buildings can be technically unfeasible without specific boundary conditions (e.g. proper space around the building).

To overcome these barriers, newly and innovative seismic and energy integrated retrofit solutions have been recently investigated to specifically meet the current needs of cost-effectiveness, quick installation and reduced users' disturbance.

In this framework, the use of CLT panels as strengthening elements to increase the seismic capacity of the existing buildings has showed great potentiality as alternative and environmentally sustainable retrofit solution, thanks to the high mechanical performance of this engineered wood product.

Different applications of CLT panels on the existing buildings envelope have been investigated for retrofit purpose, which include the use of both CLT shell-solutions, CLT infilled shear walls and rocking CLT walls. The recent and rich literature on the topic shows that these studies are of great interest, but also that the development of these system is at a preliminary stage. In particular, the application of a new outer CLT-shell on the buildings envelope well meets the current retrofit needs. On the one side, the installation from the outside of the building avoids the occupants' relocation during works and supplemental demolition interventions. Hence, it reduces implementation time and costs and minimizing waste production. On the other side, this solution turns out to be highly versatile, since it does not requires excessive space around the building, without affecting the building geometry and appearance.

Highly potential in further reducing costs and implementation time is showed by the increase of the prefabrication level of CLT components that integrate insulation and finishing layers.

The use of dissipative devices as connection systems between the CLT panels and the building envelope can also increase the effectiveness of this solution, since the

supplemental dampers dissipate part of the seismic energy, thus reducing the displacement demand of the structure.
However, the research on potential dampers for this use is still at a preliminary stage. The dampers investigated so far have been mainly conceived to allow seismic energy dissipation by exploiting their ductility capacity. This dissipation mode is not very effective in terms of technological and operational efficiency, since it requires the replacement of the dampers and the removal of the CLT panels after the seismic event.
Based on the above, there is a need for new and innovative potential CLT-shell retrofit solutions provided with more effective and widely applicable seismic dampers.

2.4 References

[1] Federico, M.; Zuccaro, G. Seismic and energy retrofitting of residential buildings: A simulation- Based approach. UPLanD 2016, 1, 11–25.

[2] Marini, A.; Belleri, A.; Feroldi, F.; Passoni, C.; Preti, M.; Riva, P.; Giuriani, E.; Plizzari, G. Coupling energy refurbishment with structural strengthening in retrofit interventions. *Conference proceeding. SAFESUST workshop,* Ispra, November 26-27, 2015.

[3] Chandrakar, J.; Singh A.K. Study of Various Local and Global Seismic retrofitting strategies – A review. *International Journal of Engineering Research & Technology* 2017, 6 (06), 824-831.

[4] Bournas, D. Innovative Materials for Seismic and Energy Retrofitting of the Existing EU Buildings; EUR 29184 EN, Publications Office of the European Union: Luxembourg, 2018.

[5] Gorai, S.; Maiti, P.R. Advanced retrofitting techniques for reinforced concrete structures: a state of an art review. *i-manager's Journal on Structural Engineering* 2016, 5 (1), 6-18.

[6] Advanced Fibre-Reinforced Polymer (FRP) Composites for Structural Applications; J Bai, 2013.

[7] Lau, D.; Qiu, Q.; Zhou, A.; Lun, C. Long term performance and fire safety aspect of FRP composites used in building structures. *Construction and Building Materials* 2016, 126, 573–585.

[8] Tetta, Z.C.; Koutas, L.N.; Bournas, D.A. Textile-reinforced mortar (TRM) versus fiber-reinforced polymers (FRP) in shear strengthening of concrete beams. *Composites Part B* 2015, 77, 338-348.

[9] Raoof, S. M.; Bournas, D.A. Bond between TRM versus FRP composites and concrete at high temperatures. *Composites Part B* 2017, 127, 150-165.

[10] European Commission. *Technology options for earthquake resistant, eco-efficient buildings in Europe: Research needs.* Publications Office of the European Union: Luxembourg: 2014, ISBN 978-92-79-35424-3.

[11] Image available online: https://www.ediltecnico.it/85672/inserimento-di-pareti-strutturali/.

[12] Tsionis, G.; Apostolka, R.; Taucer, F. Seismic strengthening of RC buildings; EUR 26945 EN, Publications Office of the European Union: Luxembourg, 2014.

[13] Ireland, M. G.; Pampanin, S.; Bull, D. K. Experimental investigations of a selective weakening approach for the seismic retrofit of R.C. walls. *New Zealand Society for Earthquake Engineering Conference*, Palmerston North, New Zealand, 2007.

[14] Neri, F.; La Guzza, M.; Russo, A. L'utilizzo di controventi dissipativi per la protezione sismica del plesso scolastico Cappuccini a Ramacca (CT).

[15] Image available online: https://www.airesingegneria.it/it/progetti/adeguamento-sismico-liceo-vito-capialbi/.
[16] Rahimi, A.; Maheri, M. R. The effects of steel X-brace retrofitting of RC frames on the seismic performance of frames and their elements. *Eng. Struct.* 2019, 206.
[17] Mazza, F.; Pucci, D. Static vulnerability of an existing r.c. structure and seismic retrofitting by CFRP and base-isolation: A case study. *Soil. Dyn. Earthq. Eng.* 2016, 84, 1-12.
[18] Trombetta, P. L.; Castellano, M. G.; Cocchio D. Adeguamento Sismico di Edifici mediante Isolamento Sismico (In Italian).
[19] Christopoulos, C.; Filiatrault, A. Principles of Passive Supplemental Damping and Seismic Isolation; IUSS Press: Pavia, Italy, 2006.
[20] Barbagallo F.; Bosco M.; Marino E.M.; Rossi P.P.; Stramondo P.R. A multi-performance design method for seismic upgrading of existing RC frames by BRBs. *Earthquake Engineering and Structural Dynamics* 2017, 46, 1099–1119.
[21] Schiavoni S, D'Alessandro F, Bianchi F, Asdrubali F. Insulation materials for the building sector: a review and comparative analysis renew. *Sustain Energy Rev* 2016; 62:988–1011.
[22] Bournas, D.A. Concurrent seismic and energy retrofitting of RC and masonry building envelopes using inorganic textile-based composites combined with insulation material: A new concept. Compos. Part B 2018, 148, 166-179.
[23] Baljit, S.S.S.; Chan, H.-Y.; Sopian, K. Review of building integrated applications of photovoltaic and solar thermal systems. *J. Clean. Prod.* 2016, 137, 677–689.
[24] D'Agata, G.; Margani, G.; Pettinato, W. Cost evaluation of seismic and energy retrofit for apartment blocks in southern Italy. In *Demolition or Reconstruction? Proceedings of the Colloqui.AT.e* 2017, Ancona, Italy, 28–29.
[25] Takeuchi, T.; Yasuda, K.; Iwata, M. Studies on Integrated Building Facade Engineering with High-Performance Structural Elements. IABSE Symp. Rep. 2006, 92 (4), 33–40.
[26] Takeuchi T.; Yasuda K.; Iwata M. Seismic retrofitting using energy dissipation façades. In Proceedings of ATC-SEI09, San Francisco, USA, 2009.
[27] Passoni C, Marini A, Belleri A, Menna C. A multi-step design framework based on Life Cycle Thinking for the holistic renovation of the existing buildings stock. CESB19 Central Europe towards Sustainable Building 2019, July 2 - 4, 2019, Prague; 2019.
[28] Marini, A.; Passoni, C.; Belleri, A.; Feroldi, F.; Preti, M.; Metelli, G.; Riva, P.; Giuriani, E.; Plizzari, G. Combining seismic retrofit with energy refurbishment for the sustainable renovation of RC buildings: a proof of concept. *Eur. J. Environ. Civ. Eng.* 2017, 21, 1-21.

[29] Passoni, C.; Guob, J.; Christopoulosc, C.; Alessandra Marini, A.; Riva, P. Design of dissipative and elastic high-strength exoskeleton solutions for sustainable seismic upgrades of existing RC buildings. *Engineering Structures* 2020, 221.

[30] D'Urso, S.; Cicero, B. From the Efficiency of Nature to Parametric Design. A Holistic Approach for Sustainable Building Renovation in Seismic Regions. *Sustainability* 2019, *11*, 1227.

[31] ProGETone. https://www.progetone.eu/

[32] Ferrante, A.; Mochi, G.; Predari, G.; Badini, L.; Fotopoulou, A.; Gulli, R.; Semprini, G. A. European Project for Safer and Energy Efficient Buildings: Pro-GET-onE (Proactive Synergy of integrated Efficient Technologies on Buildings' Envelopes). *Sustainability* 2018, 10(3), 812.

[33] Prota A. Interventi integrati leggeri, rapidi e a basso impatto per costruzioni in cemento armato. Webinar ReLUIS: "La ricerca italiana in ingegneria sismica e le attività di ReLUIS a 40 anni dal terremoto lucano-campano", 23 November 2020.

[34] European Commission. Integrated techniques for the seismic strengthening and energy efficiency of existing buildings. Publications Office of the European Union: Luxembourg: 2021, ISBN 78-92-76-30255-1.

[35] Ecosism. Geniale cappotto sismico. Available online: http://www.ecosism.com/moduli/geniale/

[36] Ferrimix. SismaCoat. Available online: https://www.ferrimix.it/ferrimix-sismacoat/

[37] Paver. Cappotto sismico Paver. Available online: https://www.paver.it/blocchi/cappotto-sismico-termico.

[38] Pohoryles, D.A..; Bournas, D.A. iRESIST+ Innovative seismic and energy retrofitting of the existing building stock; EUR 30583 EN, Publications Office of the European Union: Luxembourg, 2018.

[39] da Porto, F.; Donà, M.; Verlato, N.; Guidi, G. Experimental testing and numerical modellingof robust unreinforced and reinforced clay masonry infill walls, with and without openings. *Frontiers in Built Environment*, Vol. 6, 2020, pp. 591985.

[40] Artino, A.; Evola, G.; Margani, G. Seismic and Energy Retrofit of Apartment Buildings through Autoclaved Aerated Concrete (AAC) Blocks Infill Walls. *Sustainability* 2019, *11*, 3939.

[41] World Green Building Council Technical Report Bringing Embodied Carbon Upfront; World Green Building Council: London, UK, 2019.

[42] Brandner, R.; Flatscher, G.; Ringhofer, A.; Schickhofer, G.; Thiel, A. Cross laminated timber (CLT): overview and development. Eur. J. Wood Prod. 2016, 74, 331–351.

[43] EN 338:2016. structural timber - Strength classes.

[44] Presutti, A.; Evangelista, P. Edifici multipiano in legno a pannelli portanti in XLAM. Dario Flaccovio Editore: Palermo, 2014; p. 36.

[45] Ringhofer, A.; Brandner, R.; Blass, H.J. Cross laminated timber (CLT): Design approaches for dowel-type fasteners and connections. *Engineering Structures* 2018, *171*, 849-861.
[46] EN 16351:2015 Timber structures - Cross laminated timber – Requirements.
[47] Jeleč, M.; Varevac, D.; Rajčić, V. Cross-laminated timber (CLT) – a state of the art report. *GRAĐEVINAR, 70* (2018) 2, 75-95.
[48] Brandner, R. Production and Technology of Cross Laminated Timber (CLT): A state-of-the-art Report. In Focus Solid Timber Solutions - European Conference on Cross Laminated Timber (CLT), 2013, University of Bath.
[49] Pei, S.; Van de Lindt, J. W.; Popovski, M.; Berman, J. W.; Dolan, J. D.; Ricles, J.; Sause, R.; Blomgren, H.; Rammer, D.R. Cross-Laminated Timber for Seismic Regions: Progress and Challenges for Research and Implementation. *J. Struct. Eng.*, 2016, 142(4).
[50] Tesfamariam, S.; Stiemer, S.F.; Dickof, C.; Bezabeh, M.A. Seismic vulnerability assessment of hybrid Steel-Timber structure: Steel moment-Resisting frames with clt infill. *J. Earthq. Eng.* 2014, 18, 929–944.
[51] Brock Commons Tallwood House. https://www.thinkwood.com/projects/brock-commons-tallwood-house.
[52] Dalston Lane. https://waughthistleton.com/dalston-works/
[53] https://www.dezeen.com/2020/02/17/cf-moller-architects-tallest-kajstaden-tall-timber-building-sweden/.
[54] Loss, C.; Frangi, A. Experimental investigation on in-plane stiffness and strength of innovative steel-timber hybrid floor diaphragms. *Eng. Struct.* 2017, 138, 229–244.
[55] Lucchini, A.; Mazzucchelli, E. S.; Mangialardo, S.; Persello, M. "Façadism and CLT technology: An innovative system for masonry construction refurbishment" Proceedings of the 40th IAHS World Congress on Housing, Funchal, Portugal, 2014.
[56] Riccadonna, D.; Giongo, I.; Shiro, G.; Rizzi, E.; Parisi, M.A. Experimental shear testing of timber-masonry dry connections for the seismic retrofit of unreinforced masonry shear walls. Constr Build Mater. 2019, 211, 52-72.
[57] Pozza, L.; Evangelista, F.; Scotta, R. CLT used as seismic strengthener for existing masonry walls. Proceedings of the 17th Conference ANIDIS – L'ingegneria sismica in Italia, Pistoia, Italy, 2017.
[58] A. Björnfot, F. Boggian, A. Nygård, R. Tomasi. Strengthening of traditional buildings with slim panels of cross-laminated timber (CLT). 4th international conference on structural health assessment of timber structures (SHATIS'17), Istanbul, 20-22 September, 2017.
[59] I. Sustersic, B. Dujic. Seismic strengthening of existing URM and RC structures using Xlam timber panels. International conference on Earthquake Engineering, Skopie, Macedonia, 2013.

[60] Sustersic, I.; Dujic, B. Seismic shaking table testing of a reinforced concrete frame with masonry infill strengthened with cross laminated timber panels. World Conference on Timber Engineering, Quebec City, Canada, 2014.

[61] Zanni, J.; Cademartori, S.; Marini, A.; Belleri, A.; Giuriani, E.; Riva, P.; Angi, B.; Franchini, G.; Marchetti, A.L.; Odorizzi, P.; G. Luitprandi, G. Riqualificazione integrata e sostenibile di edifici esistenti con esoscheletri a guscio prefabbricati: il caso studio AdESA. Convegno Ar.Tec. - Colloqui.AT.e 2020, Catania, Italia.

[62] AdESA system. https://www.sistemaadesa.it/

[63] Marini A. Life cyycle thinking e indici prestazionali integrati per la concezione e valutazione degli interventi. Webinar ReLUIS: Interventi integrati, rapidi e a basso impatto per la riduzione della vulnerabilità sismica e dei consumi. 25-06-2020. Available online: http://www.reluis.it/index.php?option=com_content&view=article&id=686&Itemid=205&lang=it

[64] Rhinoceros-wood. https://www.woodbeton.it/sistemi/rhinoceros-wall/

[65] Haba, R.; Kitamori, A.; Mori, A.; Fukuhara, T.; Kurihara, T.; Isoda, H. Development of clt panels bond-in method for seismic retrofitting of RC frame structure. J. Struct. Constr. Eng. 81, 1299–1308, 2016 (In Japanese).

[66] Haba, R.; Kitamori, A.; Mori, T.; Isoda H. Development of clt panels bond-in method for seismic retrofitting of RC frame structure. Kyoto University Research Information Repository. Available online: https://repository.kulib.kyoto-u.ac.jp/dspace/handle/2433/225876.

[67] F. Stazi, M. Serpilli, G. Maracchini, A. Pavone. An experimental and numerical study on CLT panels used as infill shear walls for RC buildings retrofit. Constr. Build. Mater. 211, 605-616, 2019.

[68] A. Sandoli, M. Pinto, S. Pampanin, B. Calderoni. Protezione sismica di edifici esistenti in c.a. mediante l'utilizzo di pareti lignee post-tese. Proceedings of 17th Conference ANIDIS – L'ingegneria sismica in Italia, Pistoia, Italy, 2017 (In Italian)

3

Research goals and methodology

3.1 Research aim

According to the remarks resulting from the state-of-the-art review on the topic of retrofitting of RC framed buildings through CLT-based solutions, this work aims at investigating the potential of an integrated CLT-shell retrofit technology equipped with innovative dissipative systems (Figure 3.1). Specifically, the proposed retrofit solution provides to apply structural CLT-based panels (called e-CLT) to the existing outer walls, by connecting them to the RC frame by means of novel friction dampers able to meet the needs of structural, technological, and industrial efficiency. The system is conceived so that in occurrence of moderate ground motions the CLT panels increase the seismic capacity of the existing structure, while in occurrence of stronger ground motions dampers dissipate part of the input seismic energy, thus reducing the seismic demand of the structure.

The concept idea is also to combine the e-CLTs with non-structural panels (called e-PANEL) to be applied on the outer windowed walls and equipped with new high-performing windows that replace the existing ones. Since the e-PANELs have no structural role, they are conceived with a lightweight wooden frame to ensure easier manufacture, low environmental impact, and cost savings.

The overall system is conceived to be totally prefabricated and installed with dry technologies to reduce implementation costs and time. Therefore, both e-CLTs and e-PANELs integrate insulation materials, waterproof breather membranes and the desired finishing layer (e.g. wood, plaster, ceramic, stone, porcelain stoneware, glass, PV modules, etc.). The new prefabricated shell is intended to act as an energy-efficient and seismic-resistant skin for the existing building, contributing also to renovate its architectural image.

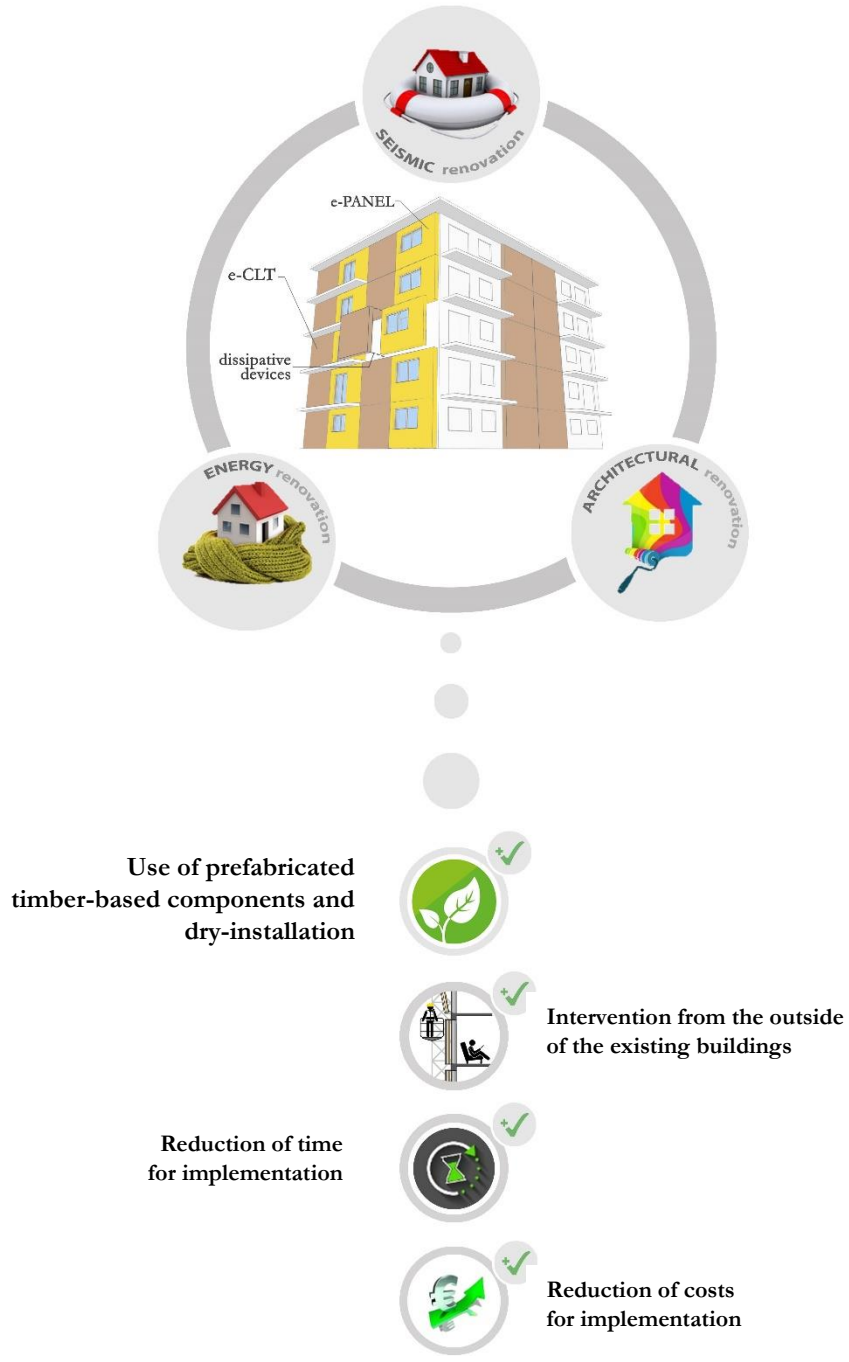

Figure 3.1 Concept of the proposed integrated retrofit solution

3.2 Research objectives and methods

Figure 3.2 reports the objectives defined to attain the stated research aim.

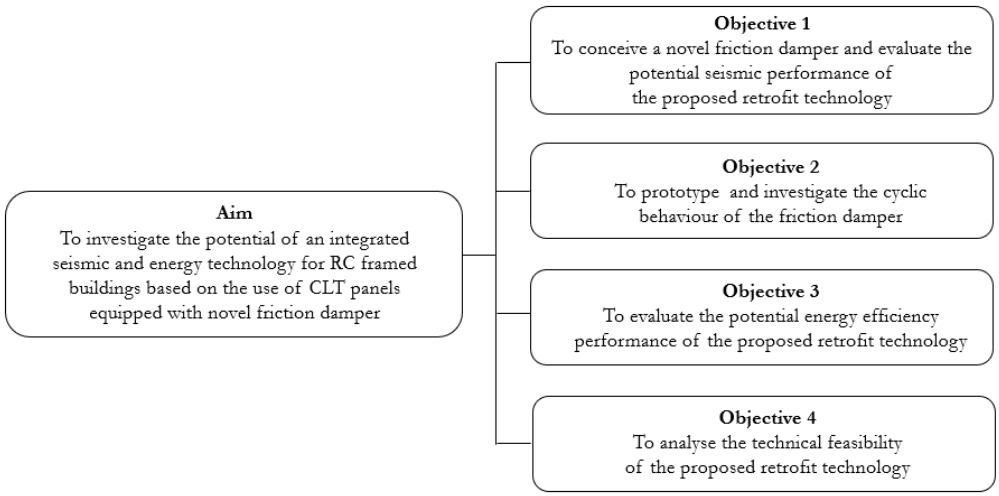

Figure 3.2 Research aim and objectives

The proposed CLT-shell retrofit technology has been investigated in terms of seismic performance, energy efficiency, and technical feasibility.
The research methodology was based on the parallel investigation of seismic and technological aspects, considering the synergistic correlation between the scientific areas involved as the main point of the actual success of the retrofit intervention.
Specifically, the main research objective concerned the conception of a novel friction damper able to connect the CLT-based panels to the existing building envelope. The damper has been developed with the support of an academic partner, the Norwegian University of Life Sciences (NMBU), and an industrial partner, the Italian company Adveco Srl. NMBU is specialized in wooden constructions, while Adveco is specialized in the production of hardware for wooden structures.
The potential impact of the e-CLT system (CLT panels equipped with the proposed dampers) on the response of existing RC framed structures has been preliminarily verified. To this purpose, numerical models of RC frames designed considering gravity loads only and equipped with the e-CLT system have been implemented in OpenSEEs environment. Then, the nonlinear responses of the investigated systems

at pre- and post-intervention state have been assessed by monotonic and cyclic pushover analyses and the impact of the intervention has been investigated in terms of stiffness, strength, and energy dissipation capacity improvement.
After that the potential of the proposed seismic retrofit system was demonstrated, four damper configurations have been prototyped at Adveco to verify their technical and economic feasibility. Cyclic loading tests have been designed and performed on each damper prototype at the NMBU laboratories to investigate their cyclic response, highlight limits and advantages of each configuration, and identify the optimal one.
The CLT-shell retrofit technology has been analysed also in terms of energy efficiency and technical feasibility. Specifically, dynamic thermal simulations have been carried out on typical multi-storey residential apartment buildings through EnergyPlus, both pre- and post-intervention. These simulations allowed evaluating the impact of the proposed retrofit solution in terms of reduction of the seasonal energy demand.
Moreover, a construction analysis of the proposed retrofit technology has been conducted, both at system and component level, to investigate its technical feasibility, versatility, and main technical requirements.

4

Concept of the friction damper and analysis of the proposed seismic retrofit technology

Summary

This chapter describes the novel friction damper conceived to connect the structural CLT panels to the existing building envelope. Then, the potential impact of the proposed seismic retrofit solution (e-CLT system) on existing RC framed structures is investigated in terms of stiffness, strength, and energy dissipation capacity improvement. To this purpose, a case study RC frame was designed according to old building regulations and a set of single-storey frames with and without the application of the e-CLT system was simulated, considering a different number of CLT panels and friction dampers, and the presence of infill walls with different mechanical properties. Hence, numerical models of the investigated frames at pre- and post-intervention state were implemented in OpenSees environment. Their nonlinear response was assessed and compared by monotonic and cyclic pushover analyses.

4.1 Damper concept

The first research stage involved the design of a new dissipative connection device to attach the e-CLT panels of the investigated retrofit solution to the outer envelope of the existing RC framed building.

The idea was to concentrate the non-linear behaviour of the proposed seismic upgrading solution at the connection devices only, thereby protecting the CLT panels from damage. Furthermore, the device is conceived to ensure the durability of its structural efficiency even after seismic events. This feature avoids the need of its removal and replacement, which in turn would involve the removal of the attached e-CLT panel too.

The requirements of easy and quick manufacture, installation and maintenance have been also considered to conceive the damper. On the one hand, the easy damper manufacturing results in lower work time and workforce for the industry companies, thus reducing costs and increasing the potential commercial success of the damper. On the other hand, the easy and fast installation reduces the time and costs for the implementation of the retrofit intervention, making it more widely applicable. The damper easy maintenance also provides for its longer service life.

To meet the need of structural efficiency even after seismic events, the research activity has been oriented toward the design of a device that dissipates seismic energy by friction.

Friction dampers (also known as slip-friction connectors or slotted-bolt connectors) have been originally investigated to dissipate energy in steel moment resisting frames [1-2]. These devices mainly consist of steel plates clamped together by means of preloaded bolts (Figure 4.1). The presence of slotted holes in one plate allows it to slide over the other plate under a specified force, i.e. the design slip force, thus enabling the dissipation of seismic energy by means of the friction exerted in the contact surfaces. The slip force is a function of preload force of the bolts and friction coefficient of the contact surfaces. Shim materials can be also inserted between the steel plates to reduce wear and tear, which in turn enhance the stability of the hysteretic loops of the damper [3-4].

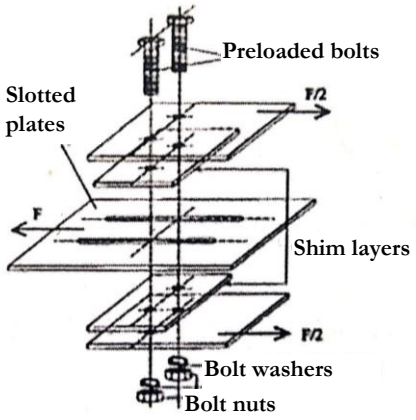

Figure 4.1. Components of friction dampers

The typical behaviour of friction dampers is elastic-perfectly plastic. The elastic branch occurs when the applied force is lower than the activation slip force and its slope is equal to the lateral stiffness of the device. The plastic branch occurs when the slip force is attained, and the sliding takes place. The maximum relative displacement between the steel plates is equal to the length of the slotted holes.
The sliding mechanism of friction dampers can be either symmetric or asymmetric [5-8] (Figure 4.2).

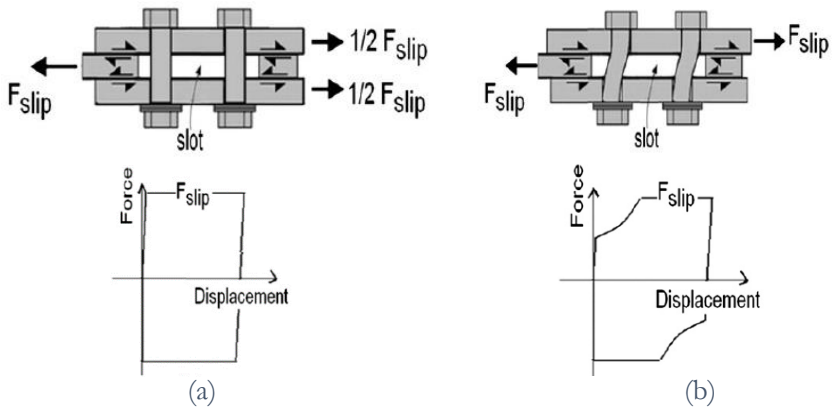

Figure 4.2. Types of friction dampers configurations and their typical hysteretic behaviour: (a) symmetric configuration; (b) asymmetric configuration [7].

Friction dampers in symmetric configuration present a slotted centre-plate where the slip force F_{slip} is applied, and two external plates that resist half of the applied force F_{slip} (Figure 4.2a) [7]. Instead, in asymmetric friction damper, loads are applied to the slotted centre-plate and only to a single external plate, providing asymmetric loading condition (Figure 4.2b). During sliding, the external plate that is not directly loaded is dragged along by the bolts, resulting in slight instability in the damper hysteretic loop [7-8].

Overall, friction dampers have been proven to have one of the most efficient and damage-free energy dissipation mechanism, without degradation of resistance and energy dissipation capacity over time. For this reason, in last decades, interest of the scientific community on the use of friction dampers in earthquake resistant structures, including timber-based structures, has gradually increased. Filiatrault [9] firstly investigated the use of friction dampers for timber sheathed shear walls. Loo et al. [10-11] and Hashemi et al. [12] analysed the application of slip friction connections in replacement of traditional hold-downs at the two base corners of rocking laminated veneer lumber (LVL) and coupled CLT walls, respectively. These devices showed remarkable seismic performance in terms of both hysteretic behaviour stability and reduction of damage in timber panels, compared to traditional systems where energy dissipation is provided by yielding of fasteners (nails and screws) and crushing of wood fibres [13-14]. The resilient slip friction (RSF) joints were the advancement of the above-mentioned slip-friction hold-downs since they have been investigated to provide them with an additional self-centering mechanism [15]. Recent studies investigate innovative friction dampers used in the form of frame-to-wall connectors in timber-steel hybrid structure [16-17]. These studies have demonstrated the high potential of such devices in mitigation of earthquake-induced damage in the structure.

Considering the benefits of friction energy dissipation on the overall performance of the structure, the dissipative device investigated in the framework of this thesis has been conceived as a friction damper having a geometry optimized to meet also the needs of industrial and technological efficiency (Figure 4.3).

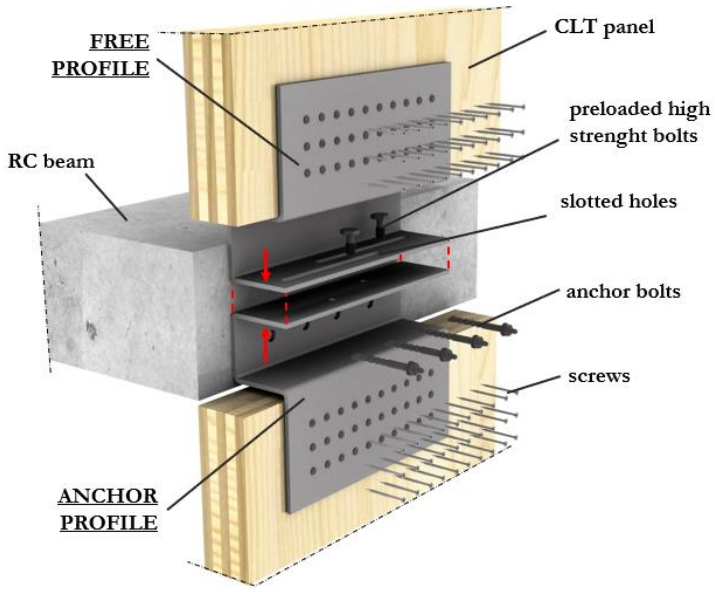

Figure 4.3. Proposed friction damper

The damper consists of two cold bent steel profiles that connect the CLT panels of two consecutive storeys with the existing interposed RC beam. One profile, called "anchor profile", is connected to the RC beam by anchor bolts. The other profile, called "free profile", is provided with slotted holes and is connected to the "anchor profile" by preloaded high strength bolts. Common timber screws connect the two steel profiles to the CLT panels. The shear force is transmitted between the two profiles by means of the friction exerted in the contact surface. During an earthquake, when the force transmitted by the damper attains the value of the friction force, the "free profile" slides on the "anchor" one thanks to the slotted holes, thus dissipating seismic energy (Figure 4.4). The activation of the sliding movement between the two profiles by a predefined force allows to control the internal forces on both the damper components (steel profiles and fasteners) and CLT panels, thus properly dimensioning them and limiting or avoiding damage of these elements and the need of their replacement after the seismic event. Furthermore, the length of the slotted holes should be designed in accordance with the maximum allowable lateral drift of the building to be renovated, in order to avoid the shear failure of the preloaded bolts before that the RC structure could exploit its maximum drift capacity.

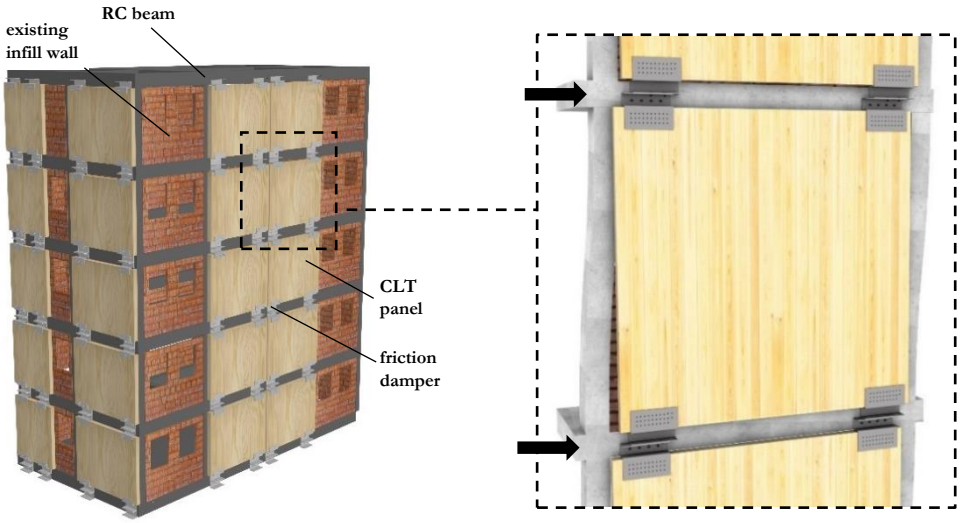

Figure 4.4. Behaviour of the proposed friction damper under seismic loads

The detailed explanation of the potential advantages of the proposed damper in terms of industrial and technological efficiency are reported in the following Sections.

4.1.1 Industrial issue: manufacturing process

On an industrial scale, the innovative design of the proposed friction damper enables an easy and efficient manufacturing process, since the "anchor" and "free profiles" have the same development in size and are produced by cutting, drilling, press bending and welding of steel sheets. These manufacturing are ordinary and commonly performed in factories specialized in the production of construction metal works. Press bending is the main process involved. Specifically, three press-bending operations are required to realize the damper profiles (Figure 4.5). The ease and speed of these operations depend mainly to the overall size of the damper. Press bending plays a key role in mechanical processing, since it enables to give form to steel sheets by means of advanced machines that allow much freedom to the bender workers. The process consists in plastically deforming steel sheets along a single axis, thus involving few fibres of the material, with consequent high internal stresses. The ability of the bender worker is thus to tame steel material and its variability factors (e.g. cladding, lamination direction, external temperature, thickness tolerance etc.)

by means of technique and experience, transforming an industrial process into a real art [18].

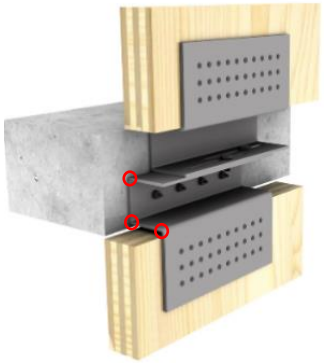

Figure 4.5. Press-bending operations required to realize the proposed friction damper

Hydraulic press brakes are commonly used for bending processes. The base tools consist in a press ram equipped with a *punch* and a *die* having V-groove that is installed on the workbench of the machine (Figure 4.6a). The steel sheet is put between the punch and the die. In this way, when the machine is activated, the ram moves down and the punch pushes the workpiece into the die cavity, applies a force higher than the yield force of the steel sheet, and thus forces it to bend (Figure 4.6b).

(a) (b)

Figure 4.6. (a) Base tools of a press brake and (b) press brake in action

The three main press bending methods are reported in Figure 4.7 and following described:

- **Air bending:** In this method, the workpiece is not forced completely into the die but touches only the two edges of the die and the tip of the punch throughout the entire bending process. When the press force is released, the workpiece "springs back" to form the final angle. The V-groove of the die is approximately between 78 and 30 degrees. It is the most common bending method since it allows the use of lower press forces than other methods. Conversely, the springback effect is higher, resulting in the need of repeating the bending process.
- **Bottom bending:** Compared to air bending method, dies having V-groove between 88 and 85 degrees are generally used, that allow the material springback, but forcing it up to the maximum limit allowed by the die V-opening. The result is a higher stability in the bending process.
- **Coining:** In this method, the workpiece is conformed to the exact angle of the punch and die, avoiding the springback effect. Accordingly, the use of die with V-opening of 90 degrees is required for squared folds. Compared to the other methods, higher press forces are required (about 4.5 times higher than that used for common air bending). Steel sheets having fine thicknesses can be effectively bent through this method [18].

Figure 4.7. Press bending methods

4.1.2 Technological issue: installation process

The proposed friction damper allows fast and easy installation of the e-CLT system. In particular, the "anchor profiles" of each damper can be pre-assembled on the top of CLT panels off-site (Figure 4.8a). In this way, the e-CLT installation involves: (1) to lift and place the panel next to the existing outer wall, by means of a mobile lifting equipment and (2) to connect the panel to the existing RC beams through anchors dowels, which are inserted into the holes of the "anchor profiles". Then, the "free profiles" of the same dampers are installed on-site, in order to properly align and connect the friction surfaces of the two steel profiles.
The same installation of the e-CLT system can be applied also if the building has balconies (Figure 4.8b), thus making the system more adaptable. In this case, friction dampers are located at the lower edge of the CLT panels and the "anchor profiles" of each damper are thus fixed to the existing RC beam or directly to the balcony RC slab.

Figure 4.8. Installation of the e-CLT panels equipped with proposed friction dampers in (a) no-balcony façade and (b) balcony façade.
(e-CLTs and e-PANELs are reported without insulation and cladding layers).

Furthermore, it is also possible to allow dampers inspection and maintenance (e.g. to preload friction bolts that may have loosened after a seismic event) by adopting proper cladding solutions to cover the dampers after the installation of the panels. Even the swift removal and replacement of the dampers is possible, since the "anchor" and "free profiles" are connected to the external side of CLT panels.

4.2 Impact of retrofit of RC frames by CLT panels and friction dampers

The impact of the e-CLT system (CLT panels equipped with the proposed friction dampers) on the seismic response of RC framed structures has been evaluated through numerical analyses on a case study frame, assuming a rigid-plastic cyclic behaviour of the proposed friction dampers. Different features of the case study (with and without infill walls) and importance levels of the retrofit solution were considered.

The following Sections describe the case study, the examined e-CLT configurations and the numerical models which have been implemented. Hence, the results of the numerical analyses are reported and discussed.

4.2.1 Description of the case study

The case study is a one-storey, three-bay RC frame having net height and net width of 3.2 m and 11.1 m, respectively (Figure 4.9a). It represents the first storey of a 4-storey frame. The columns have cross-section of 30x30 cm and are reinforced by four rebars with diameter of 14 mm. The beams have cross-section of 30x50 cm and are reinforced by nine rebars with the 14 mm diameter arranged as shown in Figure 4.9b.

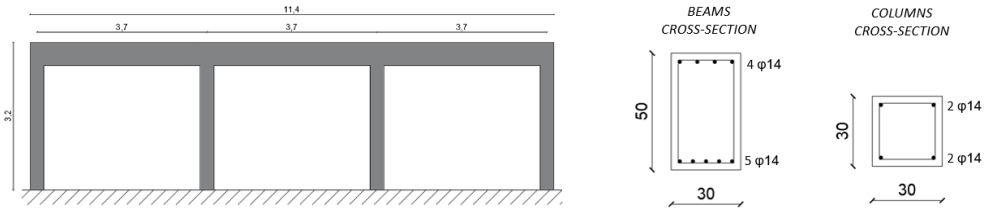

(a) (b)

Figure 4.9. (a) Case study frame and (b) cross-sections of RC members

Both columns and beams have been designed according to the regulations in force in Italy during the 1970s [19-20], as well as the construction practices of that period. In particular, the cross-sections size and the steel reinforcements area of the frame

members have been designed by means of the allowable stress method [20], considering gravity loads only.
Columns have been designed to resist only axial force and to work at 70% of the allowable stress of concrete $\overline{\sigma}_c$. Hence, the minimum required cross-section area of the column $A_{c,req}$ has been calculated by the following relation:

$$A_{c,req} = \frac{N}{0.7\,\overline{\sigma}_c}$$

where N is the design axial force, which has been evaluated considering a tributary area of 3.7x3.54 m^2 (length of the beam span x width of the slab sustained by the beam) and 4 storeys in elevation. The rebars area A_s in the columns is not smaller than the minimum value $A_{s,min}$:

$$A_{s,min} = \max\left(0.003A_c; 0.006\,A_{c,req}\right)$$

As regard beams, the cross-section size 30x50 cm is consistent with the construction practice of the 1970s and the rebars area A_s has been calculated as:

$$A_s = \frac{M}{0.9\,d\,\overline{\sigma}_s}$$

where $\overline{\sigma}_s$ is the allowable stress of steel and M is the bending moment from the design loads.
Steel grade Feb38K with a characteristic yield stress f_{yk}=375 MPa has been assumed for rebars, while the characteristic compressive cubic strength R_{ck} of concrete has been assumed equal to 20 MPa (corresponding to cylinder strength f_{ck} equal to 17 MPa). The values of the allowable stresses are 7.4 MPa and 215 MPa for concrete and steel, respectively.
The case study frame has been analysed considering both the bare and the infilled configuration. Specifically, the infill wall has been assumed made of two leaves of hollow clay bricks (8-cm and 12-cm thick, internally and externally, respectively) with an intermediate air cavity. This infill type is consistent with the construction techniques used in Southern Italy between the 1950s and the 1980s. The presence

of window openings has been also considered, both in the two lateral bays of the frame and in the central one (Figure 4.10).

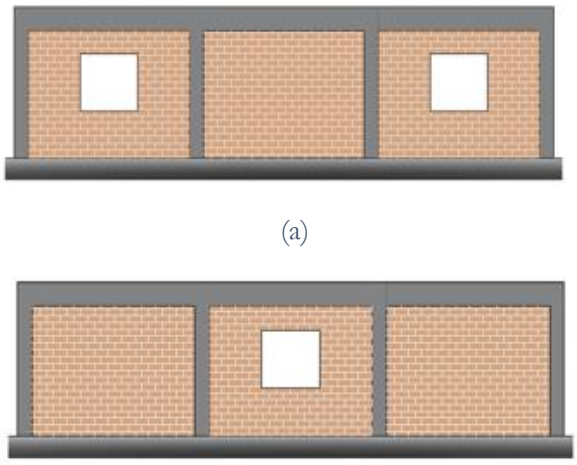

(a)

(b)

Figure 4.10. Infilled configurations of the case study having window openings (a) on the two lateral bays of the frame and (b) on the central one.

4.2.2 Retrofit configurations under investigation

The impact of the e-CLT system on the seismic response of both bare and infilled case study frame has been investigated considering two different configurations of the seismic retrofit system (configurations 1 and 2 in Figures 4.11 and 4.12). Specifically, in configuration 1 (Figure 4.11) a single CLT panel equipped with two friction dampers is applied to the central bay of the frame, while in configuration 2 (Figure 4.12) the RC frame is retrofitted by two CLT panels that are applied to the lateral bays of the frame by using a total of four friction dampers (two damper per CLT panel). The dampers connect the bottom of each CLT panel to the foundation of the RC frame, while CLT panels are connected to the RC beam by means of two "anchor profiles" arranged on their top.

In both the investigated configurations, 3-ply CLT panels having a total thickness of 10 cm (layers thickness: 30-40-30 mm) and made of C24-class spruce boards have been assumed. In Table 4.1 the mechanical characteristics of C24-class spruce wood are reported.

CONFIGURATION 1

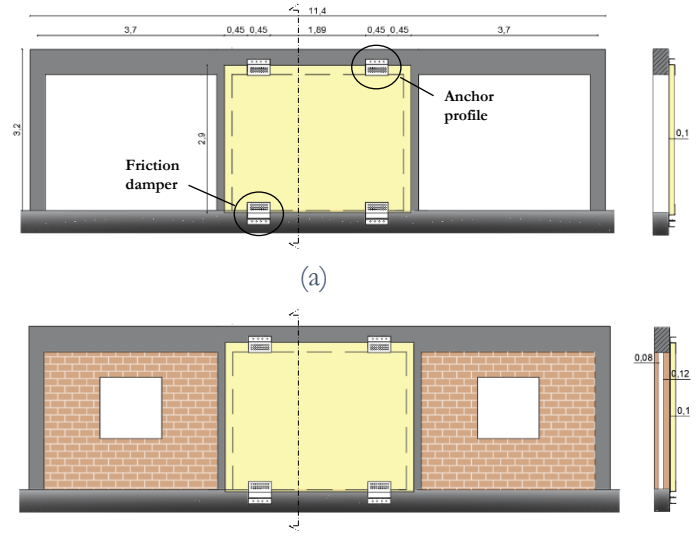

Figure 4.11. (a) Bare and (c) infilled frame with e-CLT in configuration 1.

CONFIGURATION 2

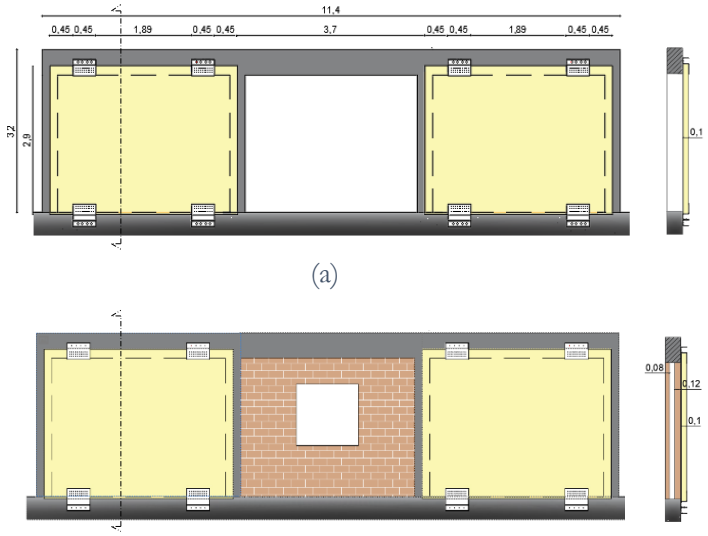

Figure 4.12. (a) Bare and (c) infilled frame with e-CLT in configuration 2.

The friction dampers are 450-mm wide and 8-mm thick. This size has been evaluated as the maximum to ease the processes of drilling and press bending the steel sheets, as well as to control the damper weight in view of a good handing during both manufacturing and installation process. The dampers are arranged symmetrically to each other, at a distance of 0.45 m from the side edge of the panel. The CLT-connections consist of 30 screws having diameter of 8 mm, which have been designed in accordance with Eurocode 5 [22], producers' technical approval [23] and relative literature [24], by assuming to arrange them on three rows of 10 screws each. A slip force of 30 kN for the friction damper has been assumed to design the screw connections.

$E_{0,m}$ [MPa]	$E_{90,m}$ [MPa]	G_m [MPa]	$f_{m,k}$ [MPa]	$f_{t,0,k}$ [MPa]	$f_{t,90,k}$ [MPa]	$f_{c,0,k}$ [MPa]	$f_{c,90,k}$ [MPa]	$f_{v,k}$ [MPa]	ϱ_m [kg/m^3]
11,000	370	690	24	14.50	0.40	21	2.50	4	420

Table 4.1. Mechanical characteristics of C24-class spruce wood according to EN 338 [21]. $E_{0,m}$ and $E_{90,m}$: mean values of the parallel-to-grain and perpendicular-to-grain moduli of elasticity; G_m: mean shear modulus; $f_{m,k}$: characteristic bending strength; $f_{t,0,k}$ and $f_{t,90,k}$: characteristic values of the parallel-to-grain and perpendicular-to-grain tensile strength; $f_{c,0,k}$ and $f_{c,90,k}$: characteristic values of the parallel-to-grain and perpendicular-to-grain compressive strength; $f_{v,k}$: characteristic shear strength; ϱ_m mean density.

4.2.3 Numerical modelling in OpenSees environment

A numerical model has been implemented trough the framework OpenSees (Open System for Earthquake Engineering Simulation) [25] to analyse the nonlinear response of the investigated RC frame at pre- and post-intervention state, considering the configurations described in Section 4.2.2.

The global reference system of the numerical model consists of a cartesian triad having positive axes X, Y and Z in the directions shown in Figure 4.13. A local reference system has been also used for the individual structural member, where: (i) the x-axis is that connecting the two nodes of the member; (ii) the y-axis is parallel and concordant to the global X-axis for the column-elements, while is parallel and opposite to the global Z-axis in case of beam-elements; (iii) the z-axis is orthogonal

to the plane xy and is oriented according to the right-hand rule. Instead, the local reference system for the cross section of CLT panels and the other components of the numerical model has been set equal to the global one.
The columns are restrained at the base (Figure 4.13). All the other elements are constrained to move along both the global Z-axis and to rotate around the global X and Y-axes.
Figure 4.14 shows the numerical model scheme, referring to a single infilled bay of the case study frame, equipped with CLT panel and friction dampers. The detailed description of the parts of the numerical model (RC frame, CLT panel, friction damper and infill) is reported in the following Sections.

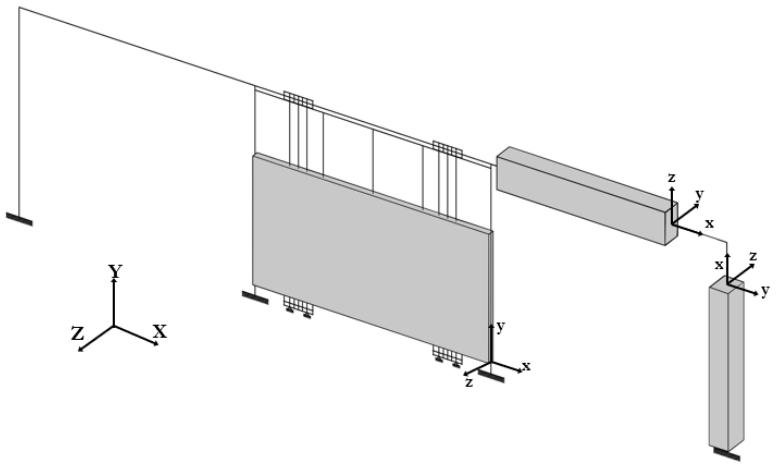

Figure 4.13. Reference systems for the numerical model in OpenSees environment.

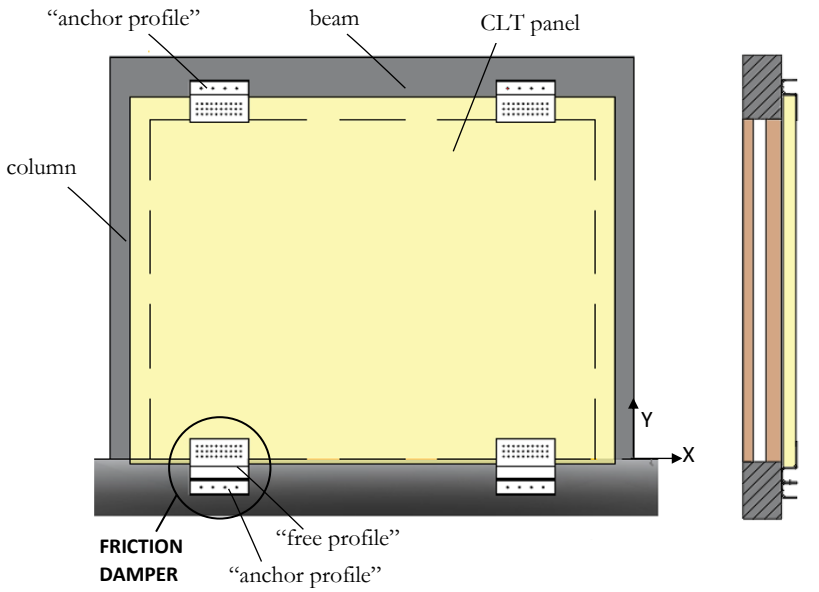

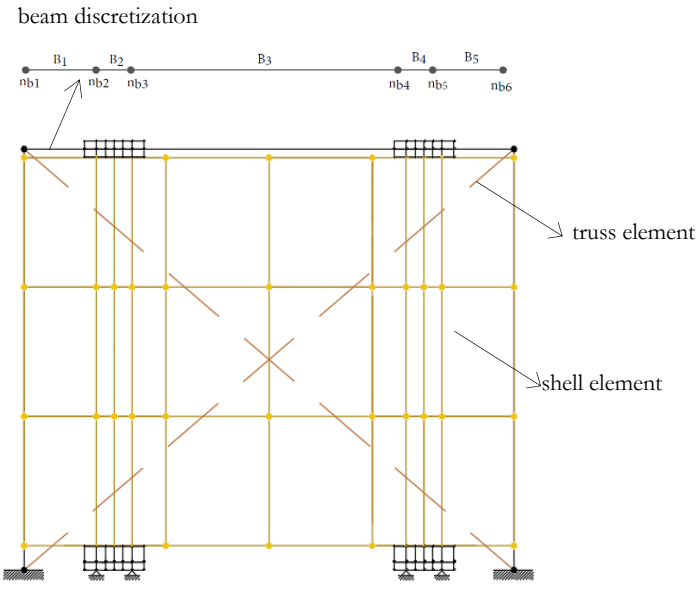

Figure 4.14. Numerical model scheme, referring to a single infilled bay of the case study frame at post-intervention state.

4.2.3.1 RC frame

Beams and columns of the RC frame have been modelled differently. Specifically, columns have been modelled by using the OpenSees feature "beamWithHinges Element". This element consists in a member with a linear-elastic region in the middle and plastic hinges at its ends (Figure 4.15a). The length of the plastic hinges has been set equal to the depth of the column cross section, while the linear-elastic portion has been modelled by assigning the Young's Modulus and the shear modulus of the concrete, the area of the element cross-section and the moment of inertia about the local Z-axis and Y-axis as well as the torsional moment of inertia.
The beams where the CLT panels are fixed at post-intervention state have been discretized in five elements (elements B_1-B_5 in Figure 4.14). The intent was to locate along each beam four intermediate nodes (nodes n_{b2}, n_{b3}, n_{b4} and n_{b5} in Figure 4.14) to connect the beam and the two "anchor profiles". Specifically:

- the two lateral beam portions (elements B_1 and B_5) and the central one (element B_3) have been modelled by nonlinear force-based beam-column elements able to replicate the spread of plasticity along the member (Figure 4.15b) by means of the numerical integration option based on Gauss-Lobatto quadrature rule [26]. In particular, three and five Gauss integration points have been assigned to the lateral and central portions of the beam, respectively;
- the beam portions B_2 and B_4 have been modelled as linear-elastic members, assuming that plastic hinges form outside of the damper length. The OpenSees feature "elasticBeamColumn Element" has been used to model them, which requires the same input parameters mentioned above for the linear-elastic portion of the "beamWithHinges Element".

Finally, the beams belonging to the spans without CLT panels have been modelled by nonlinear force-based beam-column elements having plasticity distributed along the members, by assigning five Gauss integration points to each one.
A fibre cross section has been assigned to each plastic zones of nonlinear RC members, considering both the concrete part and steel rebars, as shown in Figure 4.15c. The concrete part is dived into fibres having constant 5-mm depth and width equal to that of cross section. Instead, single fibres enclosed in the cross section are used to model the steel rebars.

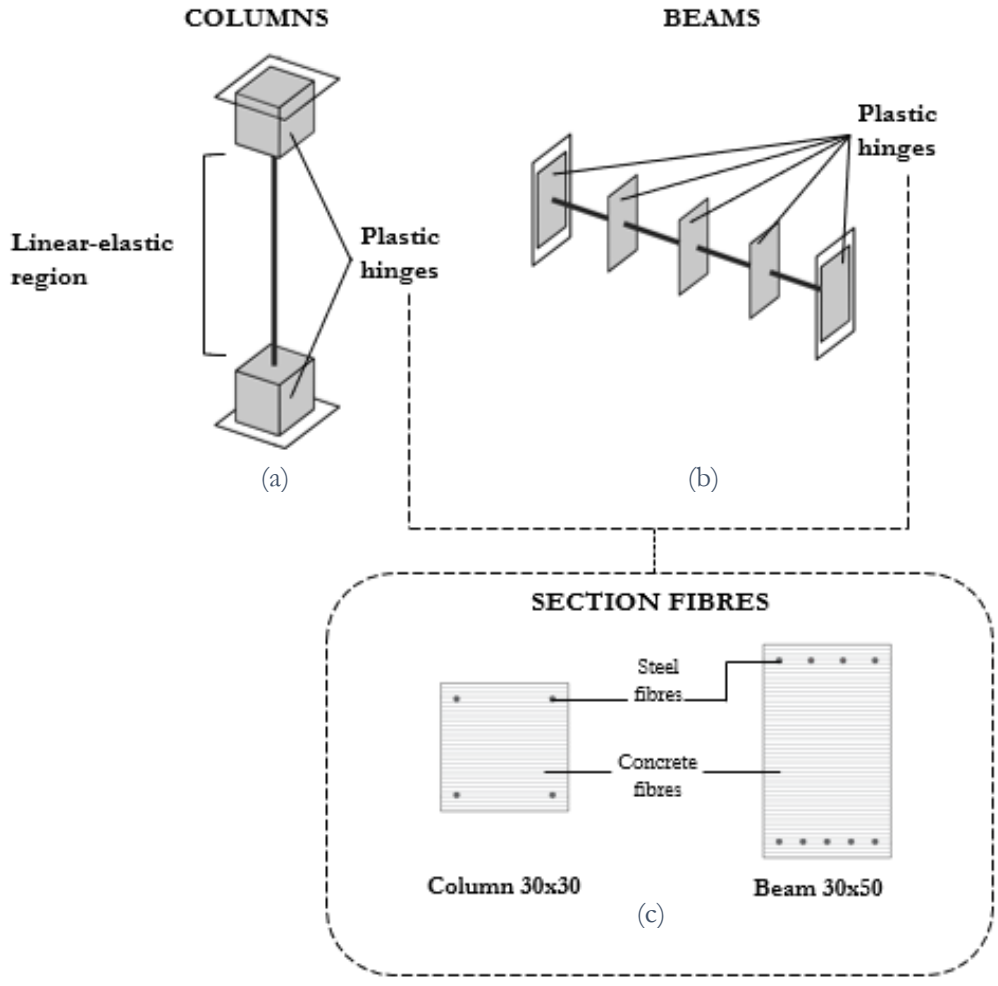

Figure 4.15. Schema of the elements used to model the inelastic response of (a) columns and (b) beams (elements B_1, B_3, B_5 in Figure 4.14)**;** (c) fibre modelling of the cross-section of each plastic zone.

The "Concrete 04" uniaxial material has been assigned to the concrete fibres. This material is based on the Mander constitutive law (Figure 4.16) and the following mechanical parameters have been set to define it:

f_c Compressive strength.
It has been assumed equal to the average value f_{cm} = 25 MPa.
No difference between the core and the cover of the members cross section has been made, neglecting the confinement effect of the stirrups to simulate their scarcity in the structural members.

ε_c, ε_{cu} Strain at maximum strength and at crashing strength, respectively.
These values have been assuming equal to $2x10^{-3}$ and $3.5x10^{-3}$, respectively. No difference between the core and the cover of the members cross section has been made.

E_c Young's modulus.
It has been assumed equal to 31,500 MPa.

f_t, ε_t Maximum tensile strength and ultimate tensile strain, respectively.
Tensile strength of concrete has been neglected and these values have been assumed equal to zero.

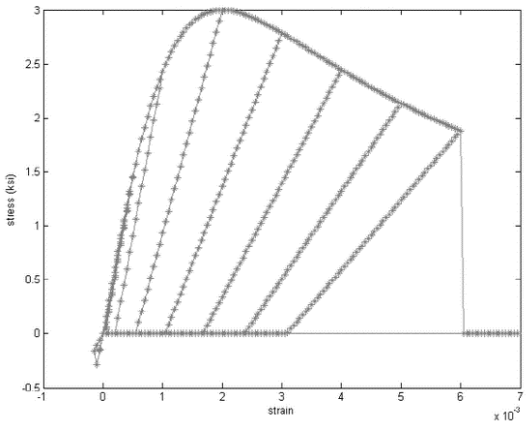

Figure 4.16. Cyclic tension compression response envelope of the OpenSees feature "Concrete04 Material"[25].

An elastic-plastic material with isotropic strain hardening, "Steel 02" uniaxial material (Figure 4.17) has been assigned to steel rebars. The following mechanical parameters have been set to define the material:

f_y Yielding strength
It has been assumed equal to the average value f_{ym} = 380 MPa.

E_s Young's modulus.
It has been set equal to E_s = 200,000 MPa.

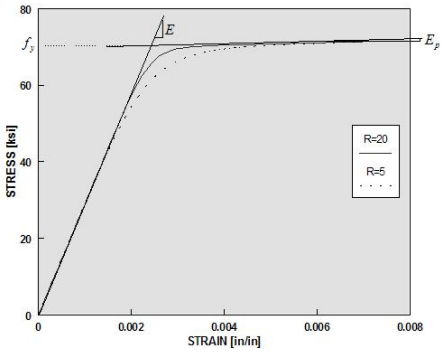

Figure 4.17. Monotonic envelope of the OpenSees feature "Steel02 Material"[25].

The mechanical parameters of RC frame members are summarized in Table 4.2.

Concrete		
Compressive strength	f_c =	25 MPa
Strain at maximum strength	ε_c =	0.002
Strain at crashing strength	ε_{cu} =	0.0035
Young's modulus	E_c =	31,500 MPa
Rebars		
Yielding strength	f_{ym} =	380 MPa
Young's modulus	E_s =	200,000 MPa

Table 4.2. Material properties of RC frame members

4.2.3.2 CLT panel

The mechanical behaviour of CLT differs from usual timber products due to the crosswise build-up. The strength and stiffness values of solid wood panels with cross layers depend on the loading direction regarding both the panel plane (in plane or out of plane), as well as the direction of the grain of the outer layers.
At present, CLT is not provided in current structural Eurocodes and its mechanical properties are inconsistently regulated in technical approvals [27].
The method proposed by Blass and Fellmoser [28] has been adopted in the present investigation to define the mechanical properties of CLT. This method is widely adopted for the needs of seismic modelling, when building nonlinear behaviour is mostly localized in connections [29-33]. It is based on the reduction of a multi-layer material into a single-layer orthotropic one by means of reduction coefficients (named composition factors) that modify the stiffness and strength values assuming a plane stress state of the timber panel. By definition, the composition factor is the ratio between the strength or stiffness value of the selected CLT cross section and the strength or stiffness values of a fictitious homogeneous cross section having the grain direction of all the layers parallel to the direction of the stress. The effective values of strength and stiffness for solid wood panels with cross layers and the composition factors k_i for different types of stress are reported in Tables 4.3 and 4.4, respectively.

Loading	To the grain of outer skins	Effective strength value	Effective stiffness value
Perpendicular to the plane loading			
Bending	Parallel	$f_{m,0,ef} = f_{m,0} \cdot k_1$	$E_{m,0,ef} = E_0 \cdot k_1$
	Perpendicular	$f_{m,90,ef} = f_{m,0} \cdot k_2 \cdot a_m / a_{m-2}$	$E_{m,90,ef} = E_0 \cdot k_2$
In-plane loading			
Bending	Parallel	$f_{m,0,ef} = f_{m,0} \cdot k_3$	$E_{m,0,ef} = E_0 \cdot k_3$
	Perpendicular	$f_{m,90,ef} = f_{m,0} \cdot k_4$	$E_{m,90,ef} = E_0 \cdot k_4$
Tension	Parallel	$f_{t,0,ef} = f_{t,0} \cdot k_3$	$E_{t,0,ef} = E_0 \cdot k_3$
	Perpendicular	$f_{t,90,ef} = f_{t,0} \cdot k_4$	$E_{t,90,ef} = E_0 \cdot k_4$
Compression	Parallel	$f_{c,0,ef} = f_{c,0} \cdot k_3$	$E_{c,0,ef} = E_0 \cdot k_3$
	Perpendicular	$f_{c,90,ef} = f_{c,0} \cdot k_4$	$E_{c,90,ef} = E_0 \cdot k_4$

Table 4.3. Effective values of strength and stiffness for solid wood panels with cross layers [28].

	k_i
	$k_1 = 1 - \left(1 - \frac{E_{90}}{E_0}\right) \cdot \frac{a_{m-2}^3 - a_{m-4}^3 + \ldots \pm a_1^3}{a_m^3}$
	$k_2 = \frac{E_{90}}{E_0} + \left(1 - \frac{E_{90}}{E_0}\right) \cdot \frac{a_{m-2}^3 - a_{m-4}^3 + \ldots \pm a_1^3}{a_m^3}$
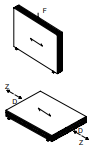	$k_3 = 1 - \left(1 - \frac{E_{90}}{E_0}\right) \cdot \frac{a_{m-2} - a_{m-4} + \ldots \pm a_1}{a_m}$
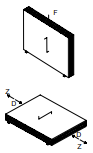	$k_4 = \frac{E_{90}}{E_0} + \left(1 - \frac{E_{90}}{E_0}\right) \cdot \frac{a_{m-2} - a_{m-4} + \ldots \pm a_1}{a_m}$

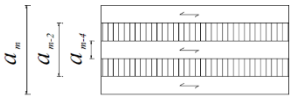

Table 4.4. Composition factors k_i for solid wood panels with cross layers [28].

According to the above assumption, the 3-ply CLT panel has been modelled as an assembly of elastic and homogenized-orthotropic four-nodes shell elements. Specifically, each panel has been discretized in 30 shell elements (Figure 4.14), by using the Opensees "MITC4 Shell Element" command. The size of each shell element is not constant but differs according to the number of nodes that has been required to model the connections systems by which the panel is attached to the RC frame, i.e. the friction dampers on the bottom and the "anchor profiles" on the top (Figure 4.14).

The orientation of the outer layers of CLT has been assumed along the global Y-axis.

The following parameters have been set to define the homogenized-orthotropic material, according to the local reference system of CLT panel mentioned in Section 4.2.3:

E_{wx} – E_{wy} – E_{wz} Elasticity moduli of the CLT panel in the local X-axis (perpendicular-to-grain of the outer boards, in panel plane), Y-axis (parallel-to-grain of the outer boards) and Z-axis (perpendicular-to-grain of the outer boards, out of panel plane), respectively.

The elasticity moduli E_{wx} and E_{wy} have been calculated as:

$$E_{wx} = E_0 k_4 = E_0 \left[\frac{E_{90}}{E_0} + \left(1 - \frac{E_{90}}{E_0}\right)\frac{a_1}{a_3}\right]$$

$$E_{wy} = E_0 k_3 = E_0 \left[1 - \left(1 - \frac{E_{90}}{E_0}\right)\frac{a_1}{a_3}\right]$$

where E_0 and E_{90} are the mean values of the elasticity moduli parallel-to-grain and perpendicular-to-grain of C24-class spruce wood, respectively (see Table 4.1). The parameters a_1 and a_3 are, instead, the inner layer thickness (40 mm) and the total thickness (100 mm) of the adopted CLT panel (see Section 4.2.2 and Table 4.4).
The elasticity modulus E_{wz} has been assumed equal to E_{90}.

$G_{xy} - G_{yz} - G_{zx}$ Shear moduli in the three perpendicular planes of the local reference system.

The value of shear modulus G_{xy} has been reduced to 500 MPa compared to the medium value G_m of the C24-class spruce wood (see Table 4.1), assuming no-bonding on the CLT narrow face [27] . The values of shear moduli G_{yz} and G_{zx} have been neglected, not considering out-of-plane stress in the present investigation.

$\nu_{xy} - \nu_{yz} - \nu_{zx}$ Poissont's ratios in the three perpendicular planes of the local reference system.

The values of Poissont's ratios have been neglected assuming no-bonding on the CLT narrow face [33].

ϱ Density.
It has been assumed equal to the mean value of the C24-class spruce wood (see Table 4.1)

The material properties of the homogenized CLT material are reported in Table 4.5.

CLT		
Perpendicular-to-grain Young's modulus	E_{wx} =	4622 MPa
Parallel-to-grain Young's modulus	E_{wy} =	6748 MPa
Perpendicular-to-grain Young's modulus	E_{wz} =	370 MPa
Shear modulus	G_{xy} =	500 MPa
Poissont's ratios	ν =	0.0
Density	ϱ =	420 kg m^{-3}

Table 4.5. Material properties of CLT panel.

4.2.3.3 Friction damper and connection elements

The scheme of the damper numerical model is reported in Figure 4.18. As described in Section 4.1, the investigated friction damper is basically made by two steel profiles (i.e. "anchor profile" and "free profile"), which mainly consist of a middle web and two side flanges. The OpenSees "ShellMITC4 Element" and "Truss Element" have been used to model both these components. Specifically, the web of each profile has been modelled by five 8-mm thick shell elements, while the flanges have been modelled by 8x100-mm truss elements, which connect the edge nodes of the above-mentioned shell elements. An elastic material has been assigned both to web and flanges of the steel profiles, assuming that they do not yield. The Young modulus of steel (E_s=210.000 MPa) is considered for the assigned material.
"ZeroLength Elements" have been used to connect the adjacent nodes of the "anchor profile" and "free profile" of each friction damper. Different behaviours in the X and Y directions are attributed to each element. Specifically, in the X direction an elasto-plastic material with strain kinematic hardening constitutive law ("Steel01" uniaxial material) has been assigned to each element, in order to model the sliding movement of the "free profile" when the shear force attains a value of friction force equal to 30 kN. In the Y direction, two of these elements are characterized by a large stiffness, in order to simulate the preloaded high strength bolts that connect the "anchor profile" and "free profile". Instead, an elastic material having large stiffness in compression and no tension resistance has been assigned to the other ZeroLength elements by means of the OpenSees comand "Elastic-No Tension Material", in

order to simulate the contact between the two steel profiles in compression and the separation of the nodes of the two profiles in tension, respectively.

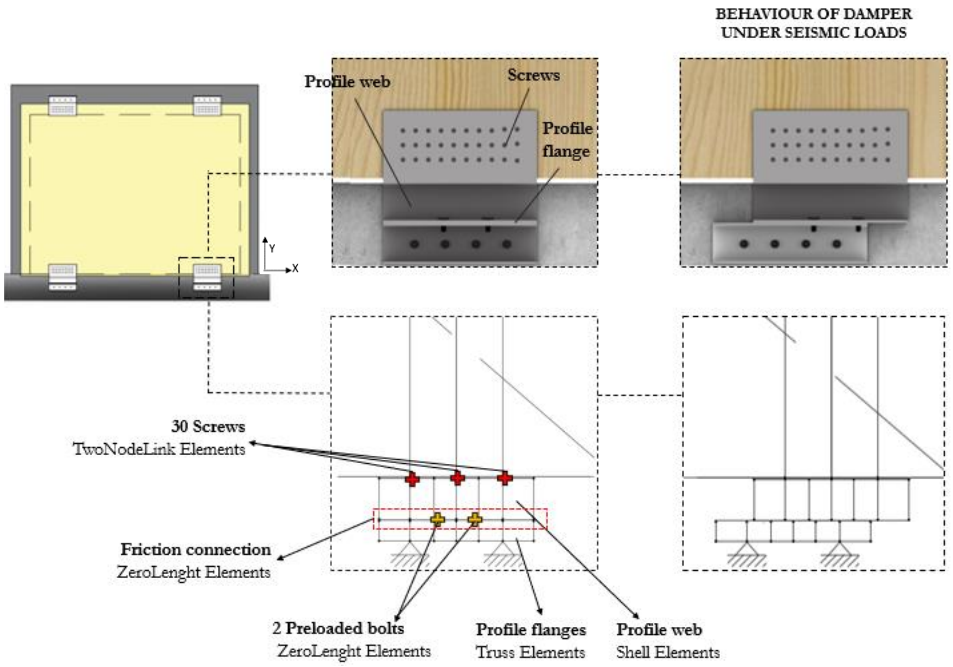

Figure 4.18. Scheme of the damper numerical model.

The "Two Node Link Elements" have been used to model the connection between the friction damper and CLT panel by means of timber screws. In particular, three elements have been used to simulate 30 screws for each damper (see Section 4.2.2), by supposing that each element represents 10 screws, respectively. The length of each element has been set equal to 5 mm in order to simulate the gap intentionally left between CLT panel and friction damper. Because of this gap, the transmission of the forces between the two elements takes place only by mean of the screws. An elastic material has been also assigned to each element, whose stiffness has been calculated and set in accordance with the prescriptions reported in Eurocode 5 for the steel-to-timber connections made by screws [22].
The same modelling has been used for the "anchor profiles" on the top of each CLT panel. In addition, "ZeroLength Elements" having large stiffness have been used to

connect the nodes of the profile's web to the nodes of the RC beams, in order to simulate the presence of anchor bolts.
Both the "anchor profiles" on the top of each CLT panel and the "free profiles" of the friction dampers are constrained to move along the global Z-axis and to rotate around the global X and Y-axes. Instead, the "anchor profiles" of the friction dampers are base constrained by means of hinges that allow rotation movement only around the global Z-axis.

4.2.3.4 Infill wall

The infill walls have been modelled by a pair of diagonal "Truss Elements", which connect the top of each column with the bottom of the subsequent one (Figure 4.14). These elements are supposed to have no tension resistance and their force-displacement relationship is calibrated to replicate the shear force-drift relationship of the infill panel, as proposed by Panagiotakos and Fardis [34] and Celarec et al. [35]. This relationship consists of four branches (Figure 4.19): a first elastic branch up to the first cracking of panel, a second branch with a lower stiffness up to the complete cracking of panel, a degrading branch and a last branch with a residual resistance. The values of stiffness K and maximum force F for each branch has been determined according to the equations proposed in [35]. The multi-linear force-displacement relationship thus obtained is then converted into an equivalent stress-strain relationship. The values of stress and strain corresponding to the three corners of the envelope have been assigned to the truss member by means of the "Hysteretic" uniaxial material implemented in OpenSees.
The force-displacement relationship has been first determined for the infill without openings assuming that the infill thickness is 20 cm, as reported in Section 4.2.1, the shear cracking strength is 0.28 MPa, while Young modulus and shear modulus are 4130 and 1240 MPa, respectively. The ordinates of this force-displacement relationship have been reduced to 50% for the infill with openings. These relationships define a layout of infills with high mechanical properties.
Other two infill layouts have been defined by reducing the ordinates of the force-displacement relationships of the first layout to 80% and 60%, in order to represent infills with lower mechanical properties and/or window openings having larger size.

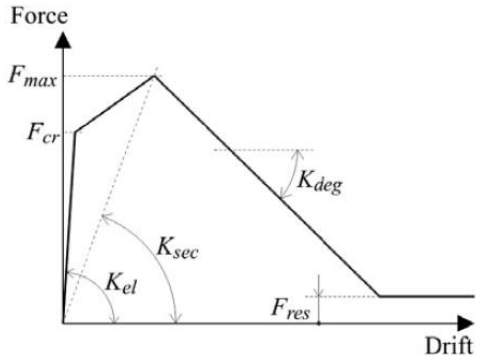

Figure 4.19. Schematic quadrilinear force-displacement relationship of the diagonal trusses, according to [35].

4.2.4 Analyses and results

Monotonic and cyclic pushover analyses in displacement control have been carried out both on bare and infilled RC frame at pre- and post-intervention state (Figure 4.20) to compare their seismic responses and quantify the potential impact of the e-CLT system. The loading conditions included both concentrated loads at the top of each column and distributed loads on each beam. These loads are consistent with those used to design the frame and include a vertical load of 292.5 kN at the top of the two central columns, a vertical load of 146.25 kN at the top of the two lateral ones, and a uniformly distributed load of 26 kN/m on each beam.

The ultimate top horizontal displacement has been set equal to 80 mm and corresponds to the near collapse limit state of the bare RC frame. This displacement value has been determined through monotonic pushover analysis on the bare frame, by increasing the top horizontal displacement until in one column the chord rotation has attained its ultimate value according to Eurocode 8 – part 1-3 [36]. For the cyclic analyses, the ultimate top displacement has been applied according to the incremental loading protocol at 5-steps reported in Figure 4.21.

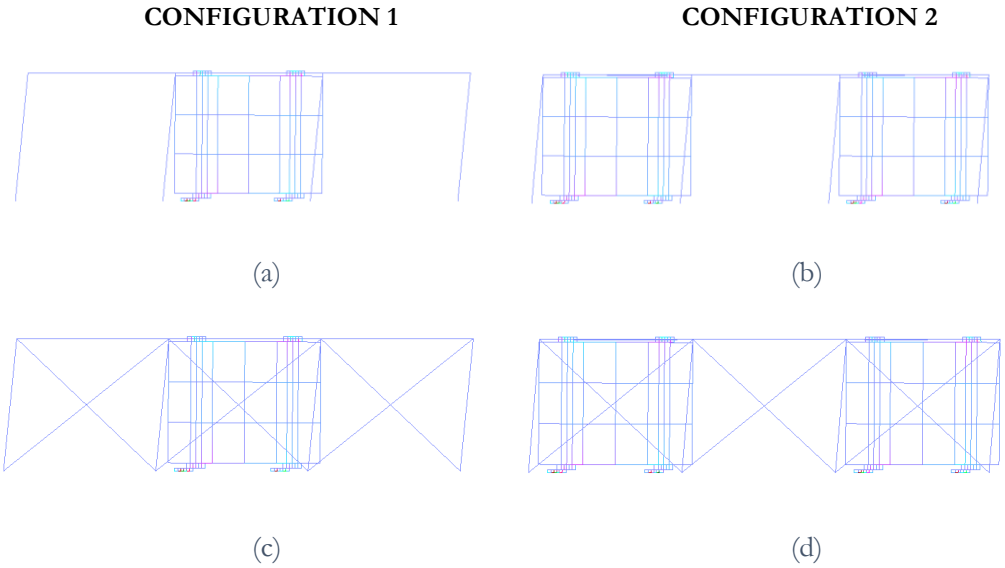

Figure 4.20. Pushover analysis on (a,b) bare and (c,d) infilled frame at post-intervention state, with e-CLT system in (a,c) configuration 1 and (b,d) configuration 2

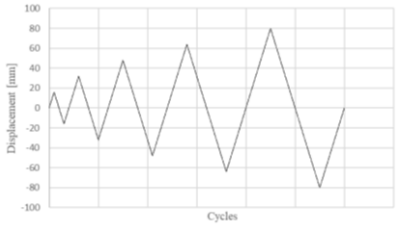

Figure 4.21. Loading protocol.

The hysteretic response of both bare and infilled frame is shown in Figures 4.22-4.25. The impact of the e-CLT system on the seismic capacity of the investigated frames has been examined in terms of the achieved increase of lateral strength, stiffness, and energy dissipation capacity. The lateral strength is assumed equal to the maximum horizontal force sustained by the system during monotonic loading. The lateral stiffness is calculated as the ratio of the lateral strength to the corresponding displacement. Finally, energy dissipation capacity is quantified as the energy dissipated during cyclic loading, which is calculated as the area enclosed by the hysteresis loops. The percentage increase of the above-mentioned seismic

parameters after the application of the e-CLT system in both the investigated configurations are reported in Figure 4.26.

Bare frame

The monotonic curves and hysteretic loops of the bare frame at pre- and post-intervention state (Figures 4.22-4.23) show a considerable increase of the seismic capacity after the application of the e-CLT system.

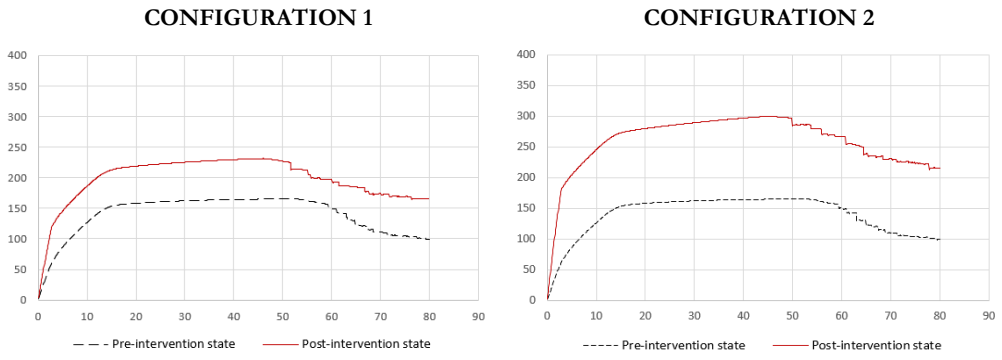

(a) (b)

Figure 4.22. Monotonic curves of the investigated bare frame at pre- and post-intervention state, with e-CLT system in (a) configuration 1 and (b) configuration 2.

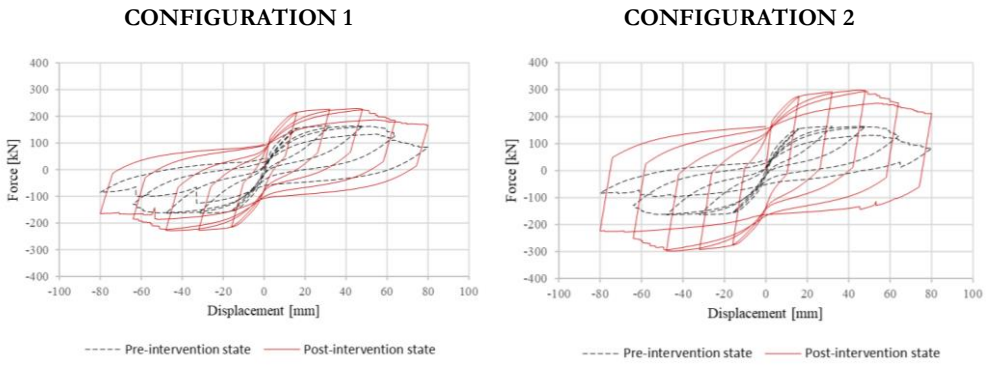

(a) (b)

Figure 4.23. Hysteretic loops of the investigated bare frame at pre- and post-intervention state, with e-CLT system in (a) configuration 1 and (b) configuration 2.

In particular, the lateral resistance of the structure upgraded by the e-CLT in configurations 1 and 2 reaches the values of 231 kN and 300 kN. Compared to the lateral strength of 165 kN at pre-intervention state, the achieved percentage increase is 40% and 82% for configurations 1 and 2, respectively. Furthermore, the application of a single CLT panel equipped with two friction dampers (configuration 1) provides the RC frame with an increase of lateral stiffness and energy dissipation capacity by 93% and 128%, respectively. Instead, by adding two CLT panels and four friction dampers (configuration 2) the stiffness of the structure increases by 165%, while the energy dissipation capacity by 275%.

Infilled frame

As mentioned in Section 4.2.3.3, the seismic response of the masonry infilled frame has been investigated assuming three different levels of quality of masonry infill, i.e. stiffness and strength equal to 100%, 80% and 60% of the reference infill defined in the same Section 4.2.3.3.

As shown by the comparison of both the monotonic curves and hysteretic loops of the infilled frame at pre- and post- intervention state (Figures 4.24-4.25), the impact of the e-CLT system on the seismic capacity of infilled frames is less remarkable. In particular, the lateral stiffness of the frame up to the first cracking of the infills does not change by applying the CLT panels, while the increase of the stiffness up to the complete cracking of the infills is negligible.

The increase of lateral strength is also low, with higher percentage increase for infills with low mechanical properties (increase by 16% and 26% in configuration 1 and 2, respectively), while in case of stronger infills the lateral strength increases by 10% and 17%, respectively.

However, the introduction of the e-CLT still leads to a significant increase of the lateral residual strength of the RC frame after the infill failure and even a more remarkable increase of energy dissipation capacity. The percentage increase of the lateral residual strength achieved by the e-CLT retrofit in configuration 1 and 2 is around 38% and 77%, respectively. Finally, the percentage increase of energy dissipation capacity achieved after the e-CLT application for infills with high, intermediate and low mechanical properties is 82%, 89.5% and 98.5%, respectively, in configuration 1 and 146%, 162.7% and 182.6%, respectively, in configuration 2.

CONFIGURATION 1 **CONFIGURATION 2**

Values of masonry infill at 100%, high mechanical properties

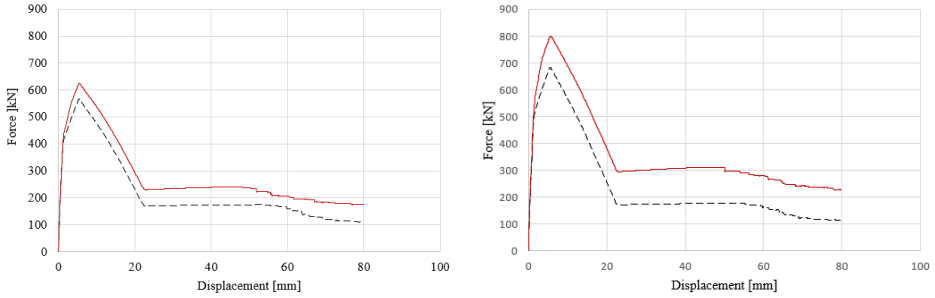

(a) (b)

Values of masonry infill at 80%, intermediate mechanical properties

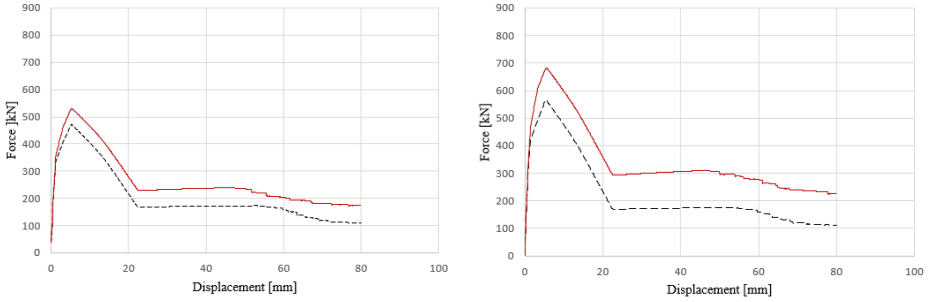

(c) (d)

Values of masonry infill at 60%, low mechanical properties

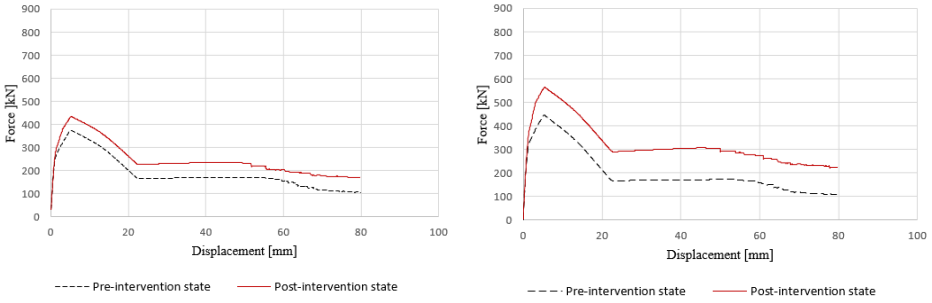

(e) (f)

Figure 4.24. Monotonic curves of the investigated infilled frame at pre- and post-intervention state, with e-CLT system in (a-c-e) config. 1 and (b-d-f) config. 2.

CONFIGURATION 1 **CONFIGURATION 2**

Values of masonry infill at 100%, high mechanical properties

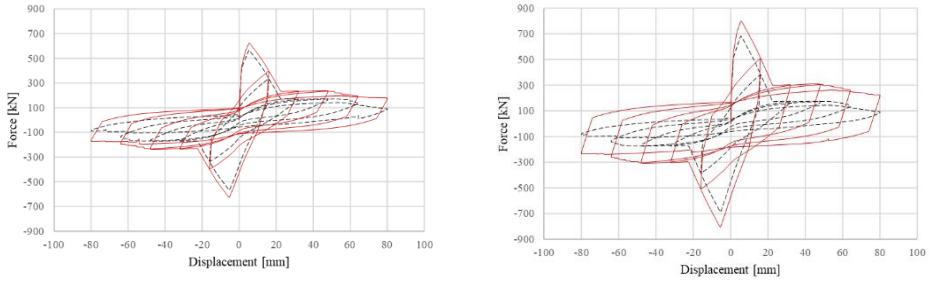

(a) (b)

Values of masonry infill at 80%, intermediate mechanical properties

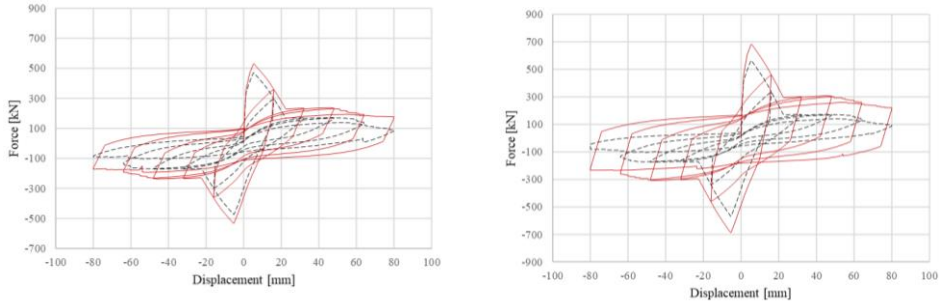

(c) (d)

Values of masonry infill at 60%, low mechanical properties

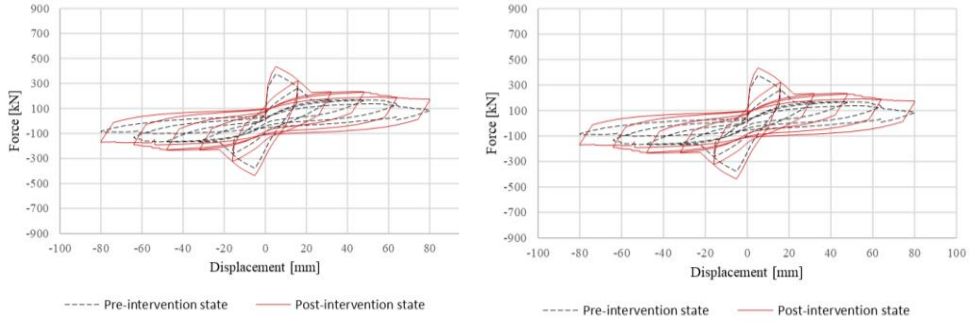

(e) (f)

Figure 4.25. Hysteretic loops of the investigated infilled frame at pre- and post-intervention state, with e-CLT system in (a-c-e) config. 1 and (b-d-f) config. 2.

CONFIGURATION 1 **CONFIGURATION 2**

Lateral strenght improvement

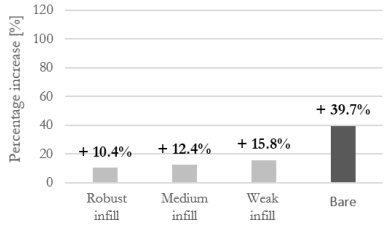

(a)

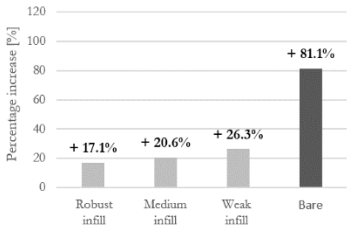

(b)

Lateral stiffness improvement

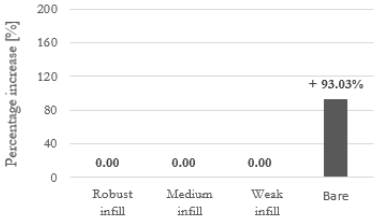

(c)

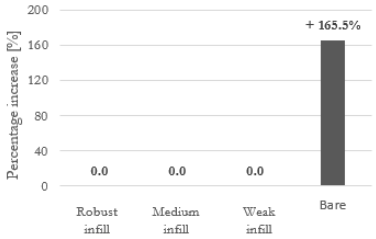

(d)

Lateral residual strenght improvement

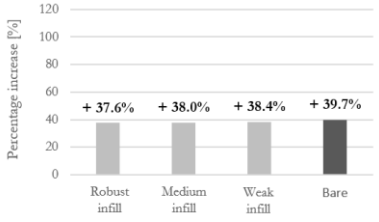

(e)

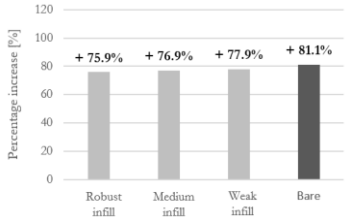

(f)

Energy dissipation improvement

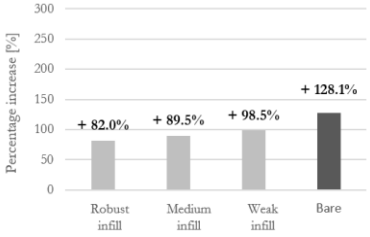

(g)

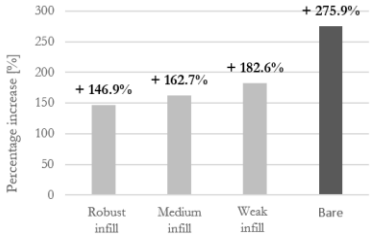

(h)

Figure 4.26. Percentage increase [%] of the (a,b) lateral strength, (c,d) lateral stiffness, (e,f) lateral residual strength and (g,h) energy dissipation capacity of the investigated frame after the application of the e-CLT system in (a,c,e,g) configuration 1 and (b,d,f,h) configuration 2.

4.2.5 Discussion

The results of the pushover analyses on the one-storey, three bay RC frame considered as case study evidence the potential of the e-CLT system in enhancing the seismic performance of existing RC framed buildings. The parametric study considers different features of the buildings to be upgraded (with and without infill walls) and different importance level of the retrofit solution (with reference to the case study, one or two CLT panels equipped with two dampers for panel).

In the case of the bare RC frame, even the configuration with a single CLT panel equipped with two friction dampers leads to a significant improvement of all the seismically relevant features of the building, i.e. the lateral strength, stiffness and energy dissipation capacity. The largest impact is on the energy dissipation capacity, that increases more than double. The impact on the lateral stiffness is also significant, in compliance with the main results of recent literature on the topic. The above-mentioned seismic features result approximately doubled in the configuration with two CLT panels and four friction dampers.

The impact of the e-CLT system on the seismic capacity of infilled frames is less remarkable since the infills make the frame very stiff and strong, regardless of the infills mechanical properties. Even considering the solution with two CLT panels, the impact on the lateral stiffness is negligible. The improvement of the lateral strength is also low, while a significant increase of the lateral residual strength of the RC frame after the infill failure is achieved, which increases by more than 1.3 times and 1.7 times by applying one and two CLT panels, respectively.

The improvement achieved in terms of increase of energy dissipation capacity is also significant, with higher values in case of weak infills. In fact, even in the case of the stiffest and strongest considered infill, the energy dissipation capacity increases by 1.8 times and 2.4 times by using two and four friction dampers, respectively.

Based on these results, the e-CLT system appears to be a promising solution for seismic upgrading of RC framed buildings. Its effectiveness is expected to be relevant in fulfilling the Near Collapse performance objective, which relies mostly on energy dissipation capacity of the structure. Instead, when the improvement of seismic performance is mainly related to the increase of lateral stiffness, as in the case of damage limitation performance objective, the effectiveness of the-CLT system could be limited when it is applied to infilled frames.

4.3 References

[1] Grigorian, C. E.; Yang, T. S.; Popov, E. P. Slotted Bolted Connection Energy Dissipators. *National Science Foundation*. Washington, DC., July 1992, 36 p.

[2] Pall, A. S., and Marsh, C. Optimum Seismic Resistance of Large Panel Structures Using Limited Slip Bolted Joints. *Proceedings of the 70th World Conference on Earthquake Engineering*. Istanbul, Turkey, 1980. Vol. 4, pp. 177-184.

[3] Golondrino, J., MacRae, G., Chase, J., and Rodgers, G. "Behaviour of asymmetrical friction connections using different shim materials." *New Zealand Society for Earthquake Engineering Conference*, 2012.

[4] Zheng Li, Minjuan He, Hanlin Dong, Zhan Shu, Xijun Wang. Friction performance assessment of Non-Asbestos Organic (NAO) composite-to-steel interface and Polytetrafluoroethylene (PTFE) composite-to-steel interface: Experimental evaluation and application in seismic resistant structures. *Construction and Building Materials*. 2018, 174, 272–283.

[5] Loo, W. Y., Quenneville, P., and Chouw, N. A new type of symmetric slip-friction connector. *Journal of Constructional Steel Research*. 2014, 94, 11–22.

[6] Chanchi Golondrino, J. C., MacRae, G. A., Chase, J. G., Rodgers, G. W., and Clifton, G. C. Seismic behaviour of symmetric friction connections for steel buildings. *Engineering Structures*. 2020, 224, 111200.

[7] G.C. Clifton, G.A. MacRae, H. Mackinven, S. Pampanin, J. Butterworth, Sliding hinge joints and subassemblies for steel moment frames, Palmerston North, New Zealand: Proc of New Zealand Society for Earthq Eng Conf, 2007.

[8] Chanchi Golondrino, J. C., MacRae, G. A., Chase, J. G., Rodgers, G. W., and Clifton, G. C. Asymmetric friction connection (afc) design for seismic energy dissipation. *Journal of Constructional Steel Research*. 2019, 157, 70–81.

[9] A. Filiatrault. Analytical predictions of the seismic response of friction damped timber shear walls. Earthquake Eng. Struct. Dyn. 1990. 19 (2), 259-273.

[10] W.Y. Loo, P. Quenneville, N. Chouw, A numerical study of the seismic behaviour of timber shear walls with slip-friction connectors, *Eng. Struct.* 2012, 34, 233–243.

[11] W.Y. Loo, C. Kun, P. Quenneville, N. Chouw, Experimental testing of a rocking timber shear wall with slip-friction connectors, Earthquake Eng. Struct. Dyn. 2014, 43 (11), 1621–1639.

[12] Hashemi A, Masoudnia R, Quenneville P. A numerical study of coupled timber walls with slip friction damping devices. Construction and Building Materials 2016. 121: 373-385

[13] A. Ceccotti, C. Sandhaas, M. Okabe, M. Yasumura, C. Minowa, N. Kawai, SOFIE project – 3D shaking table test on a seven-storey full-scale cross-laminated timber building, Earthquake Eng. Struct. Dyn. 2013, 42 (13), 2003–2021.

[14] I. Gavric, M. Fragiacomo, A. Ceccotti, Cyclic behaviour of typical metal connectors for cross-laminated (CLT) structures. Mater. Struct. 2014, 48 (6), 1841–1857.

[15] Hashemi A, Zarnani P, Masoudnia R, Quenneville P. Experimental Testing of Rocking Cross-Laminated Timber Walls with Resilient Slip Friction Joints. *Journal of Structural Engineering* 2018; 144(1):1-16.

[16] Zheng, Li; Hanlin, D.; Xijun, W.; Minjuan He. Experimental and numerical investigations into seismic performance of timber-steel hybrid structure with supplemental dampers. *Engineering Structures* 2017. 151: 33-43.

[17] Minjuan, He; Qi, L.; Zheng, Li; Hanlin, D.; Minghao, Li. Seismic performance evaluation of timber-steel hybrid structure trough large-scale shaking table tests. *Engineering Structures* 2018. 175: 483-500.

[18] Corrieri E. (2017) La piegatura della lamiera: Le basi e le tecniche operative. Milano: Tecniche nuove.

[19] Italian Ministry of Public Works: Law n. 1086, 5/11/1971, Norme per la disciplina delle opere in conglomerato cementizio normale e precompresso ed a struttura metallica (Regulations for constructions of normal and pre-stressed reinforced concrete and with steel structure), Gazzetta Ufficiale Serie generale n. 321, 21/12/1971, Rome. (in Italian)

[20] Italian Ministry of Public Works: Ministry Decree, 30/05/1974, Norme tecniche per l'esecuzione delle opere in cemento armato normale e precompresso e per le strutture metalliche (Technical regulations for constructions with reinforced concrete, prestresses concrete and steel structure), Gazzetta Ufficiale Serie generale, 29/07/1974, Rome (In Italian).

[21] EN 338:2016. Structural timber - Strength classes.

[22] EN 1995-1-1:2004 Eurocode 5: Design of timber structures - Part 1-1: General - Common rules and rules for buildings

[23] European Technical Assessment ETA-11/0030.

[24] Mohammad, M; Blaβ, H.J.; Salenikovich, A.; Ringhofer, A.; Line, P.; Rammer, D.; Smith, T.; Li, M. Design approaches for CLT connections. *Wood and Fiber Science.* 2018, 50, 27-47.

[25] OpenSees, Open System for Earthquake Engineering Simulation, http://opensees.berkeley.edu/

[26] Scott, M. Numerical Integration Options for the Force-Based Beam-Column Element in OpenSees, 2011.

[27] Brandner, R.; Flatscher, G.; Ringhofer, A.; Schickhofer, G.; Thiel, A. Cross laminated timber (CLT): overview and development. Eur. J. Wood Prod. 2016, 74, 331–351.
[28] H. Blass, P. Fellmoser. Design of solid wood panels with cross layers. World Conference on Timber Engineering. Lahti, Finland, June 14-17, 2004.
[29] Sustersic I, Fragiacomo M, Dujic B. Influence of connection properties on the ductility and seismic resistance of multi-storey cross-lam buildings. *CIB-W18*. Alghero, Italy, 2011.
[30] I. Sustersic, B. Dujic. Seismic strengthening of existing URM and RC structures using Xlam timber panels. International conference on Earthquake Engineering, Skopie, Macedonia, 2013.
[31] M. Fragiacomo, B. Dujic, I. Sustersic, Elastic and ductile design of multi-storey crosslam massive wooden buildings under seismic actions, *Eng. Struct.* **33**, 11, 3043–3053, 2011.
[32] Porcu, M.C.; Bosu, C.; Gavric, I. Non-linear dynamic analysis to assess the seismic performance of cross-laminated timber structures. Journal of Building Engineering. 2018,19, 480-493.
[33] C. Aranha, J. Branco, P. Lourenço, G. Flatscher, G. Schickhofer. Finite element modelling of the cyclic behaviour of CLT connectors and walls. World Conference on Timber Engineering, Vienna, Austria, August 22-25, 2016.
[34] T. B. Panagiotakos, M.N. Fardis, Seismic response of infilled RC frame structures. 11th world conference on earthquake engineering, Acapulco, Mexico, June 23-28 1996.
[35] D. Celarec, P. Ricci, M. Dolšek, The sensitivity of seismic response parameters to the uncertain modelling variables of masonry-infilled reinforced concrete frames, Engineering Structures 35, 165-177, 2012.
[36] CEN. Eurocode 8: Design of structures for earthquake resistance. Part 1-3: Assessment and retrofitting of buildings. European Committee for Standardization, Brussels; 2005

5

Prototyping and mechanical characterization of the friction damper

Summary

This chapter describes the specimens of the proposed damper that have been designed and prototyped to be tested under cyclic loading to investigate the hysteretic behaviour of the steel-to-steel friction connection. Hence, the results of the experimental campaign are presented and discussed.

5.1 Damper prototyping

After that the potential of the proposed seismic retrofit system was demonstrated, four damper configurations (Figure 5.1) have been prototyped to detect potential limits and advantages of each one and identify the optimal option.

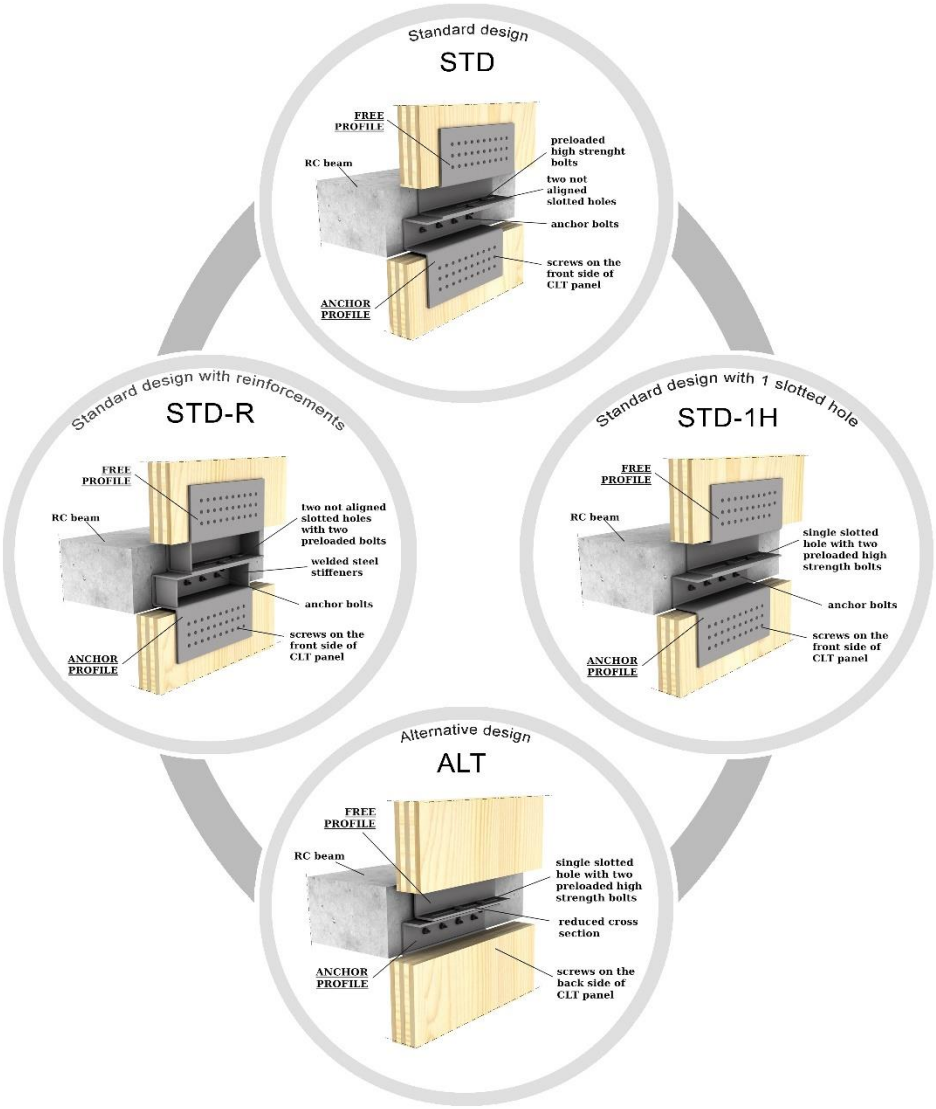

Figure 5.1. Friction damper configurations

The conceived damper configuration (named "standard" in Figure 5.1) provides two preloaded bolts located in not aligned slotted holes. This design has also been investigated in two modified configurations, characterized by: (i) additional steel stiffeners welded at the outer edges of the bent sections of the profiles (damper STD-R in Figure 5.1); (ii) the arrangement of the two preloaded bolts in a single centred slotted hole (damper STD-1H in Figure 5.1). The intent was to analyse the effects of using additional stiffeners, considering potential deformations due to the breadth in depth of the two profile flanges, and one or two slotted holes for the overall stability of the friction connection.

The fourth configuration (damper ALT in Figure 5.1) is the one that mostly differs from the standard one. Hence, it is named ALTernative. In this configuration the connections between damper and CLT panel (CLT-steel connections) are on the internal side of the CLT panel (i.e. the side facing the existing façade). The number of bends of each profile is reduced and two preloaded bolts are arranged in a single centred slotted hole, which is closer to the vertical edge of the "free profile" with respect to the slotted holes of the other configurations. The ALT design derives from the results of preliminary numerical investigations presented in [1] that showed torsional deformations in the other damper configurations due to the multiple bends in the profiles and large eccentricity between the point of application of friction force and reaction force transmitted by the CLT panel. For this design, both the steel profiles consist of two separate plates, welded together with a small overlap to create a gap to fit the screw heads without risking rubbing between the profiles and the RC beams. Countersunk holes in steel plates may solve this problem, but they have been avoided because they make the industrial production of the damper more complex.

Compared to the other configurations, the ALT design requires to pre-assemble the CLT panels off-site with both the profiles at the edges, and then connect them to each other and to the RC beams on-site. This is due to the back fitting of the CLT-steel connection, that makes the damper installation more complex since the adjustment of the friction surfaces alignment cannot be guaranteed on-site. Furthermore, dampers replacement results more time consuming, since the removal of the panels is required.

The specimens of the investigated four damper configurations are shown in Figure 5.2.

	Damper configuration	Damper specimen
STD	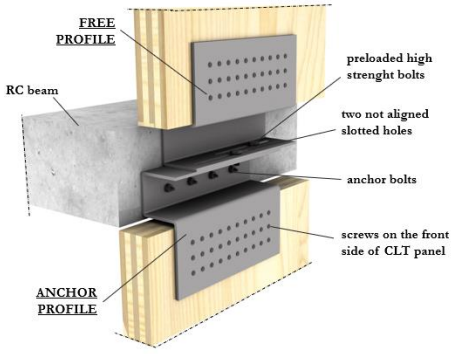	
STD-R	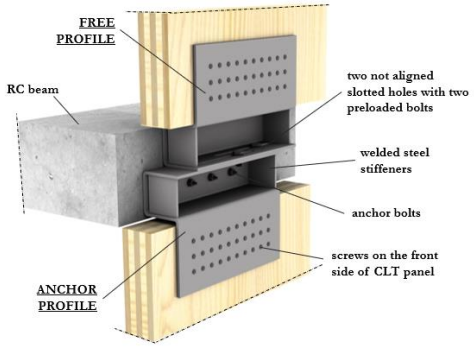	
STD-1H	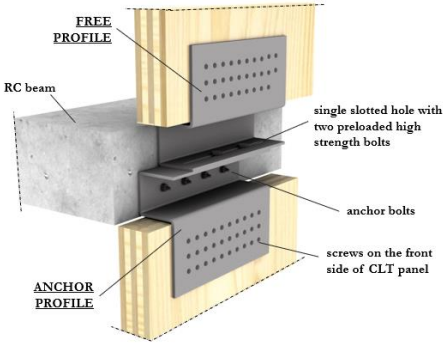	

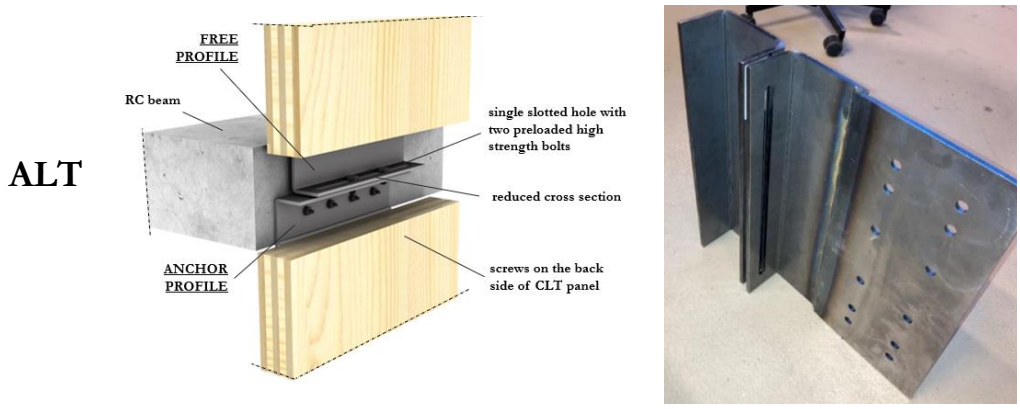

Figure 5.2. Specimens of the investigated four damper configurations

These specimens have been realized to be tested under cyclic loading. Each specimen is composed by two profiles. One profile is shaped as the "free profile" of the corresponding design and presents holes to be fixed by means of bolts to a steel column, which simulates the CLT panel. Instead, the other profile is C-shaped and simulates the "anchor profile" fixed to the RC beam, which is replicated by a steel element. The drawings of each damper specimen are reported at the end of this Section.

All the specimens are 8-mm thick and 450-mm long (see Chapter 4, Section 4.2.2.). The flanges are 121-mm depth in all the standard configurations (configurations STD, STD-R and STD-1H), assuming to connect a 100-mm thick CLT panel, while they are 78.5-mm depth in the ALT configuration. The overall height of each specimen is 445 mm (120 mm the "anchor profile" and 325 mm the "free profile"). All the specimens were made of steel S235 JR, that has been chosen since it is softer and thus easier to be bent compared to other structural steels.

The "anchor profile" of each specimen has 4 round holes in the web and 2 round holes in one flange, in order to be connected to the test setup and the "free profile", respectively. Instead, each "free profile" has 12 holes for the connection to the test setup, and one/two slotted holes on the interface surface with each "anchor profile", in order to provide for the sliding between the two profiles. The slotted holes are 240-mm long in the two-holes damper configurations and 370-mm long in the single-hole one. The length of the slotted holes is determined assuming an ultimate value of storey drift equal to 100 mm, which corresponds to about 3% of the common RC building storey height, i.e. 3 m, and an additional 20-mm tolerance in

both sliding directions. All the holes have a diameter of 15 mm to accommodate M14 bolts. In particular, the specimens have been designed by assuming a slip force equal to 30 kN, in accordance with other testing campaigns of similar devices [2]. As regard the friction connections, two high-strength M14 bolts (grade 10.9) conformed with European Standard EN 14399 [3] have been used, according to the prescriptions of EN 1993-1-8 par. 3.9.1 [4]. Specifically, the characteristic slip strength $F_{s,Rk}$ of a preloaded high-strength bolt is given as:

$$F_{s,Rk} = k_s n \mu F_{p,C}$$

where:
k_s is the shape coefficient
n is the number of friction surfaces
μ is the friction coefficient
$F_{p,C}$ is the preload force, calculated as: $F_{p,C} = 0.7\ f_{ub}\ A_s$ (where f_{ub} and A_s are the ultimate tensile strength and the bolt resistant area)

Thus, the slip resistance of the investigated friction connections, made of two M14 bolts grade 10.9 (f_{ub}= 1000 MPa and A_S= 115 mm^2) each one, has been preliminary calculated as:

$$F_{s,Rk,\,tot} = n_{bolts}\ F_{s,Rk,}$$
$$F_{s,Rk,\,tot} = 2\ (k_s\, n\, \mu\, F_{p,C}) = 30.4\ \text{kN}$$

where:
$k_s = 0.63$ (shape coefficient for bolts in long slotted holes having slot axis parallel to the direction of load transfer)
$n = 1$
$\mu = 0.3$ (friction coefficient for steel surface cleaned by wire-brushing or flame cleaning, with loose rust removed)
$F_{p,C} = 80.5$ kN

The spacing and edge distance of bolts have been designed also in accordance with [4].

As regard the manufacturing process, the most common "air bending" method has been used to realize each damper specimen. Specifically, an 88-grade punch and a die having 50-mm V-opening have been used. The selected die allowed the 90°-bending of 8-mm thick steel sheet, ensuring low bending internal radius Ri (Figure 5.3), and observing the minimum edge B that needs to be without holes in order to keep the bending line unchanged and avoid deformations during the press bending process.

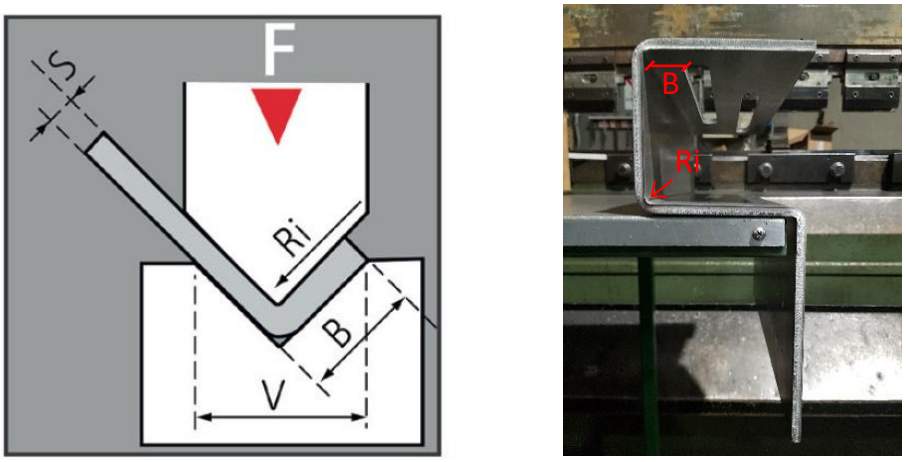

Figure 5.3. Bending parameters: V=die opening; Ri=internal radius; B=minimum edge; F= press force; S= sheet thickness

"FREE PROFILE"

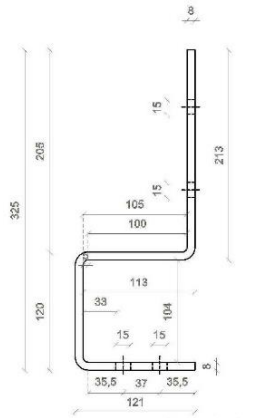

Lateral view

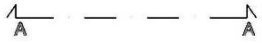

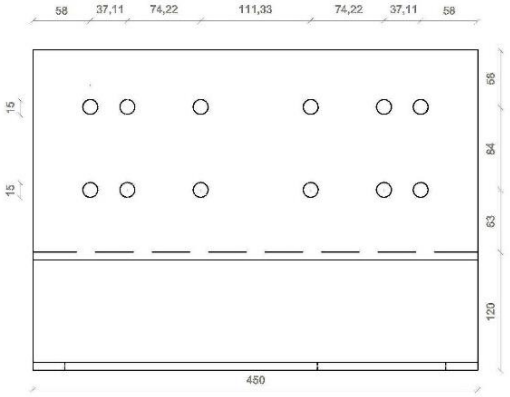

Front view

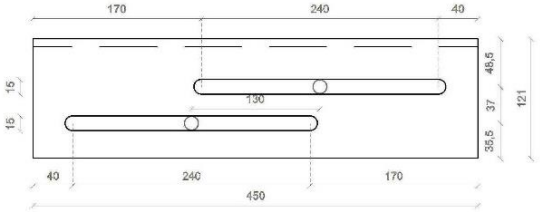

View A-A

"ANCHOR PROFILE"

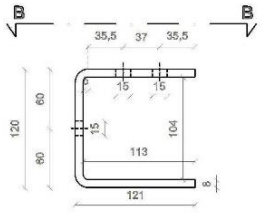

Lateral view

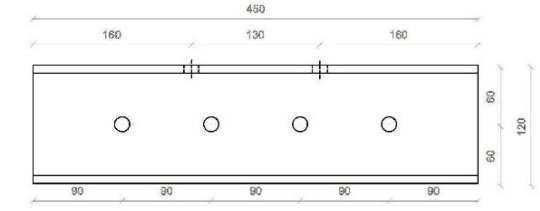

Front view

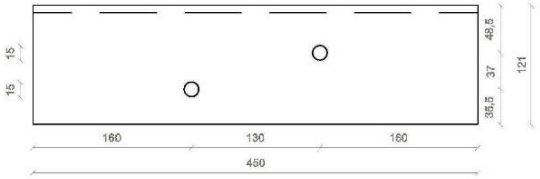

View B-B

Specimen
STD

"FREE PROFILE"

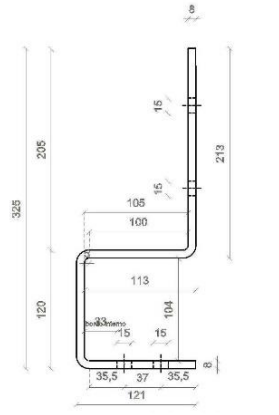

Lateral view
(stiffeners not reported)

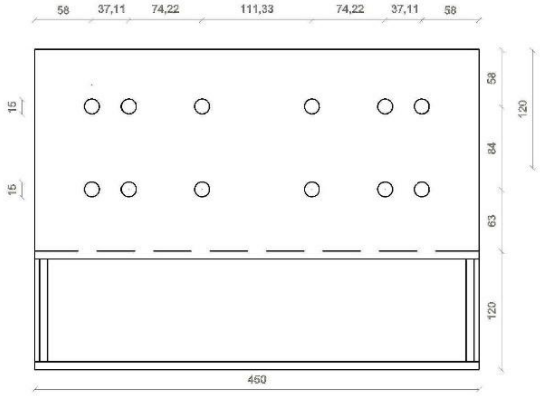

Front view

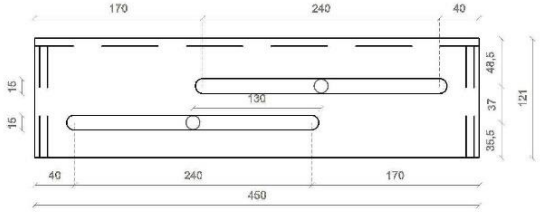

View A-A

"ANCHOR PROFILE"

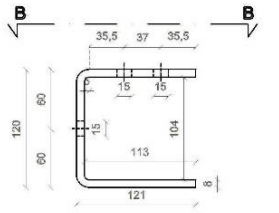

Lateral view
(stiffeners not reported)

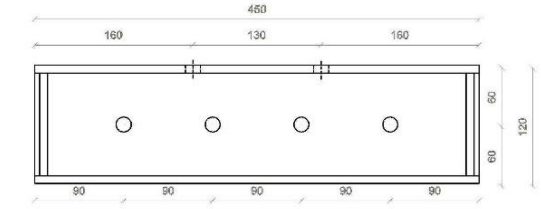

Front view

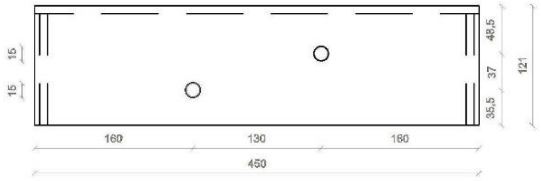

View B-B

Specimen
STD-R

"FREE PROFILE"

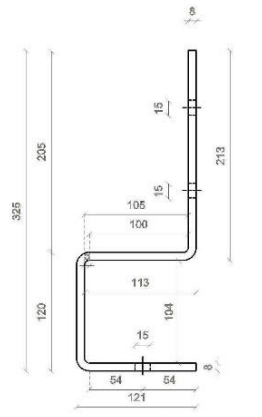

Lateral view

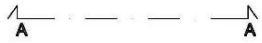

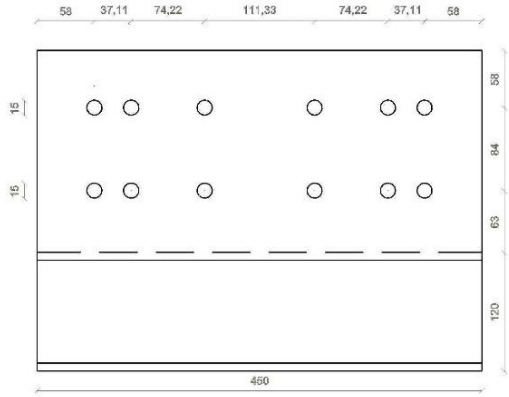

Front view

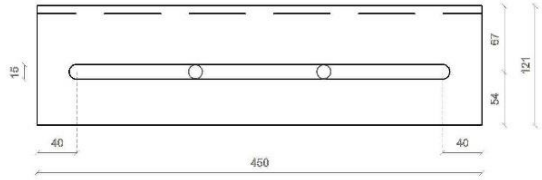

View A-A

"ANCHOR PROFILE"

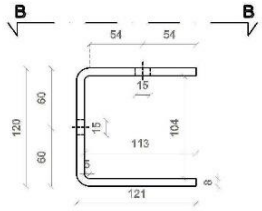

Lateral view

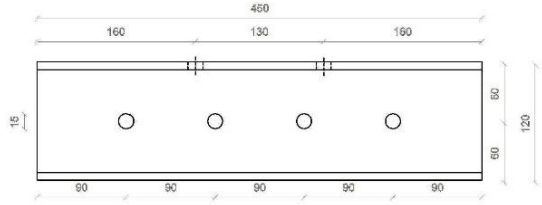

Front view

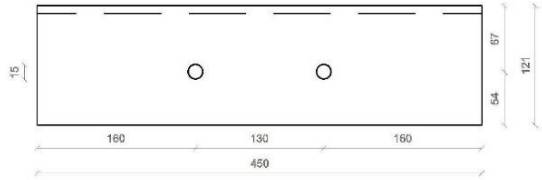

View B-B

Specimen
STD-1H

"FREE PROFILE"

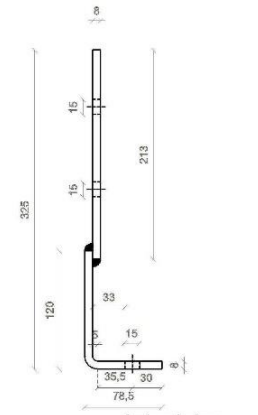

Lateral view

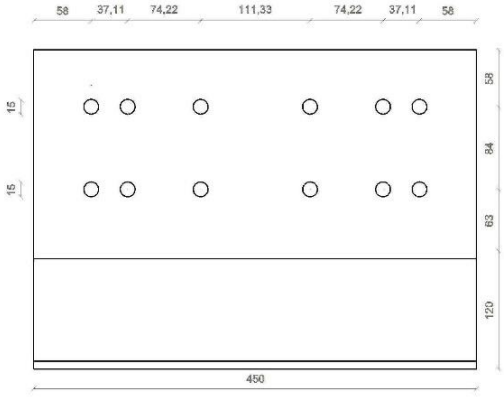

Front view

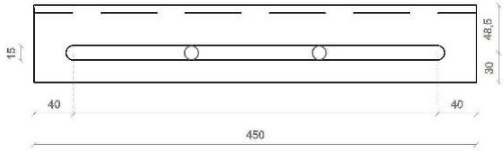

View A-A

"ANCHOR PROFILE"

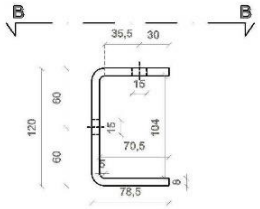

Lateral view

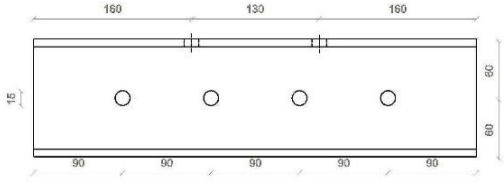

Front view

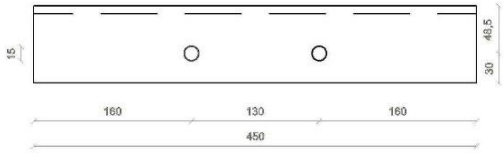

View B-B

Specimen
ALT

5.2 Mechanical characterization

Cyclic loading tests in displacement control have been carried out on each damper specimen to investigate the hysteretic behaviour of the steel-to-steel friction connection, analysing the slip force stability and the energy dissipation capacity. A sliding force equal to 30 kN, the stability of the sliding force and a displacement capacity of 100 mm have been set as main targets to be achieved.
In the following Sections the test setup is described, and the results of the experimental campaign are reported and discussed.

5.2.1 Test setup

A universal Instron electromechanical testing machine having 100-kN and 50-kN capacity in monotonic and cyclic testing, respectively, has been used to test the cyclic behaviour of the four damper specimens. Figure 5.4 shows the test setup, which consists of a rigid steel frame fixed to the machine by means of a 25-mm thick steel base plate.
The steel frame is made of two columns having 12.5-mm thick hollow cross sections 100x200, which are connected each other by a C-shaped profile bolted on their front sides. On the other hand, a stiffened T-shaped steel element is fixed to the load cell of the machine.
The "free profile" of each specimen is fixed on the right column (Figure 5.4b), while the "anchor profile" is connected to the load cell of the testing machine by means of the T-shaped element, which thus ensures the load transfer to the specimen. Based on this setup, the "anchor profile" is moved up and down by the press machine, to simulate the movement of the RC beam in a real building during earthquake, while the attachment of the "free profile" to the right column simulates the connection to the CLT panel. This column presents steel stiffeners at the base to avoid any deformation due to the eccentricity between the "free profile" and the point of load application.

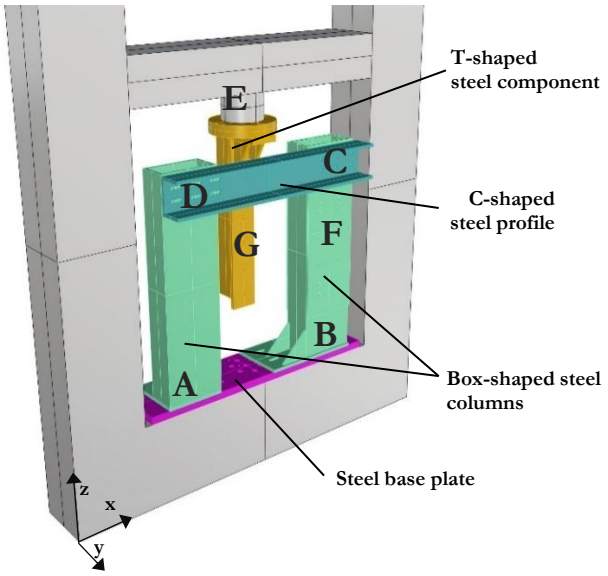

(a)

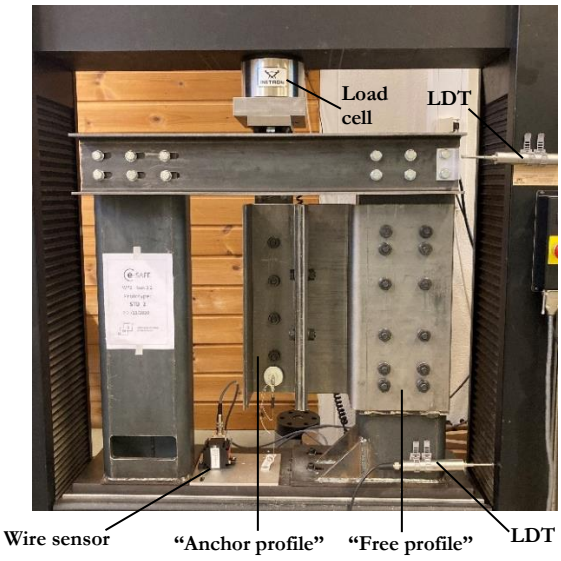

(b)

Figure 5.4. Test setup: (a) 3D model of the setup before damper placement; (b) setup installed.

The damper-setup connections are shear oversized and are marked in Figure 5.4a as follows:

A Connection between left column and base plate is made of 4 M10 bolts in round holes.

B Connection between right column and base plate is made of 6 M10 bolts in slotted holes to allow the column movement along the X direction.

C Connection between C-shaped profile and right column is made of 6 M12 bolts in round holes.

D Connection between C-shaped profile and left column is made of 6 M12 bolts in slotted holes to allow the profile movement along the X direction.

E Connection between T-shaped element and load cell is made of 4 M12 bolts in slotted holes to allow the profile movement along the Y direction.

F Connection between "free profile" and right column is made of 12 M14 full thread hexagon screws, which are preloaded to avoid any slip during testing. To do this, bolts are inserted with the head on the internal side of the column, in order to apply washers and nuts from the outside and thus proceed with their tightening.

G Connection between "anchor profile" and T-shaped element is made of 4 M14 bolts, which are preloaded to avoid any slip during testing.

Connections B, D and E have been provided with slotted holes to mitigate potential inaccuracies in specimens manufacturing.
The test setup also includes an external wire sensor to measure the displacement of the "anchor profile" and compare it to that which drive the displacement-controlled test. The wire sensor is fixed to the steel base plate and is connected to the "free profile" by a magnet (Figure 5.4b). Furthermore, two Linear Displacement Transducers (LDTs) are placed at the top and bottom of the right column to detect any undesired sliding or rotation movements.

5.2.2 Test overview

Table 5.1 summarizes the cyclic loading tests carried out on each damper specimen.

Test	Specimen	Loading protocol	Test speed [mm s^{-1}]	Bolts preload [kN]	Additional shim layers and cap plate
STD.1	STD_1	A	0.5	24.1	No
STD.2	STD_1	A	0.5	24.1	No
STD.3	STD_2	A	0.5	24.1	Yes
STD-R.1	STD-R_1	A	0.5	24.1	Yes
STD-1H.1	STD-1H_1	A	0.5	24.1	Yes
STD-1H.2	STD-1H_1	A	0.5	45.3	Yes
ALT.1	ALT_1	A	0.5	24.1	Yes
ALT.2	ALT_1	A	0.5	36	Yes
ALT.3	ALT_1	A	2	36	Yes
ALT.4	ALT_1	B	2	36	Yes

Table 5.1. Cyclic loading test on each damper specimen

The same specimen was used for multiple tests, except for the STD damper for which two specimens were tested.
The experimental tests have been performed in displacement control by adopting incremental loading protocols in accordance with ISO 16670 [5] and EN 15129 [6]. Specifically, the loading protocols A and B in Figure 5.5 have been used, where the maximum amplitude was set equal to 50% and 100% of the displacement capacity of the damper specimens, respectively. Test speed has been set equal to 0.5 mm s^{-1} in tests STD.1÷ALT.2, and 2 mm s^{-1} in tests ALT.3÷ALT.4, as reported in Table 5.1.
The bolts preload value used for each specimen is reported also in Table 5.1. Specifically, each specimen has been firstly tested by tightening friction bolts with a preload force equal to 24.1 kN, that corresponds to 30% of the standard preload suggested in [4] for the selected high strength bolts (see Section 5.1). This preload value was set according to the results of a preliminary monotonic test on an additional STD specimen, where the use of the standard preload value to tight friction bolts resulted in the sliding of the "anchor profile" for a force much higher

than the cyclic capacity of the test machine. Higher bolts preloads have been also used for the cyclic loading tests, as reported in Table 5.1.
Moreover, in tests STD.1-STD.2 friction damper has been investigated in its original configuration, which includes only two steel friction surfaces. In the other tests (tests STD.3 ÷ ALT.4), an 8-mm thick steel plate has been added in each specimen near the slotted plate of the "free profile", as well as two 2-mm thick aluminium plate as shim layers between the friction surfaces, as illustrated in Figure 5.6 referring to the STD configuration of the damper.

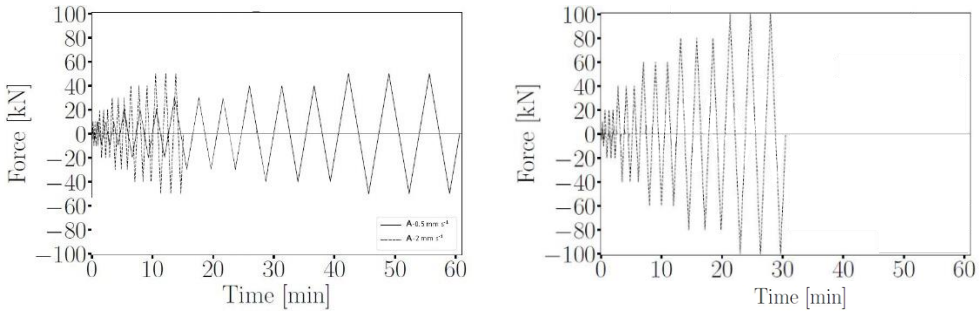

(a) (b)

Figure 5.5. (a) Loading protocol A (1x 5mm + 3x 10-20-30-40-50mm) with test speed 0.5 mm s^{-1} and 2 mm s^{-1}; (b) loading protocol B (1x 5-10mm + 3x 20-40-60-80-100mm) with test speed 2 mm s^{-1}

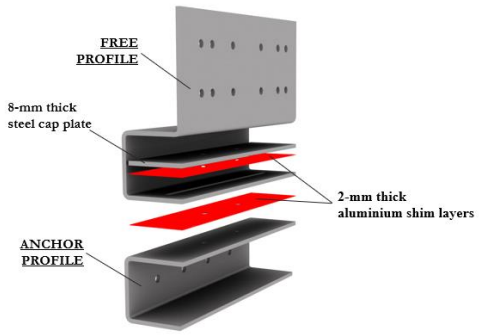

Figure 5.6. Addition of a steel cap plate and two aluminium shim layers in the STD configuration of the damper.

5.2.3 Results

The results of the cycling loading tests for each damper specimen are reported below. Specifically, the hysteretic behaviour of the damper specimens and the energy dissipated over time are reported for each cyclic test.

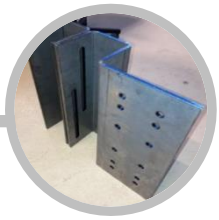

STD specimen

The three cyclic loading tests (tests STD.1, STD.2 and STD.3) on the STD specimens showed an unstable and unpredictable hysteretic behaviour of the damper, resulting in not constant energy dissipation over time (Figure 5.7).

Test STD.1

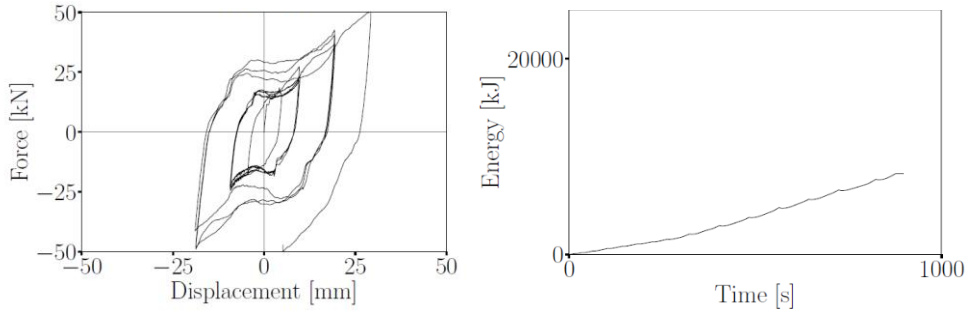

Test STD.2

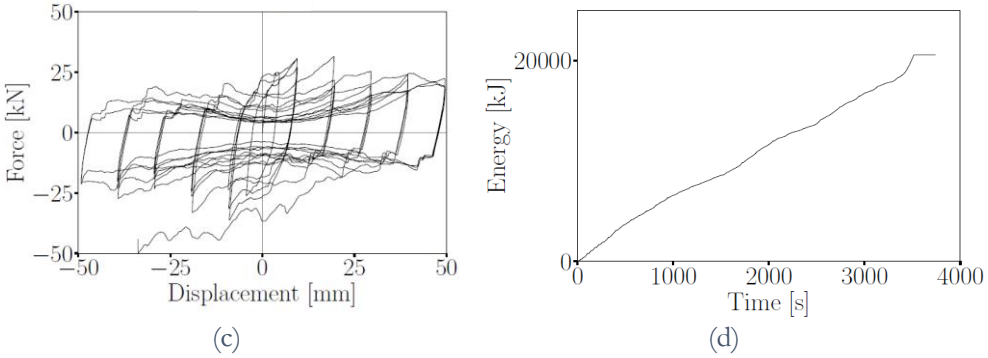

Test STD.3

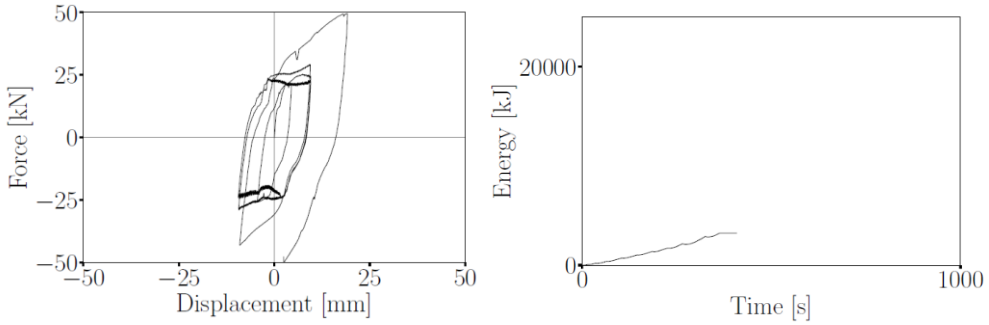

(e) (f)

Figure 5.7. (a,c,e) Hysteretic response and (b,d,f) energy dissipated by the STD specimens in tests (a,b) STD.1, (c,d) STD.2 and (e,f) STD.3.

Tests STD.1 and STD.2 have been performed on the same specimen. In test STD.1, the slip force increased rapidly (Figure 5.7a), reaching the maximum load capacity of the test machine, i.e. 50 kN, at 30-mm load cycle, which caused the stopping of the test before completing the whole loading protocol. Instead, in test STD.2 the limit load value has been reached during one of the last load cycles (Figure 5.7c), but the hysteretic loop resulted high unstable, presenting a sudden drop in force after the initial peaks. Compared to test STD.1, scraping effect between the bolt washers and the edges of slotted holes have been observed (Figure 5.8), as well as preload losses in the bolts at the end of the test. A relative twisting effect between the contact surfaces of the two damper profiles (Figure 5.9) has been also observed in both tests, and significant deformations of the two outer bends of the "free profile" (Figure 5.10), whose external radius deviated in positive and negative compared to the original 90° degree.

Based on these results, a new STD specimen has been tested (test STD.3), by adding a steel cap plate and two aluminium shim layers in the friction connection (see Figure 5.6 in Section 5.2.2) to avoid the bolt washers scraping observed in test STD.2 and the wear of the steel surfaces, as well as to enhance the hysteretic stability of the damper. However, the results of test STD.3 (Figure 5.7e) were not satisfactory. The force has increased rapidly again, reaching the load capacity of the machine at 20-mm load cycle. Once more, both friction surfaces twisted and the outer bends of the "free profile" deformed. Rather, any scraping and wear effect has been observed.

For this reason, the steel cap plate and the aluminium shim layers have been added also to the STD-R, STD-1H and ALT specimens tested later.

Figure 5.8. Scraping effect between bolt washers and edges of slotted holes

Figure 5.9. Twisting effect between the friction surfaces of the two damper profiles

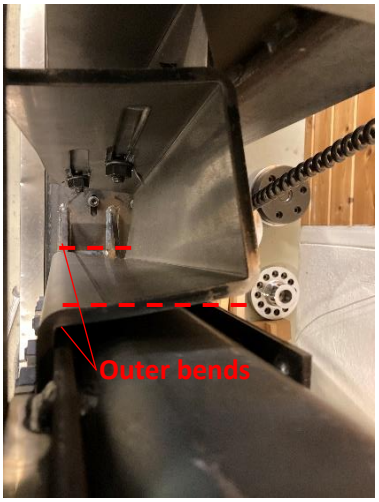

Figure 5.10. Deformations in the outer bends of the "free profile"

STD-R specimen

The results of test STD-R.1 are comparable to the STD.3 ones (Figure 5.11). The test stopped at 20-mm load cycle upon reaching the load capacity of the testing machine, and relevant deformations have been noted on the "free profile". The twisting effect between the friction surfaces has been observed also in this specimen, while no scraping between the contact surface was detected. According to these results, no other tests were performed on this specimen.

Test STD-R.1

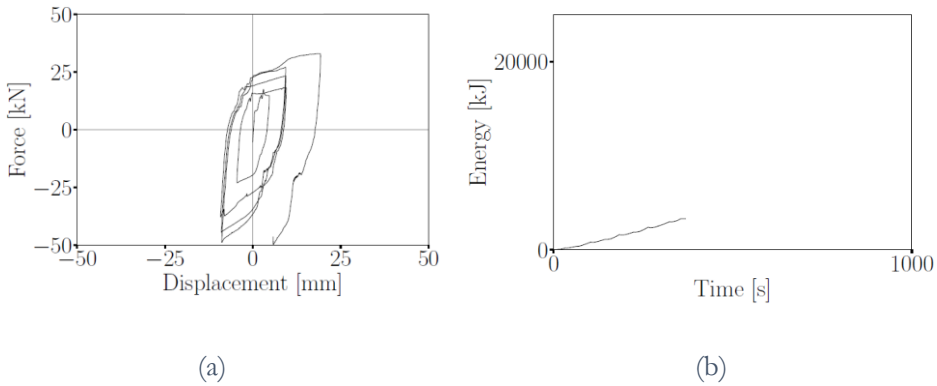

(a) (b)

Figure 5.11. (a) Hysteretic response and (b) energy dissipated by the STD-R specimen in test STD-R.1.

STD-1H specimen

The STD-1H specimen showed a more stable behaviour than specimens STD and STD-R in both the cyclic tests that have been performed on it, as shown in Figure 5.12.

Specifically, the specimen exhibited an almost rectangular loop behaviour in first test STD.1H.1 (Figure 5.12.a), but it activated for a slip force lower than the target one. The slip force had a first peak value of around 16 kN, which then drop to an almost constant value of 8 kN. The twisting between the friction surfaces was significantly lower compared to STD and STD-R specimens, without noticeable deformation in the two steel profiles.

In the second test STD-1H.2, the bolts preload force has been increased to achieve higher slip force value. Specifically, a ratio of 1.51 between the bolt preload and the target slip force of 30 kN has been considered, in accordance with the results of tests STD-1H.1.

As shown in Figure 5.12.c, the slip force reached higher values during the first load cycles, and then it decreased up to reach a constant value of around 25-30 kN. The test stopped at the last load cycle, when the 50-kN load limit was reached. During the test, the twisting of the contact surfaces was more evident than in the previous

case, even if much more limited compared to the other damper specimens. Instead, the deformation of the "free profile" at the outer bends was bigger.

Test STD-1H.1

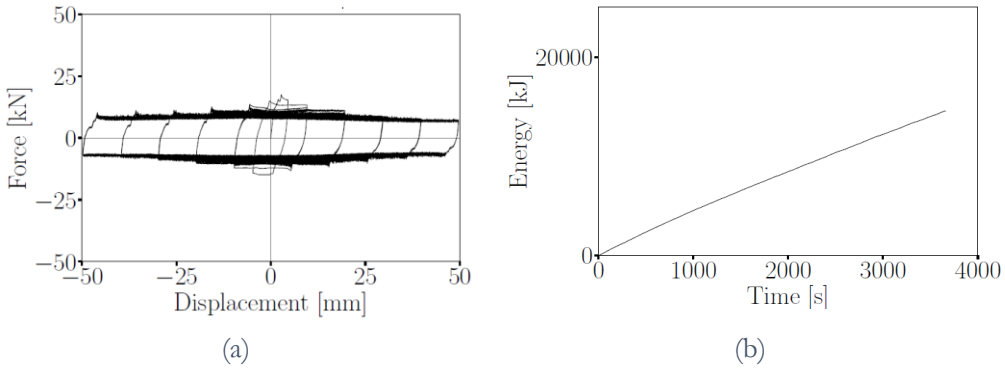

Test STD-1H.2

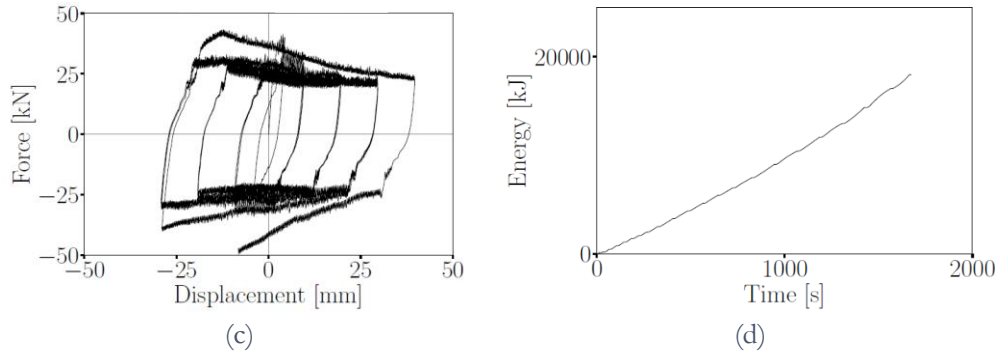

Figure 5.12. (a,c) Hysteretic response and (b,d) energy dissipated by the STD-1H specimen in tests (a,b) STD-1H.1 and (c,d) STD-1H.2

ALT specimen

Promising results have been obtained from the four cyclic loading tests of the ALT specimen (Figure 5.13).

Test ALT.1

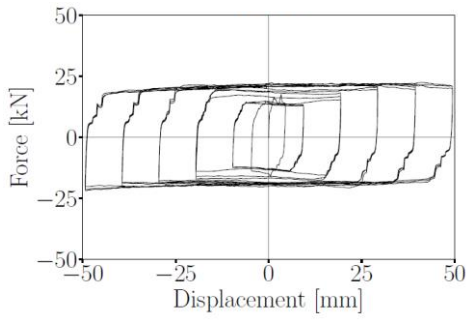

(a)

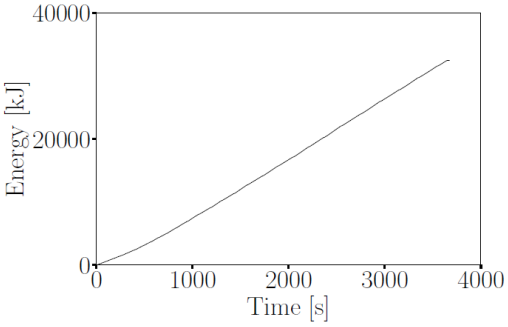

(b)

Test ALT.2

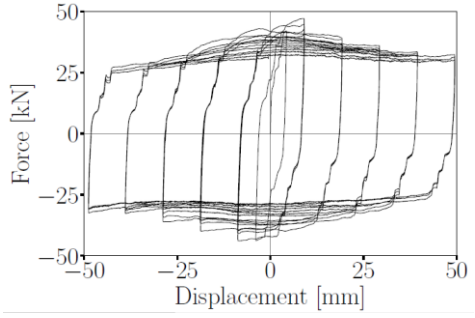

(c)

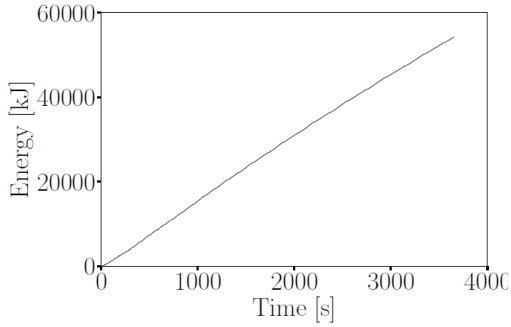

(d)

Test ALT.3

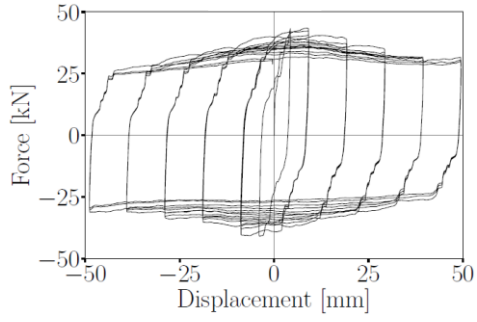

(e)

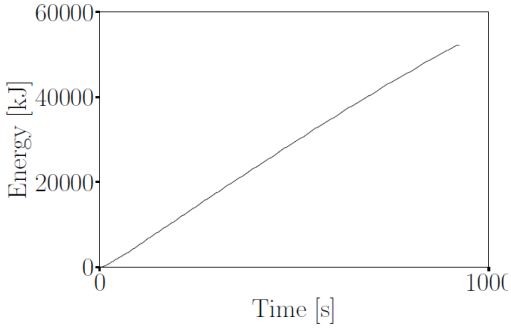

(f)

Test ALT.4

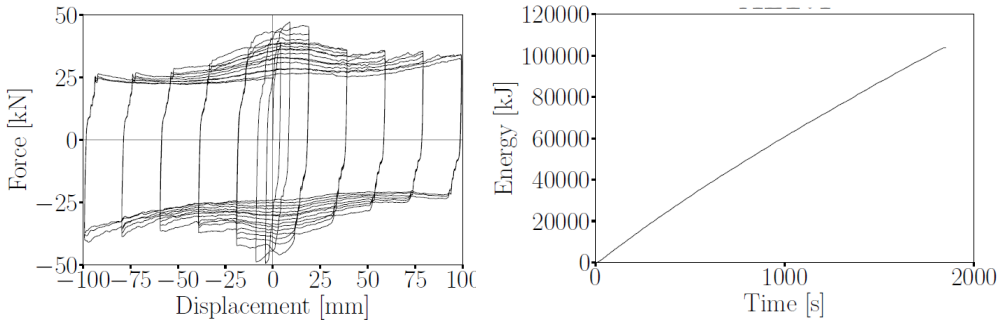

Figure 5.13. (a,c,e,g) Hysteretic response and (b,d,f,h) energy dissipated by the ALT specimen in tests (a,b) ALT.1, (c,d) ALT.2, (e,f) ALT.3 and (g,h) ALT.4.

Figure 5.13 (a-d) show the results of the first two tests (tests ALT.1 and ALT.2) carried out on the ALT specimen by using different bolt preloads, at a speed of 0.5 mm s^{-1}.

Specifically, the specimen exhibited a stable hysteretic behaviour by tightening bolts with the low preload of 24 kN (Figure 5.13a). The slip force value was lower in first load cycles and then it increased until stabilizing for a value of around 18 kN. The behaviour of the specimen resulted slightly less stable by increasing the bolts preload in accordance with the results of test ALT.1, by considering a ratio of 1.2 between the bolt preload and the target slip force of 30 kN. In this case, the hysteretic loop presented load peaks in the first load cycles (Figure 5.13c), which then gradually declined reaching a stable slip force level of around 30 kN.

The test ALT.3 has been performed with the same bolt preload of test ALT.2, but at a speed of 2 mm s^{-1} instead of 0.5 mm s^{1}. The hysteretic response and the energy dissipated recorded by the test ALT.3 (Figure 5.13e,f) were comparable to those of test ALT.2 (Figure 5.13c,d).

In the last test ALT.4, the displacement protocol reached the full 100mm-sliding capacity of the slotted hole. During the test, the specimen exhibited the same behaviour of previous tests up to 50mm-displacement (Figure 5.13f), while a moderate loop instability was manifested for higher levels of displacements. Overall, no torsional deformation of the steel profiles was observed during each test, while preload losses in the bolts occurred at the end of each one.

Table 5.2 reports the energy E dissipated by the specimens and the slip force F_{slip} measured for each cyclic loading test.

Test	Dissipated energy E [kJ]	Slip force F_{slip} [kN]
STD.1	8,25	19.99
STD.2	20,54	12.00
STD.3	3,23	19.51
STD-R.1	3,31	20.49
STD-1H.1	14,55	8.10
STD-1H.2	18,19	22.74
ALT.1	32,46	18.20
ALT.2	54,18	30.79
ALT.3	52,15	29.57
ALT.4	103,73	28.79

Table 5.2 Results of cyclic loading tests

Specifically, the energy E dissipated by each specimen has been calculated as the area enclosed by the relative hysteresis loop:

$$E = \sum_{i=0}^{n} E_i = \sum_{i=0}^{n} \left| \frac{F_{i+1} + F_i}{2} . (\delta_{i+1} - \delta_i) \right|$$

where E_i is the energy at the i-th time step, F_i and δi are force and displacement at the same time step, respectively.
By defining the cumulative distance of travel D as the sum of the displacement time steps:

$$D = \sum_{i=0}^{n} |\delta_{i+1} - \delta_i|$$

the slip force value F_{slip} has been evaluated according to [7] as follows, since its definition from the experimental data was not unique:

$$F_{slip} = \frac{E}{D}$$

5.2.4 Discussion

The results of the cyclic loading tests on the damper specimens are here discussed. Overall, the insertion of two aluminium shim layers and a steel cap plate in the friction connection avoided both the wear of the damper profiles and the scraping of the bolt washers on the edges of the slotted holes. Based on this configuration, when the "anchor profile" slides on the "free profile", the cap plate slides together with the first one, according to the concept of "asymmetric sliding friction connections". The slight instability in the hysteretic loop of the test specimens when loading direction changes confirmed the asymmetric behaviour of the damper due to the dragging of the cap plate by the bolts.
The main results of the four analysed damper configurations are summarized as follows:

- STD and STD-R damper configurations showed an unstable and unpredictable behaviour under cyclic loading, mainly due to the high deformations suffered in the outer bends of the "free profiles" (Figure 5.10 in Section 5.2.3). The main cause of these deformations is the large eccentricity between the point of application of the slip force and the reaction force transmitted by the steel column (Figure 5.14). This eccentricity generates a bending moment that deforms the "free profile" in its weak parts, i.e. the multiple bends. Moreover, the arrangement of the preloaded bolts in two non-aligned slotted holes contributes to the twisting of the friction surfaces that has been observed during the sliding of the "anchor profile" (Figure 5.9 in Section 5.2.3). The deformations on the outer bends of the "free profile" have been more accentuated in the STD-R damper mainly due to the presence of the steel stiffeners that had a negative role, contrary to expectations. In fact, these elements increased the stiffness of the "box" part of the "free profile", forcing all the deformations on the bends.
  The observed deformations thus made the hysteretic behaviour of both the STD and STD-R specimens unstable, causing considerable and unpredictable increase of the slip force value.

Figure 5.14. Deformation of the outer bends of the "free profile" due to the eccentricity *e* between the point of application of the slip force and the reaction force transmitted by the steel column, that represents the CLT panel

- In the STD-1H configuration of the damper the arrangement of two preload bolts in a single centred slotted hole instead of two not aligned holes enhanced the damper stability, reducing the twisting between the friction surfaces of the damper. The damper showed better stability of the hysteretic loop for low slip force. For higher force, deformations in the outer bends always occurred due to the eccentricity mentioned in the previous point.

- ALT damper configuration reduced the above-mentioned eccentricity, avoiding deformability effects on the specimen and ensuring to reach the target slip force of around 30 kN for a bolts preload value of 36 kN, corresponding to 45% of the standard preload suggested in [4].
  The specimen showed better stability of the hysteretic loop for low bolts preload value, while for higher preloads and levels of displacements the slip force reduced after initial peaks, due to the bolts preload losses that have been observed at the end of the tests.

5.3 References

[1] Tardo, C., Boggian, F., Hatletveit, M., Marino, E., Margani, G., and Tomasi, R. (2020). "Mechanical characterization of energy dissipation devices in retrofit solution of reinforced concrete frames coupled with solid wood panels." *Proceedings of the 12th International Conference on Structural Analysis of Historical Constructions*.

[2] Zheng, Li; Hanlin, D.; Xijun, W.; Minjuan He. Experimental and numerical investigations into seismic performance of timber-steel hybrid structure with supplemental dampers. *Engineering Structures* 2017. 151: 33-43.

[3] EN 14399:2015. High-strength structural bolting assemblies for preloading.

[4] EN 1993-1-8:2005. Eurocode 3: Design of steel structures - Part 1-8: Design of joints.

[5] ISO 16670:2003. Timber structures - Joints made with mechanical fasteners - Quasi-static reversed-cyclic test method.

[6] EN 15129:2018. Anti-seismic devices.

[7] Loo, W. Y., Quenneville, P., and Chouw, N. A new type of symmetric slip-friction connector. *Journal of Constructional Steel Research*. 2014, 94, 11–22.

6

Analysis of the energy performance of the proposed integrated retrofit technology

Summary

This chapter investigates the potential impact of the proposed retrofit technology on the energy performance of the renovated building, referring to two case studies. For each case study the impact of the intervention is evaluated both in terms of improvement of the thermal performance of the existing outer walls, as well as the reduction of the seasonal building energy demand.

6.1 Analysis specifications

Two buildings have been selected as case studies to investigate the potential impact of the proposed retrofit technology on their energy efficiency performance.
According to the overall concept of the retrofit system (Figure 6.1), in each case study the structural e-CLT panels have been assumed applied to the outer blind walls, with a uniform distribution on the opposite building fronts, while the e-PANELs have been applied to all the windowed walls. Of course, the number of e-CLT panels depends on the level of seismic vulnerability of the building, as well as the expected level of seismic upgrading. Both panels integrate insulation materials and finishing layers. The thickness of the insulation material has been set according to the stationary thermal transmittance (U) limits for the walls required by the current Italian regulations, according to the climatic zone. The e-PANELs also integrate new high performing windows to replace the existing ones.

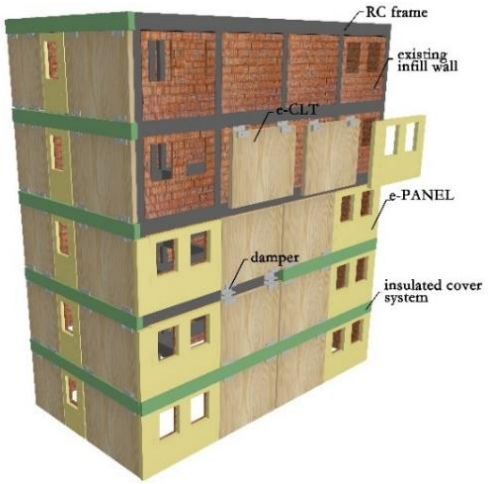

Figure 6.1. Concept of the proposed retrofit technology

The impact of the retrofit intervention on the energy performance of the selected buildings has been investigated by looking both at the improved thermal performance of the outer walls and at the reduction of the seasonal and annual building energy demand for space heating and cooling.
The thermal performance of the outer walls, before and after the intervention, has been quantified by comparing the stationary and dynamic thermal parameters.

Specifically, in addition to the U-value, the compared parameters were the periodic thermal transmittance (Y_{IE}), the decrement factor (f_a), the time shift (φ), the internal areal heat capacity (κ_i) and the surface mass (M_s).
Under the assumption of a cyclic temperature excitation acting on the outer side of the wall, the periodic thermal transmittance Y_{IE} is the ratio between the amplitude of the two cyclic functions describing the incoming heat flux and the temperature excitation, respectively. According to the current Italian regulation [1], the outer walls must have $Y_{IE} < 0.10$ W m^{-2} K^{-1}, both in new and in renovated buildings, except for the walls facing north.
The decrement factor f_a is the ratio of the periodic to the stationary thermal transmittance, while the time shift φ is the time lag between the peak outside temperature and the peak heat flux transferred indoors. Walls with $\varphi > 10$ h and $f_a \leq 0.30$ have good dynamic thermal performance.
The internal areal heat capacity κ_i describes the capability of a wall to accumulate heat after a cyclic temperature fluctuation occurring on its inner side. A wall with high internal areal heat capacity helps to attenuate the indoor overheating produced by intense heat gains, thus improving the indoor thermal comfort in summer [2]. According to some studies, $\kappa_i > 50$ kJ m^{-2} K^{-1} can be regarded as a good performance level [3].
Finally, the surface mass M_s is the mass per unit wall surface, which positively influences the thermal inertia of the wall. According to the Italian regulation [1], the outer walls should have $M_s > 230$ kg/m^2.
Instead, the seasonal buildings energy needs, before and after the intervention, have been analysed by means of dynamic thermal simulations. The simulations have been run from January to December, by applying an ideal HVAC system that is constantly able to keep the indoor air temperature at the desired level. In particular, the indoor set-point temperature for the heating and cooling season have been set to 20 °C and 26 °C, respectively. The output of the simulations consists in a sequence of hourly values for the heating and cooling power of the ideal HVAC system, which are then integrated in order to calculate the overall seasonal and annual energy demand.

6.2 Case studies

The two buildings selected as case studies are representative of the RC framed buildings erected in Italy between the 1950s and the 1980s, before the issue of the most recent and restrictive national regulations on seismic resistance and energy efficiency. For each case study, a detailed description of the thermal features of the building components at pre- and post-intervention state is presented in the following Sections.

6.2.1 Case study 1

The building is a RC framed apartment block (Figure 6.2) built in 1968 and located in Via Don Carlo Gnocchi, in the city of Catania (Southern Italy – climatic zone B). It belongs to a public housing compound and consists of two blocks (named A and B in Figure 6.2) separated by a stairwell. The two blocks have 6 and 4 storeys respectively. Residential units are in all the building storeys, except for the attic on the 6th storey of block A and the ground storey of the same block, that is used as cellar.

Figure 6.2. Multi-storey apartment building selected as case study 1

At current state, the external infill walls are made of two leaves of hollow clay bricks (8 cm-thick internal leaf and 12 cm-thick external one) with an intermediate air cavity (4.5 cm-thick) without thermal insulation. The attic floor (block A), flat roof (block B), and internal floors are characterized by RC and hollow tiles mixed slabs (24 cm-thick), without thermal insulation too. The windows have steel frames (with no thermal break), single glazing and external roller shutters as shading systems. Only the most recent windows installed to close most of the recessed balconies have PVC frames and double glazing. At post-intervention state, the e-CLT and e-PANEL components have been applied to the outer walls of the building according to the

plan layout shown in Figure 6.3a, which refers to the typical floor of the case study. The e-CLTs include 10 cm-thick CLT panel (ϱ = 420 kg m^{-3}; λ = 0.12 W m^{-1} K^{-1}) coupled with a 6.5 cm-thick wooden fibre insulation layer (ϱ = 50 kg m^{-3}; λ = 0.038 W m^{-1} K^{-1}) (Figure 6.3b). Instead, the e-PANELs have been assumed made of 10 cm-thick high-density wooden fibre insulation (ϱ = 120 kg m^{-3}; λ = 0.038 W m^{-1} K^{-1}) and an air cavity (6.5 cm-thick) to match the e-CLT thickness. They also integrate new wooden-framed double-glazing windows (U=1.56 W m^{-1} K^{-1}) to replace the existing ones. A plaster cladding has been assumed for both panels.
The U-values of the main envelope components before and after renovation are reported in Table 6.1. U-values after renovation comply with the limits set by the current regulations for the climatic zone B, equal to 0.45 W m^{-1} K^{-1} and 3.20 W m^{-1} K^{-1} for the outer walls and windows, respectively.

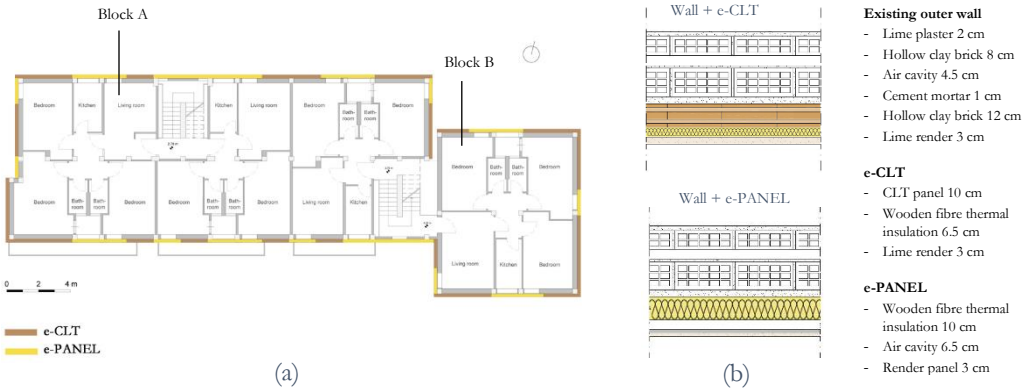

Figure 6.3. (a) Typical plan of the case study 1 and (b) stratigraphy of the outer wall after the application of the e-CLT and e-PANEL

Building Component	Pre-intervention	U-value [W m^{-2} K^{-1}]	Post-intervention	U-value [W m^{-2} K^{-1}]
External wall	Double-leaf of hollow clay bricks	1.07	Double-leaf of hollow clay bricks + e-CLT	0.29
External wall	-	-	Double-leaf of hollow clay bricks + e-PANEL	0.27
Windows	Aluminium frame, single glazing	5.9	Wooden frame, double glazing	1.56
Recessed balconies	PVC frame, double glazing	2.98	Wooden frame, double glazing	1.53

Table 6.1. U-Value of the main building components (according to the standard UNI 11300 [4] and UNI 10077 [5])

6.2.2 Case study 2

The building is a RC framed apartment block (Figure 6.4) built in 1964 and located in Via Acquicella Porto, in the city of Catania (Southern Italy – climatic zone B). It also belongs to a public housing compound and has five stories with two residential units for each one.

Figure 6.4. Multi-storey apartment building selected as case study 2.

At current state, the external infill walls have been assumed made of two leaves of hollow clay bricks (8 cm-thick internal leaf and 12 cm-thick external one) with an intermediate 10-cm thick layer (9-cm thick air cavity, plus 1 cm cement plaster on the inner face of the outer leaf) without thermal insulation, in accordance with the construction techniques of that period. Flat roof and internal floors are characterized by RC and hollow tiles mixed slabs (20 cm-thick), without thermal insulation too. The windows have metal frame without thermal break, single glazing and external roller shutters as shading systems.

At post-intervention state, the e-CLTs and e-PANELs have been applied to the building envelope according to the plan layout shown in Figure 6.5a, which refers to the ground floor of the case study. The e-CLTs include a layer of 10 cm-thick CLT panels (ϱ = 438 kg m^{-3}; λ = 0.13 W m^{-1} K^{-1}) coupled with a 6 cm-thick wooden fibre insulation layer (ϱ = 50 kg m^{-3}; λ = 0.038 W m^{-1} K^{-1}) (Figure 6.5b). The same insulation material having a thickness of 8 cm has been integrated into the e-PANELs, that present an air cavity (10 cm-thick) to match the e-CLT thickness. They also integrate new wooden-framed double-glazing windows (U= 1.5 W m^{-1} K^{-}

[1]) to replace the existing ones. Both panels are cladded with wooden staves, that provide an additional 2 cm-thick air cavity in the e-CLT panels.
The proposed envelope retrofit has been investigated in combination with the roof thermal insulation, by assuming 8 cm-thick EPS insulation layer (ϱ = 33 kg m^{-3}; λ = 0.033 W m^{-1} K^{-1}) under a floating flooring.
The U-values of the main building components before and after renovation are reported in Table 6.2. U-values after renovation comply with the limits set by the current regulations for the climatic zone B.

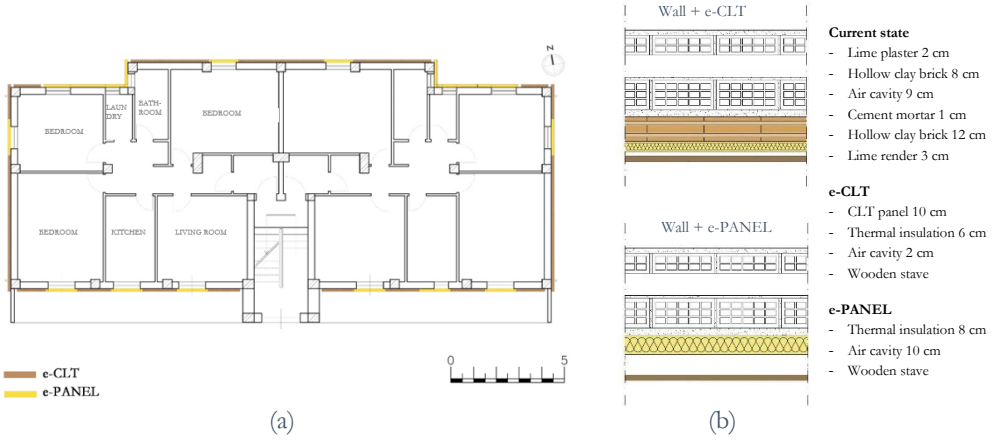

Figure 6.5. (a) Ground floor plan of the case study 2 and (b) stratigraphy of the outer wall after the application of the e-CLT and e-PANEL

Building Component	Pre-intervention	U-value [W m^{-2} K^{-1}]	Post-intervention	U-value [W m^{-2} K^{-1}]
External wall	Double-leaf of hollow clay bricks	1.07	Double-leaf of hollow clay bricks + e-CLT	0.30
External wall	-	-	Double-leaf of hollow clay bricks + e-PANEL	0.32
Flat roof	RC and hollow tiles mixed slabs	1.47	Insulated RC and hollow tiles mixed slabs	0.31
Windows	Aluminium frame, single glazing	5.9	Wooden frame, double glazing	1.5

Table 6.2. U-Value of the main building components (according to the standard UNI 11300 [4] and UNI 10077 [5])

6.3 Dynamic thermal simulations

The energy performance of the two selected buildings at pre- and post-intervention state has been evaluated by means of dynamic thermal simulations through EnergyPlus, based on a parametric model in Grasshopper (case study 1) and on a geometrical model in SketchUp (case study 2).
In the models, each room of the residential units corresponds to a heated thermal zone. The main simulation parameters are summarized in Tables 6.3 and 6.4.

Simulation parameter	Value	Unit	Boundary conditions
Ideal HVAC system:			Time setting:
- Indoor set-point temperature for heating system	20	°C	01/12 - 31/03, 8 hours a day
- Indoor set-point temperature for cooling system	26	°C	01/05 - 30/09, 12 hours a day
Natural ventilation rate	2	ACH	In case of outdoor temperature between 20 °C and 26 °C
Internal loads related to lighting	1	W m^{-2}	Assuming a typical lighting rate
Internal loads related to occupancy	100	W m^{-2}	Assuming a typical occupancy rate

Table 6.3. Simulation parameters of dynamic energy simulations on the case study 1

Simulation parameter	Value	Unit	Boundary conditions
Ideal HVAC system:			Time setting:
- Indoor set-point temperature for heating system	20	°C	30/11 - 31/03, 8 hours a day
- Indoor set-point temperature for cooling system	26	°C	31/05 - 30/09, 12 hours a day
Natural ventilation rate	0.5	ACH	winter
	1	ACH	summer
Internal loads related to lighting	0.8	W m^{-2}	Assuming a typical lighting rate
Internal loads related to occupancy	100	W m^{-2}	Assuming a typical occupancy rate

Table 6.4. Simulation parameters of dynamic energy simulations on the case study 2

Moreover, since EnergyPlus cannot simulate thermal bridges, their contribution to the energy needs has been estimated by adding 10% and 5% to the results of the total heating and cooling needs, respectively. The percent addition to the heating

needs is in line with the value suggested by UNI 11300 Standard for an existing non-insulated RC-framed building [6]. Instead, in the summer, thermal bridges have a lower impact, since heat losses have a minor role in the calculation of the cooling energy needs, if compared to internal and solar heat gains.

6.4 Results and discussion

Table 6.5 reports the stationary and dynamic parameters that quantify the thermal performance of the outer walls of both the case studies, before and after the retrofit intervention.

	Current state		**Post-intervention state**			
	Case study 1	**Case study 2**	**Case study 1**		**Case study 2**	
			e-CLT	e-PANEL	e-CLT	e-PANEL
U-Value [W m^{-2} K^{-1}]	1.15	1.07	0.29	0.27	0.3	0.32
Y_{IE} [W m^{-2} K^{-1}]	0.49	0.57	0.013	0.019	0.023	0.04
Decrement factor, fa [-]	0.43	0.54	0.04	0.07	0.08	0.13
Time shift, ϕ [h]	8.3	7.3	17.34	15.53	14.6	11.45
Internal areal heat capacity, ki [KJ m^{-2} K^{-1}]	54.15	55.18	47.36	47.38	48.42	48.77
Surface mass, Ms [kg m^{-2}]	202.04	248.04	247.29	229	294.88	252.08

Table 6.5. Stationary and dynamic thermal performance of the outer walls, before and after the proposed integrated retrofit intervention (calculation according to the algorithms reported in ISO Standard 13786 [7])

Overall, the application of the e-CLTs and e-PANELs on the existing outer walls ensures great dynamic thermal performance in terms of decrement factor ($f_a < 0.15$) and time shift ($\varphi > 11$ h). The periodic thermal transmittance complies with the current Italian regulation ($Y_{IE} < 0.10$ W m^{-2} K^{-1}) and the surface mass also considerably increases, becoming more higher than 230 kg m^{-2} in case of the e-CLT application.

These first results show the high potential of the system to improve the indoor thermal comfort in existing buildings.
Figures 6.6 and 6.7 show the results of the dynamic thermal simulations in terms of heating, cooling and total annual energy needs per unit net useful surface (kWh m^{-2}) of case studies 1 and 2, respectively. The percentage of energy saving associated to the intervention is also reported.
In particular, referring to the case study 1, the proposed retrofit intervention allows the reduction of the energy demand for heating by 65% and 70% in blocks A and B of the building, respectively (Figure 6.6b). More in detail, the current heating needs of blocks A and B are 19.65 kWh m^{-2} and 22.18 kWh m^{-2}, respectively, which decrease to 7.02 kWh m^{-2} and 6.85 kWh m^{-2} after the application of the e-CLTs and e-PANELs (Figure 6.6a). The reduction of the energy demand for cooling is lower than that for heating. In block A the current cooling needs of 10.29 kWh m^{-2} are reduced to 9.60 kWh m^{-2} (7% savings), while in block B the current cooling needs of 8.87 kWh m^{-2} fall to 6.93 kWh m^{-2} (22% savings). Overall, the application of the retrofit system provides a reduction of the annual energy demand by 44% in block A and by 56% in block B.
Equivalently, as shown in Figure 6.7b, the annual energy demand of the case study 2 decreases by 50%, with a higher energy saving for heating. In fact, the current heating needs of 32.8 kWh m^{-2} are reduced to 11.3 kWh m^{-2} (Figure 6.7a), while the cooling needs of 20.2 kWh m^{-2} are reduced to 15.02 kWh m^{-2}, which correspond to an energy saving equal to 65% and 25%, respectively.
The results of the dynamic thermal simulations on the two case studies thus confirm the high potential of the intervention to improves the energy performance of the existing building, especially in the winter.

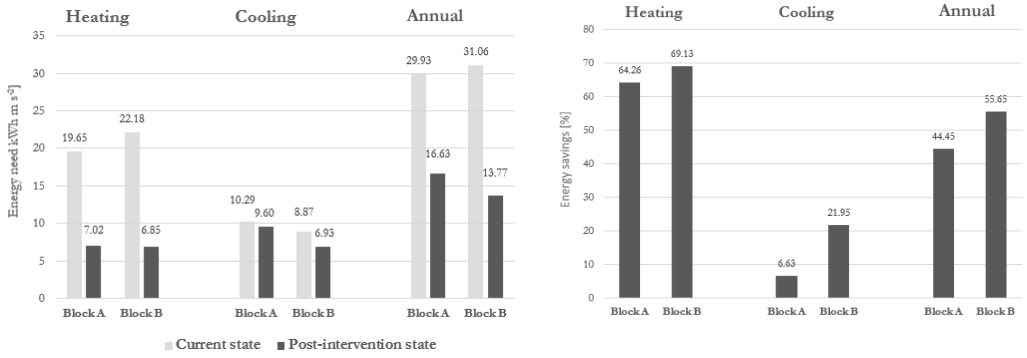

(a) (b)

Figure 6.6. (a) Heating, cooling and total annual energy needs [kWh m^{-2}] of case study 1 at pre- and post-intervention state, and (b) energy demand savings [%]

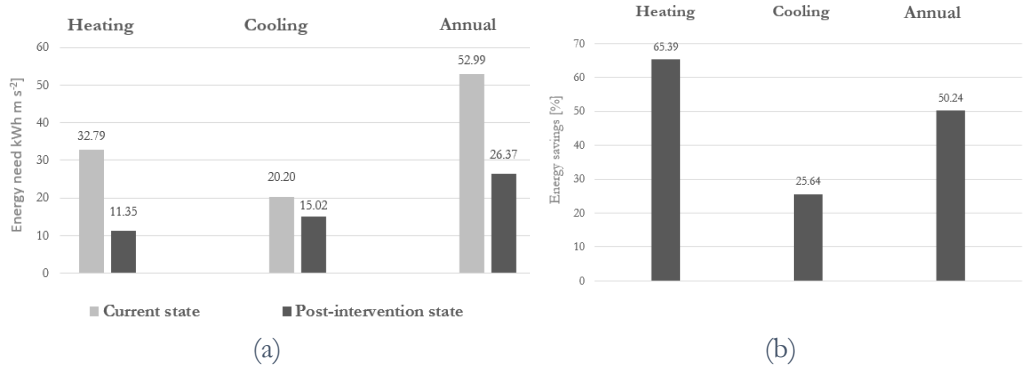

(a) (b)

Figure 6.7. (a) Heating, cooling and total annual energy needs [kWh m^{-2}] of case study 2 at pre- and post-intervention state, and (b) energy demand savings [%]

6.5 References

[1] Inter-Ministerial Decree 26.6.2015. In *Adeguamento Linee Guida Nazionali per la Certificazione Energetica degli Edifici*; Allegato 1; Gazzetta Ufficiale della Repubblica Italiana n.162 del 15.7.2015: Rome, Italy, 2015.

[2] Cascone, S.; Evola, G.; Gagliano, A.; Sciuto, G.; Baroetto Parisi, C. Laboratory and in-Situ measurements for thermal and acoustic performance of straw bales. Sustainability 2019, 11(3), 5592.

[3] Stazi, F.; Ulpiani, G.; Pergolini, M.; Di Perna, C. The role of areal heat capacity and decrement factor in case of hyper insulated buildings: An experimental study. Energy Build. 2018, 176, 310–324.

[4] Ente nazionale italiano di unificazione. Prestazioni Energetiche Degli Edifici Parte 1: Determinazione del Fabbisogno di Energia Termica Dell'edificio per la Climatizzazione Estiva ed Invernale. In UNI/TS 11300-1; UNI: Roma, Italy, 2014

[5] Ente nazionale italiano di unificazione. Prestazione Termica di Finestre, Porte e Chiusure Oscuranti–Calcolo Della Trasmittanza Termica. In UNI 10077-1; UNI: Roma, Italy, 2018.

[6] Ente nazionale italiano di unificazione. Prestazioni Energetiche Degli Edifici Parte 1: Determinazione del Fabbisogno di Energia Termica Dell'edificio per la Climatizzazione Estiva ed Invernale. In UNI/TS 11300-1; UNI: Roma, Italy, 2008-

[7] International Organization for Standardization. Thermal performance of building components-Dynamic thermal characteristics-Calculation methods. In ISO 13786; ISO: Geneva, Switzerland, 2017

7

Construction analysis of the proposed integrated retrofit technology

Summary

This chapter presents a construction analysis of the proposed integrated retrofit technology, both at system and component level, to investigate its technical feasibility, versatility and the main technical requirements. At system level the analysis focuses on potential technical solutions aimed at ensuring the operation of the technology in the event of dampers activation and the quick and easy installation of the main components, as well as their architectural integration. At component level, the analysis focuses on the main technical and safety requirements that the envelope components need to have to ensure high safety performance in use, durability and quality.

Then, the potential and limits of the application of the proposed technology to the existing building stock are examined to evaluate its replicability.

7.1 Analysis at the system level

The main technological issues related to the proposed retrofit technology are here identified to analyse potential technical solutions aimed at: (i) ensuring the correct operation of the retrofit technology during earthquakes; (ii) making the installation and maintenance of the main components quick and easy; (iii) providing a proper architectural integration of each component.
Figure 7.1 reports the overall concept of the retrofit technology.

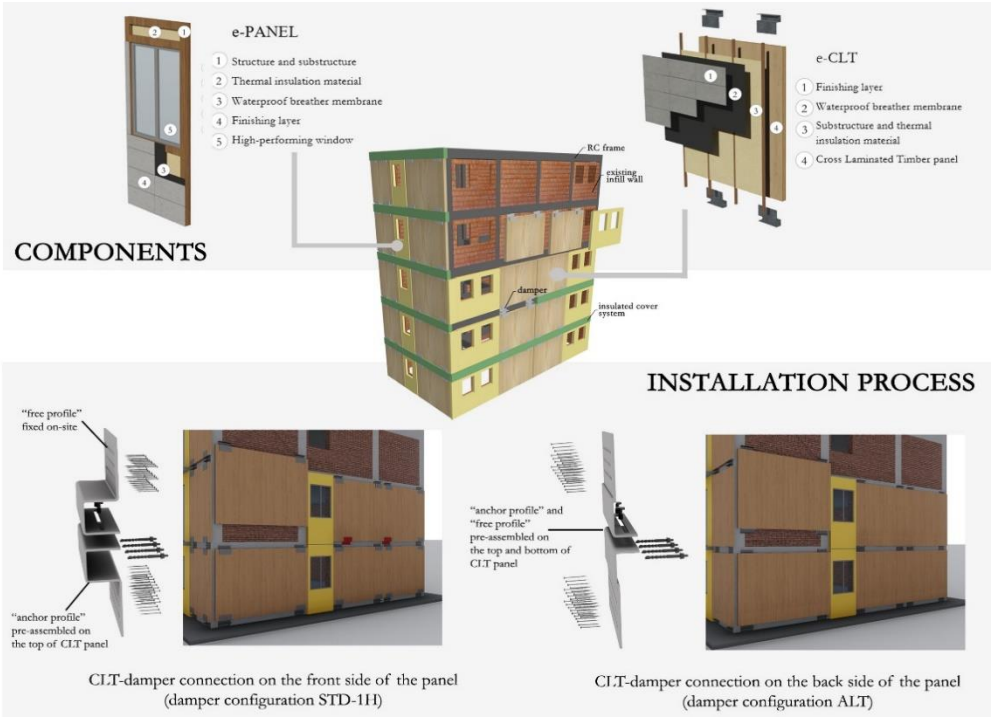

Figure 7.1. Components and installation process of the proposed retrofit technology

The system has been conceived to be prefabricated. Hence, e-CLTs and e-PANELs integrate insulation materials, waterproof breather membranes and finishing layers. The installation will be performed by means of a mobile lifting equipment (cranes, lifting platforms, etc.), which reduce the occupants' disturbance in comparison with traditional scaffodings. The panels installation starts from the ground floor of the building to the top one, by proceeding through adjacent components (from the right

corner to the left or viceversa). In particular, the e-CLT installation first requires to connect the single "anchor profiles" of the dampers located at the ground floor to the existing grade beam or to a new RC beam. Then, the e-CLT is lifted and placed next to the existing outer walls through harness accessories (e.g. tie rods and sling bars) and connected to the existing RC beams through anchors, which are inserted into the holes of the profiles pre-assembled in their top side. Mechanical anchors, in comparison to the chemical ones, may reduce the installation time, since it is not necessary to wait for the resin hardening.

Then, the "anchor profiles" of each e-CLT of a specific storey are connected to the "free profiles" of the e-CLTs applied to the walls of the upper storey. The "free profiles" are installed on-site or are pre-assembled on the bottom side of the e-CLTs, based on the specific damper configuration. More considerations on the installation process were provided in Section 4.1.2.

Unlike the e-CLTs, the e-PANELs are not equipped with friction dampers since they have not a structural role. Therefore, their application on the existing building envelope must be designed to ensure the operation of the e-CLTs in the event of dampers activation, so they need to slide horizontally following the building inter-storey drift. Accordingly, the e-PANELs need to be coupled to the adjacent e-CLTs through connection systems located on their lateral sides. Otherwise, they can be connected to the existing building envelope, providing seismic vertical joints between e-CLT and e-PANEL to let a free horizontal shift of the e-CLTs.

The system application also requires cladding solutions to cover the dampers after the panel installation and to inspect them for maintenance and/or replacement purposes. These cladding solutions need to be easy to install and remove, as well as to be integrated with thermal insulation solutions to reduce the thermal bridges at the beams level.

Overall, the system is suitable to various architectural renovation solutions. The panels can be finished by different cladding materials, according to the users' aesthetic preferences. Metallic cladding entails higher costs but reduced maintenance, while cladding layers made of wooden or plaster boards are less expensive but need more frequent maintenance; moreover, wooden claddings generally are more resistant in case of accidental collision during the shipping and installation of the panels on-site.

Based on the above, potential application solutions of the proposed retrofit technology are illustrated in the following Section to investigate its technical feasibility and versatility.

7.1.1 Application solutions

The application of the proposed retrofit technology has been simulated on the building selected as case study 2 to evaluate its energy efficiency performance (see Chapter 6, Section 6.2.2).

The case study is a five-storey apartment block and represents the residential building stock realized in Italy between the 1950s and the 1980s both for the construction system (RC framed structure with infill walls made of hollow clay bricks) as well as the building typology (multistorey apartment blocks with balconies) (Figure 7.2).

Figure 7.2. Case study building located in the city of Catania (Southern Italy)

Figures 7.3a and 7.4 schematically show the ground floor plan and the fronts of the case study after the application of e-CLTs and e-PANELs, while Figure 7.3b illustrates the stratigrafy of both prefabricated components. The panels arrangement and the thickness of the main material involved (CLT and insulation layer) have been designed according to the dynamic thermal simulations. In the e-CLTs the insulation layer (6 cm-thick wooden fibre) is interposed to 4x4-cm wooden studs. Instead, the e-PANELs consists of a lightweight wooden frame having the same thickness of the e-CLT without the finishing layer, so that the two panels are aligned in-plane. Both prefabricated panels include waterproof breather membranes and a cladding layer made, in this simulation, of wood-plastic composite (WPC) staves (4-cm thick). The total depth of each panel is 20 cm. The structural e-CLT panels have

been assumed equipped with the friction damper configuration that provides the connection to the CLT panel on its front side and two preloaded bolts in a single centred hole (i.e. configuration STD-1H in Section 5.1). This assumption has been made in consideration of the potential improvements that this damper configuration may have to increase its structural efficiency and the advantages in terms of easier installation, maintenance and replacement (see Chapter 4, Section 4.1.2). However, the technical solutions here illustrated can be applied also if the CLT-damper connection is on the back of the timber panel (e.g. using configuration ALT in section 5.1, which resulted more promising in terms of structural efficiency).

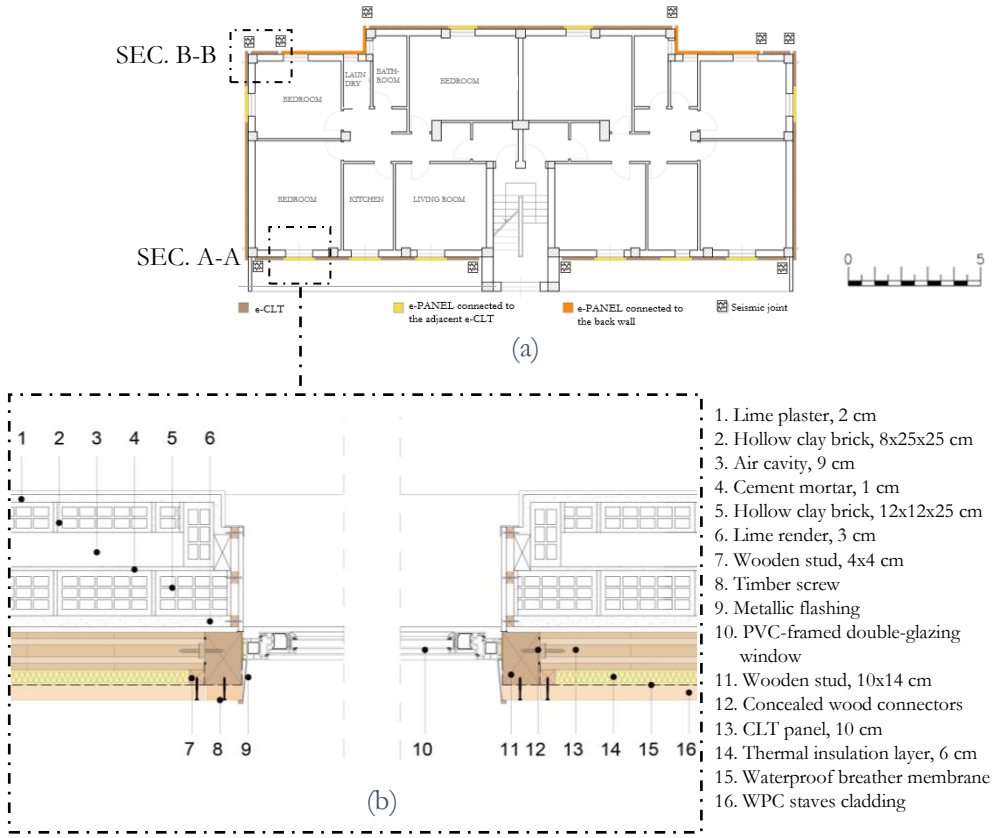

Figure 7.3. (a) Ground floor plan of the case study after the application of e-CLTs and e-PANELs and (b) section A-A (scale 1:20).

Figure 7.4. Application of e-CLTs and e-PANELs on the: (a) east front, (b) north front, (c) west front, (d) south front of the case study.

Considering the main technological issues discussed in Section 7.1, below will be discusses the potential technical solutions concerning:

- lateral connecting systems between the e-CLTs and e-PANELs, if the latter are not connected to the building envelope;
- dampers cladding solutions that allow inspection, maintenance, and possible replacement;
- seismic joints options to allow the translation of the e-CLTs in the event of dampers activation.

7.1.1.1 Lateral connecting systems between e-CLTs and e-PANELs

Common concealed hook connectors could be used as lateral connecting systems between e-CLTs and e-PANELs (Figure 7.5). Nowadays, concealed hook connectors are widely used as walls connectors both in framed and wood panel constructions, and the building market offers a wide choice in terms of sizes and mechanical resistance capacity. Basically, these connectors are made of two brackets that are pre-installed in the side edge of the timber walls to be connected, into proper recesses to avoid the walls overturning (Figure 7.5a). The connection is made by interlocking, without the use of further joints on-site.

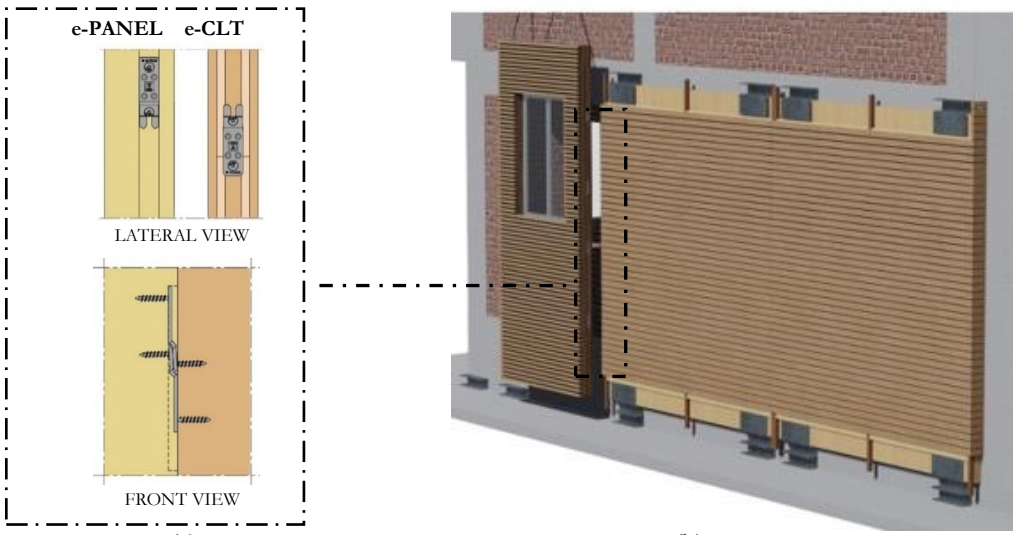

Figure 7.5. (a) example of concealed hook connector between e-CLT and e-PANEL [1] and (a) e-PANEL installation.

By using these lateral connecting systems, the e-PANEL installation requires firstly the connection to the e-CLT already installed, holding/lifting it trought the crane (Figure 7.5b). Subsequently, the adjacent e-CLT is inserted, by hooking it to the e-PANEL, and then to the existing RC beams trough the dampers. In this way, the e-PANEL will be effectively hung on the two adjacent e-CLTs and can be detached from the crane. In presence of balcony, the correct arrangement of the panels for the following mutual connection will be carried out manually, proceeding again for adjacent panels.

7.1.1.2 Dampers cladding solutions

As regards cladding solutions to cover the dampers after the panel installation, different technological solutions have been analysed.

In façades without balconies, a potential solution consists in adding insulation material on-site to avoid thermal bridges, and then fixing the finishing layer directly on the framed substructure of the e-CLT (Figure 7.6). To this end, this substructure need to be left partially exposed during the e-CLT manufacturing process, as shown in Figure 7.5b. Furthermore, a gap between the panels of consecutive storeys is required, in consideration of their relative movements in case of dampers activation. This gap need to be properly protected to prevent the rainwater infiltration, for instance through common drip caps.

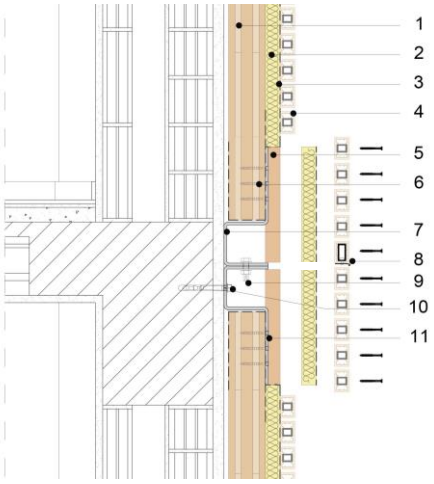

1. CLT panel, 10 cm
2. Wood fiber thermal insulation, 6 cm
3. Waterproof breather membrane
4. WPC staves cladding
5. Wooden framed, section 4x4 cm
6. Screw
7. "Free profile" of the friction damper
8. Drip cap
9. Pretensioned high strength bolt
10. Anchor
11. "Anchor profile" of the friction damper

Figure 7.6. Cladding solution to cover the friction dampers in façades without balconies: Section B-B in Figure 7.4 (scale 1:20).

In façades with balconies, the above-described cladding solution can be used to cover the steel profiles which are pre-assembled on the top of the e-CLT in order to connect them to the existing RC beam (Figure 7.7). Instead, at the bottom of the e-CLT, prefabricated elements with integrated insulation and cladding material can be used to cover the dampers. These elements are fixed to CLT panel on-site through hook connectors to facilitate the e-CLT installation. In fact, the installation solution illustrated in Figure 7.6 is much more complex in this case, since the e-CLT with the exposed framed substructure is more difficult to hand and move between two balconies.
Drip caps or proper technical solutions to protect the panel and the dampers from rainwater are also required.

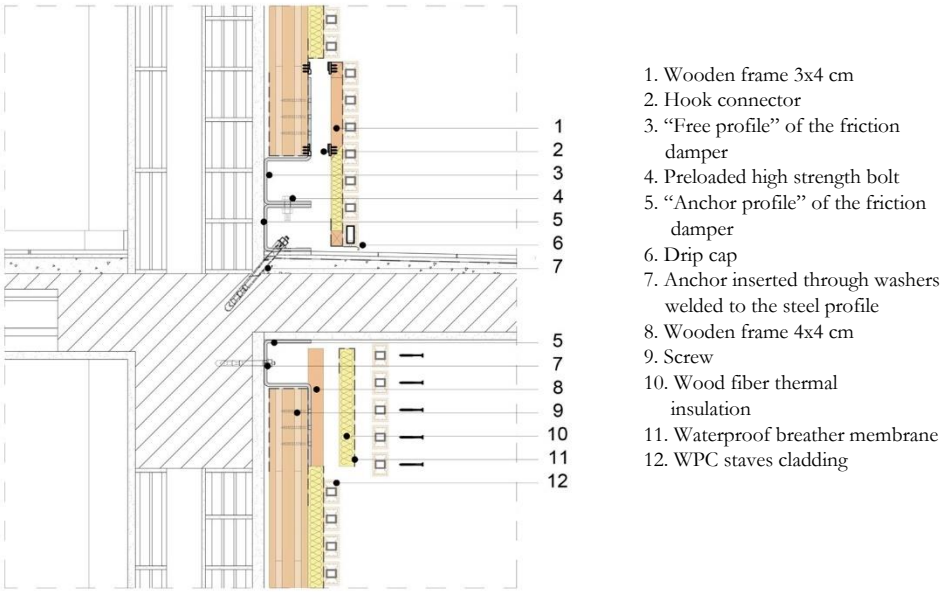

Figure 7.7. Cladding solution to cover the friction dampers in façades with balconies: Section C-C in Figure 7.4 (scale 1:20).

The above-described technical solutions provide a continuous and uniform cladding in each building fronts. These solutions are quite versatile, since they can be adopted with several cladding material, e.g. metallic or plastered cement boards etc. Other cladding options can be also used as architectural motif, e.g. by marking the façades with string courses.

7.1.1.3 Seismic joints

In case of seismic dampers activation, seismic joints are required to allow the translation of the e-CLT panels. As illustrated in Figure 7.3 these joints are needed at the corner of the building, and between the e-CLT and the e-PANEL when the latter is connected directly to the existing wall.

Figure 7.8 shows an example of waterproof and thermal insulating expansion joint which can be used to avoid thermal bridges and ensure waterproofness, but also to facilitate their installation on-site and ensure their architectural integration in the building façades (Figure 7.9a).

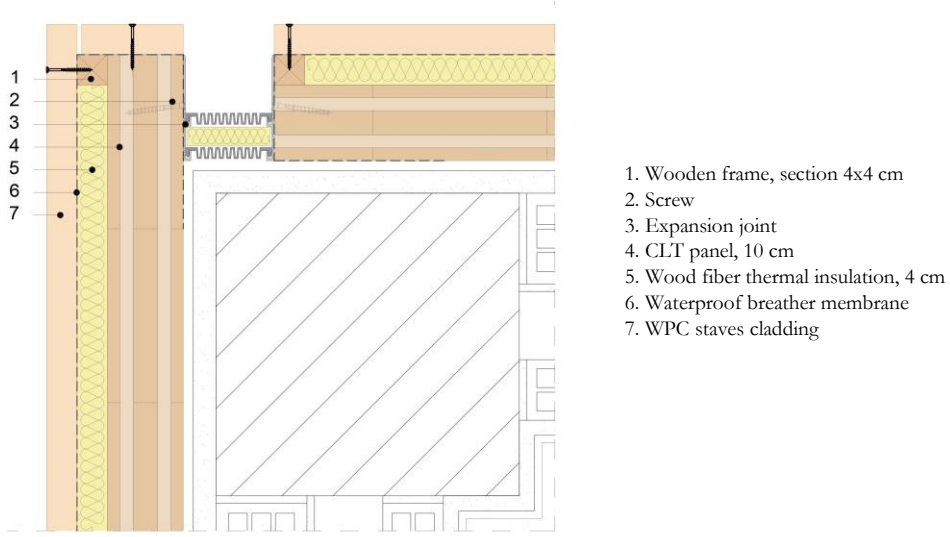

Figure 7.8. Section B-B in Figure 7.3 (scale 1:10)

Figure 7.9b shows the potential of the proposed solutions to improve the architectural image of the case study building.

(a) (b)

Figure 7.9. (a) Architectural integration of expansion joints on the building façade and (b) north front of the case study at post-intervention state.

7.2 Analysis at the component level

The e-CLTs and e-PANELs are applied on the envelope of the building to be renovated as façade elements. Therefore, they need to be designed to ensure a high level of quality and safety for occupants and pedestrians. Specifically, they need to ensure high safety performance in use, without risk of damage when subjected to different load conditions, and in case of fire, preventing or delaying its spread on the building envelope. They also need to ensure high durability and quality performance. To this end, water tightness to rainwater and melting snow under normal climatic conditions is required.
The above-mentioned technical and safety requirements are following examined, referring to the relative current European legislation and technical frameworks.

7.2.1 Fire reaction and fire resistance

The safety in the event of fire is one of the essential requirements that construction products need to have, according to the Regulation (EU) No. 305/2011 of the European Parliament concerning the harmonized conditions for the marketing of construction products. The European classification system for the fire performance of construction products involves different Euroclasses, related both to the fire reaction and fire resistance requirements (Figure 7.10)

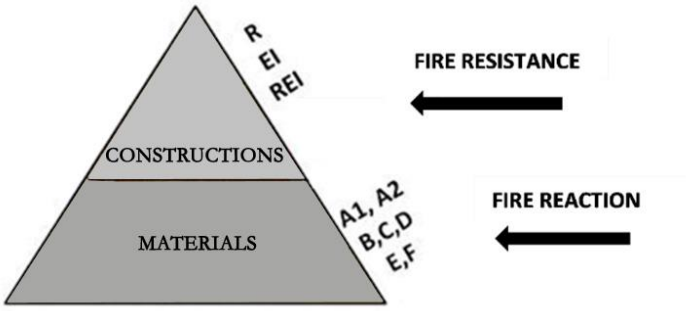

Figure 7.10. European classification system for the fire performance of construction products

The fire reaction parameter is specific to materials and represents their response in contributing by their own decomposition to a fire which are exposed to. The European fire reaction classification is set out in EN 13501-1 [2]. Specifically,

construction products are classified into seven Euroclasses (A1, A2, B, C, D, E, F) based on their reaction-to-fire performance (Table 7.1), which are reported in technical specifications or derived from specific fire tests. The taxonomy used in terms of fire behaviour considers non-combustible materials (A1, A2), very limited to medium contribution to fire (B, C, D) and high contribution to fire (E, F) materials. The European harmonisation of fire classifications also addresses the smoke class (classes s1, s2, s3) and the burning droplets one (classes d0, d1, d2), as reported in Table 7.1. In terms of smoke development, the classes considered are little or no smoke (s1), medium smoke (s2) and heavy smoke (s3). As regard the formation of flaming droplets/particles, the classes are d0 (no droplets within 600 seconds), d1 (droplet form within 600 seconds but do not burn for more than 10 seconds) and d2 (not as d0 or d1).

Definition	**Construction products**		
non-combustible materials	A1		
	A2-s1, d0	A2-s1, d1	A2-s1, d2
	A2-s2, d0	A2-s2, d1	A2-s2, d2
	A2-s3, d0	A2-s3 d1	A2-s3, d2
combustible materials- very limited contribution to fire	B-s1, d0	B-s1, d1	B-s1, d2
	B-s2, d0	B-s2, d1	B-s2, d2
	B-s3, d0	B-s3, d1	B-s3, d2
combustible materials- limited contribution to fire	C-s1, d0	C-s1, d1	C-s1, d2
	C-s2, d0	C-s2, d1	C-s2, d2
	C-s3, d0	C-s3, d1	C-s3, d2
combustible materials- medium contribution to fire	D-s1, d0	D-s1, d1	D-s1, d2
	D-s2, d0	D-s2, d1	D-s2, d2
	D-s3, d0	D-s3, d1	D-s3, d2
combustible materials - highly contribution to fire	E	|	E-d2
combustible materials - easily flammable	F		

Table 7.1. Fire reaction classification of construction products excluding floorings according to EN 13501-1 [2].

Instead, the fire resistance parameter concerns the construction elements and represents the fire exposure time, expressed in minutes, during which they ensure

specific functional performance. In accordance with the European standard EN 13501-2 [3], the fire resistance classification system is based mainly on three performance criteria (R, E, I), or their combination, which are tested by means of specific fire test methods. The tested performance criteria are the following:

- Criterion R – load bearing capacity, i.e. the ability of a construction product to preserve its mechanical characteristics and relevant load capacity under fire;
- Criterion E – integrity, i.e. the ability of a construction product to not allow the passage or production of gases, flames or smokes to areas not exposed to fire;
- Criterion I – insulation, i.e. the ability of a construction product to prevent the temperature increase in the areas non directly exposed to fire.

The test results are obtained in form of a time stamp (i.e., 15, 20, 30, 45, 60 etc.) that shows how many minutes the tested element resists the fire before the threshold for each criterion is exceeded.

The fire safety requirements of façades have a key role in preventing the spread of a fire that can break out inside or outside the building. In fact, façade spread is one of the fastest ways in which a fire can travels through the building. Furthermore, the damage of façade elements in case of fire can be dangerous both for the exodus of occupants and for the rescue workers. However, currently there is no a European harmonised approach to the fire performance assessment and classification for façade systems, but there is a methodological proposal that has been developed within the EU project "Development of a European approach to assess the fire performance of facades" [4] and is currently under definition. Examples of typical products and systems covered by this proposal include exterior thermal insulation composite systems (ETICS), metal composite material cladding systems (MCM), structural insulation panel systems (SIPS), insulated sandwich panel systems, rain screen cladding or ventilated facades, wooden façades etc.

Therefore, at present each EU member country has national regulations or guidance governing the fire performance of façades. These regulations are mainly covered by the existing European system on fire reaction and fire resistance, except for some countries that have introduced additional requirements [4]. For instance, in Italy proper fire safety requirements need to be provided for the façades of residential buildings having a "fire prevention height" (i.e. maximum floors height of the activity) higher than 12 m, and the current technical reference is the Italian guidance on "Fire safety requirements for facades (facings) on civil buildings" [5]. In the

technical guide, a minimum EU fire reaction class equal to B-s3, d0 is prescribed both for the façade insulation products, as well as gaskets sealing materials that occupy an area greater than 10% of the total façade and all the other components on a area greater than 40%. Other lower classes are also allowed if these components are protected by non-combustible materials. The design of suitable fire-resistant components is also suggested, based on the type of façade.
More prescriptive fire safety requirements based on both the building height and the type of building façade will be included in the new Vertical Technical Rule (VTR) concerning "Civil buildings closures", which is currently being trasposed into law and will be part of the Italian Technical Fire Prevention Standards
Based on the above, the e-CLT and e-PANEL components need to be designed in order to ensure specific fire performance requirements, according to the different national regulations, in order to prevent or delay the spread of a possible fire along the building envelope.

7.2.2 Impact resistance

The impact resistance of construction products is part of the requirements of safety in use.
Building façades must cope with different load conditions during their lifetime, from self-weight and wind loads to everyday bumps and scrapes. Consequently, the façades components must to accommodate these loading without risk to the safety of those around the building. At the same time, façade damage has to be minimised in order to ensure its serviceability. The main two types of façade impact are the soft body and the hard body impact. The first one results primarily from people falling or thrown against the façade and results in its general bending. The second one results from the collision of rigid objects to the façade, tending to cause localised punching (e.g. bumps from vehicles and malicious damage from objects such as hammers etc.).
According to ETAG 007 [6] concerning timber building kits, timber walls with well-known internal lining materials, such as standard gypsum boards, wood-based panel products and solid timber boards with suitable thickness and stud spacings, shall generally be accepted to have a satisfactory impact resistance for normal use in

residential housing, office buildings, etc. as long as the deemed to-satisfy conditions are met:
- stud spacing ≤ 0,65 m
- minimum thickness of internal board lining:
• Particleboard type P2-7: t ≥ 10 mm
• Plywood: t ≥ 8 mm
• OSB/2-4: t ≥ 10 mm
• Gypsum plasterboard: t ≥ 10 mm
• Solid wood lining: t ≥ 10 mm
• MDF: t ≥ 10 mm

7.2.3 Water tightness

According to ETAG 007 [6], the e-CLTs and e-PANELs components need to be sufficiently watertight in relation to water from rain and melting snow under normal climatic conditions, including driving rain and snow penetration. To this end, watertight layers need to be integrated into the prefabricated panels and proper technical solutions needs to be designed to prevent the rainwater from entering inside the envelope components provided by the retrofit system.

7.3 Overview of the main target buildings

The type of buildings that best suits the proposed retrofit system, as well as its application limits are here overviewed, according to the results achieved and discussed in this work.

Multistorey residential buildings built between the 1950s and the 1990s are the main target of this system. Overall, the proposed retrofit technology could be effectively adopted in RC framed buildings with outer blind walls where an adequate number of structural e-CLT panels should be applied to ensure the expected level of seismic upgrading.

Detached buildings are better suitable to this intervention, since the e-CLT panels can be externally added to each front. Otherwise, the internal application of the e-CLTs on the walls between two buildings might be required.

If there are colonnades at the ground story of the building, the e-CLT panels must be applied on them. This may be possible if the CLT application does not affect the the use of these areas. The presence of many garages or commercial premises with many and large shop windows may also preclude the e-CLTs application, unless the surface of the openings are reduced during the renovation works. Even a large use of bow-windows limits the application of the structural panels, which in this case cannot be connected directly to the beams of the RC structure, reducing considerably the effectiveness of this solution.

Figure 7.11 shows examples of RC framed buildings suitable to be renovated with the proposed retrofit technology.

This analysis on the main target buildings of the investigated technology is at a preliminary stage, according to the main aim of this Ph.D. thesis. More investigations are required based on the potential developments of the system.

Location: Villa Carcina (BS)

Location: Acireale (CT)

Location: Catania

Location: Concesio (BS)

Location: Catania

Location: Pisogne (BS)

Figure 7.11. Examples of potential buildings to be renovated by the proposed retrofit technology (locations under review: Catania (CT), Southern Italy, high seismic zone – Brescia (BS), Northern Italy, moderate seismic zone).

7.4 References

[1] Knapp Connectors, Walco 40. https://www.knapp verbinder.com/en/products/prefab-walls/

[2] EN 13501-1:2018. Fire classification of construction products and building elements - Part 1: Classification using data from reaction to fire tests. European Committee for Standardization; 2018.

[3] EN 13501-2:2016. Fire classification of construction products and building elements - Part 2: Classification using data from fire resistance tests, excluding ventilation services. European Committee for Standardization; 2016.

[4] Boström L.; Hofmann-Böllinghaus A; Colwell S.; Chiva R.; Tóth P.; Sjöström I.M.J.; Anderson J.; Lange D. Development of a European approach to assess the fire performance of facades, European Commission: 2018.

[5] Technical guidance on "Fire safety requirements for facades (facings) on civil buildings". Department of firefighters, public rescue and civil defense. Circular letter No 5043 of 15th April 2013 (In Italian).

[6] Guideline for European Technical approval of Timber Building Kit (ETAG 007). November 2012.

8

Conclusions

This work proposes an integrated retrofit technology for RC framed buildings, and explores its potential in terms of seismic performance, energy efficiency, and technical feasibility.

The proposed solution consists in cladding the building envelope with a new prefabricated timber-based shell that acts as seismic-resistant and energy-efficient skin for the building, contributing also to renovate its architectural image. The seismic technology that drives this intervention, named e-CLT system, is based on the use of structural CLT panels placed on the exterior walls and connected to the existing RC frame by means of innovative friction dampers. Non-structural wooden-framed panels (named e-PANELs) integrating high-performing windows are coupled to the e-CLT system and applied to the windowed walls to complete the new building envelope and ensure an aesthetic uniformity.

The friction damper has been conceived to keep its efficiency even after earthquakes, and to ensure easy and quick manufacture, installation, and maintenance. It is made by two steel profiles that connect the CLT panels of two consecutive storeys with the existing interposed RC beam. One profile is connected to the RC beam by anchor bolts and to the other one by slotted holes and preloaded high-strength bolts. During an earthquake, when the force transmitted by the damper attains the value of the friction force, the two profiles slide relatively to each other accommodating the building inter-storey drifts and dissipating seismic energy by friction.

The effectiveness of the e-CLT system has been preliminarily investigated through pushover analyses on a one-storey, three-bay RC frame (with and without masonry infills), assuming a rigid-plastic cyclic behaviour of the damper. The results evidenced that the proposed intervention can remarkably enhance the seismic performance of existing RC framed buildings. Specifically, the application of the e-CLT system to the bare frame led to a significant improvement of all the seismically relevant features of the building, i.e. lateral strength, stiffness and energy dissipation capacity. The percentage increase of these features was equal to 40%, 93% and 128%, respectively, by applying the system to a single bay of the frame, while it was approximately double by applying it to two bays. In case of infilled frames, the impact of the e-CLT system in terms of increase of the lateral strength and stiffness was negligible, since the infills make the frame very stiff and strong. Instead, the improvement achieved in terms of energy dissipation capacity remained significant, even in case of infills with high mechanical properties, resulting equal to 82% and

146% by applying the system to one or two bays of the frame, respectively. The application of the e-CLT system also allowed to increase the lateral residual strength of the RC frame after the infill failure. These results proved the potential effectiveness of the system in fulfilling the Near Collapse performance objective that relies mostly on the energy dissipation capacity of the structure.
Based on these promising results, four configurations of the proposed damper have been prototyped and then tested under cyclic loading to investigate the hysteretic behaviour of the steel-to-steel friction connection. Three damper configurations are multiple-bends and provide the connection to the CLT panel on its external side. The differences between these configurations are related to the use of a single centred slotted hole or two not aligned holes for two preloaded bolts and the addition of steel stiffeners. The fourth damper configuration is single-bend and provides the connection to the CLT panel on its internal side.
The main findings of the cyclic loading tests are that:

- The multiple-bend configurations of the damper suffer high torsional deformations due to the large eccentricity between the point of application of the friction force and the reaction force transmitted by the CLT panel. This torsion eventually determines the yielding of the profile in the bends. The arrangement of two preload bolts in a single centred slotted hole instead of two not aligned holes enhances the damper stability, reducing torsion of the damper. Instead, the presence of steel stiffeners has a negative role since it increases the deformations on the bends.
- The single-bend configuration of the damper reduces the above-mentioned eccentricity, avoiding the torsional deformations of the damper and its yielding. The stability of the hysteretic behaviour is higher in the case of low bolts preload value, while it reduces for higher bolts preloads and level of applied displacement.
- The two additional aluminium shim layers and the steel cap plate in the friction connection of the damper prevent the profiles from wearing and the bolt washers from rubbing on the edges of the slotted holes, when the damper activates.

According to the results of the experimental campaign, the single-bend configuration of the damper resulted more promising in terms of structural efficiency. Conversely, this configuration makes its installation and replacement more complex compared to the multiple-bend design. In fact, the connection of the

damper to the internal side of the CLT panel requires to pre-assemble both profiles to the edges of the panel off-site, and then to connect each other on-site. In this way, the alignment of the friction surfaces cannot be guaranteed on-site. Furthermore, the removal of the panels is required in case of dampers replacement, e.g. after an earthquake

Based on the above, future works could be aimed at further optimizing this damper configuration in view of easier installation, maintenance, and replacement.

The energy efficiency and the technical feasibility of the proposed retrofit technology have been also analysed with promising results.

Dynamic thermal simulations performed on typical Italian multi-storey residential apartment buildings, both at pre- and post-intervention state, showed a 50% reduction of the total annual energy demand for heating and cooling. The highest energy savings has been observed for winter heating, with a reduction equal or higher than 65%.

As regard the technical feasibility of the proposed system, proper technical solutions are required to ensure a proper operation of the e-CLT technology in the event of dampers activation and the architectural integration of the main components. These technical solutions concern lateral connecting systems between the two types of panels (e-CLT and e-PANEL) and cladding options for covering the dampers after the panels installation, allowing their inspection, maintenance, and replacement. Suitable expansion joints to allow the translation of the e-CLTs during dampers activation have been analysed, too.

Acknowledgements

I would like to express my sincere gratitude to my supervisors prof. Giuseppe Margani and prof. Edoardo Marino for their continuous support of my doctoral studies, for their guidance and time, for giving me the opportunity to grow as a research student, for being the best mentors for me. I will always be thankful to them.

Besides my supervisors, I would like to thank all the members of my thesis committee: prof. Gianpiero Evola, dr. Alberto Moretti, and prof. Roberto Tomasi, whose constant support has been essential for accomplishing this work. In particular, thanks to dr. Alberto Moretti for allowing the damper prototyping at the Adveco factory and providing the damper specimens, and prof. Roberto Tomasi for allowing the experimental campaign at the laboratories of the NMBU.

Many thanks to all the technical and administrative staff of the Adveco company for their continuous assistance during the dampers prototyping. Thank you all so much for having satisfied my constant curiosity, conveying me the passion for the steel processing industry.

Many thanks to eng. Francesco Boggian, for the continuous and significant remote collaboration during the experimental campaign, at the midst of the Covid-19 emergency period. Thanks to the master student Mathilde Marthinsen for her relevant contribution during the testing campaign, and the head engineer Øyvind Hansen of NMBU for his support regarding the design and production of the test setup.

Thanks to eng. Francesca Barbagallo, for her precious scientific input and her constant availability.
Thanks to eng. Martina Battiato and Giulia Fiore for their precious collaboration as undergraduates.

Thanks to the Coordinator of the XXXIV cycle of the Ph.D. Course in Evaluation and Mitigation of Urban and Land Risks of University of Catania, prof. Massimo Cuomo, and all the members of the doctoral College.

Annex

Numerical model source code

Source code of the numerical model of the case study RC frame at post-intervention state in configuration 1 (see Chapter 4, Section 4.2.2)

OpenSees v. 2.5.0 .

```
wipe;
model BasicBuilder -ndm 3 -ndf 6

############# DATASET ##############
# name of output folder
set  dataDir     Output;

#Variables set
set   x00   0.0;
set   x0    [expr $x00 + 3.7];
set   x01   [expr $x0 + 0.455];
set   x02   [expr $x01 + 0.09];
set   x03   [expr $x02 + 0.07];
set   x04   [expr $x03 + 0.065];
set   x05   [expr $x04 + 0.065];
set   x06   [expr $x05 + 0.07];
set   x07   [expr $x06 + 0.09];
set   x1    [expr $x07 + 0.165];
set   x11   [expr $x1 + 0.39];
set   x12   [expr $x11 + 0.165];
set   x13   [expr $x12 + 0.09];
set   x14   [expr $x13 + 0.07];
set   x2    [expr $x14 + 0.065];
set   x21   [expr $x2 + 0.065];
set   x22   [expr $x21 + 0.07];
set   x23   [expr $x22 + 0.09];
set   x24   [expr $x23 + 0.165];
set   x3    [expr $x24 + 0.39];
set   x31   [expr $x3 + 0.165];
set   x32   [expr $x31 + 0.09];
set   x33   [expr $x32 + 0.07];
set   x34   [expr $x33 + 0.065];
set   x35   [expr $x34 + 0.065];
set   x36   [expr $x35 + 0.07];
set   x37   [expr $x36 + 0.09];
set   x4    [expr $x37 + 0.455];
set   x5    [expr $x4 + 3.7];

set   y0     0.0;
set   y01   [expr $y0 + 0.06];
set   y02   [expr $y01 + 0.12];
set   y1    [expr $y02 + 0.005];
set   y2    [expr $y1 + 0.975];
set   y3    [expr $y2 + 0.975];
set   y4    [expr $y3 + 0.975];
set   y41   [expr $y4 + 0.005];
set   y5    [expr $y41 + 0.06];
set   y51   [expr $y5 + 0.06];

# unit of measurement: m, s, kN

###################################

file mkdir $dataDir

puts "Nodes"
### RC frame
node      01     $x00      $y0     0.0
node      02     $x0       $y0     0.0
node      03     $x4       $y0     0.0
node      04     $x5       $y0     0.0
node      11     $x00      $y5     0.0
node      12     $x0       $y5     0.0
node      13     $x4       $y5     0.0
node      14     $x5       $y5     0.0
node      71     $x02      $y5     0.0
node      73     $x06      $y5     0.0
node      77     $x32      $y5     0.0
node      79     $x36      $y5     0.0

### Damper SX
node    4111     $x01      $y0     0.0
node    4112     $x02      $y0     0.0
node    4113     $x03      $y0     0.0
node    4114     $x04      $y0     0.0
node    4115     $x05      $y0     0.0
node    4116     $x06      $y0     0.0
node    4117     $x07      $y0     0.0

node    4121     $x01     $y01     0.0
node    4122     $x02     $y01     0.0
node    4123     $x03     $y01     0.0
node    4124     $x04     $y01     0.0
node    4125     $x05     $y01     0.0
node    4126     $x06     $y01     0.0
```

```
node    4127     $x07     $y01     0.0

node    4131     $x01     $y01     0.0
node    4132     $x02     $y01     0.0
node    4133     $x03     $y01     0.0
node    4134     $x04     $y01     0.0
node    4135     $x05     $y01     0.0
node    4136     $x06     $y01     0.0
node    4137     $x07     $y01     0.0

node    4141     $x01     $y02     0.0
node    4142     $x02     $y02     0.0
node    4143     $x03     $y02     0.0
node    4144     $x04     $y02     0.0
node    4145     $x05     $y02     0.0
node    4146     $x06     $y02     0.0
node    4147     $x07     $y02     0.0

### Damper DX
node    4311     $x31      $y0     0.0
node    4312     $x32      $y0     0.0
node    4313     $x33      $y0     0.0
node    4314     $x34      $y0     0.0
node    4315     $x35      $y0     0.0
node    4316     $x36      $y0     0.0
node    4317     $x37      $y0     0.0

node    4321     $x31     $y01     0.0
node    4322     $x32     $y01     0.0
node    4323     $x33     $y01     0.0
node    4324     $x34     $y01     0.0
node    4325     $x35     $y01     0.0
node    4326     $x36     $y01     0.0
node    4327     $x37     $y01     0.0

node    4331     $x31     $y01     0.0
node    4332     $x32     $y01     0.0
node    4333     $x33     $y01     0.0
node    4334     $x34     $y01     0.0
node    4335     $x35     $y01     0.0
node    4336     $x36     $y01     0.0
node    4337     $x37     $y01     0.0

node    4341     $x31     $y02     0.0
node    4342     $x32     $y02     0.0
node    4343     $x33     $y02     0.0
node    4344     $x34     $y02     0.0
node    4345     $x35     $y02     0.0
node    4346     $x36     $y02     0.0
node    4347     $x37     $y02     0.0

### Anchor profile SX
node    4151     $x01     $y41     0.0
node    4152     $x02     $y41     0.0
node    4153     $x03     $y41     0.0
node    4154     $x04     $y41     0.0
node    4155     $x05     $y41     0.0
node    4156     $x06     $y41     0.0
node    4157     $x07     $y41     0.0

node    4161     $x01      $y5     0.0
node    4162     $x02      $y5     0.0
node    4163     $x03      $y5     0.0
node    4164     $x04      $y5     0.0
node    4165     $x05      $y5     0.0
node    4166     $x06      $y5     0.0
node    4167     $x07      $y5     0.0

node    4171     $x01     $y51     0.0
node    4172     $x02     $y51     0.0
node    4173     $x03     $y51     0.0
node    4174     $x04     $y51     0.0
node    4175     $x05     $y51     0.0
node    4176     $x06     $y51     0.0
node    4177     $x07     $y51     0.0

### Anchor profile DX
node    4351     $x31     $y41     0.0
node    4352     $x32     $y41     0.0
node    4353     $x33     $y41     0.0
node    4354     $x34     $y41     0.0
node    4355     $x35     $y41     0.0
node    4356     $x36     $y41     0.0
node    4357     $x37     $y41     0.0

```

```
node    4361     $x31      $y5     0.0
node    4362     $x32      $y5     0.0
node    4363     $x33      $y5     0.0
node    4364     $x34      $y5     0.0
node    4365     $x35      $y5     0.0
node    4366     $x36      $y5     0.0
node    4367     $x37      $y5     0.0

node    4371     $x31     $y51     0.0
node    4372     $x32     $y51     0.0
node    4373     $x33     $y51     0.0
node    4374     $x34     $y51     0.0
node    4375     $x35     $y51     0.0
node    4376     $x36     $y51     0.0
node    4377     $x37     $y51     0.0

### CLT panel
node     101      $x0      $y1     0.0
node     102     $x02      $y1     0.0
node     103     $x04      $y1     0.0
node     104     $x06      $y1     0.0
node     105      $x1      $y1     0.0
node     106      $x2      $y1     0.0
node     107      $x3      $y1     0.0
node     108     $x32      $y1     0.0
node     109     $x34      $y1     0.0
node     1010    $x36      $y1     0.0
node     1011     $x4      $y1     0.0

node     111      $x0      $y2     0.0
node     112     $x02      $y2     0.0
node     113     $x04      $y2     0.0
node     114     $x06      $y2     0.0
node     115      $x1      $y2     0.0
node     116      $x2      $y2     0.0
node     117      $x3      $y2     0.0
node     118     $x32      $y2     0.0
node     119     $x34      $y2     0.0
node     1110    $x36      $y2     0.0
node     1111     $x4      $y2     0.0

node     121      $x0      $y3     0.0
node     122     $x02      $y3     0.0
node     123     $x04      $y3     0.0
node     124     $x06      $y3     0.0
node     125      $x1      $y3     0.0
node     126      $x2      $y3     0.0
node     127      $x3      $y3     0.0
node     128     $x32      $y3     0.0
node     129     $x34      $y3     0.0
node     1210    $x36      $y3     0.0
node     1211     $x4      $y3     0.0

node     131      $x0      $y4     0.0
node     132     $x02      $y4     0.0
node     133     $x04      $y4     0.0
node     134     $x06      $y4     0.0
node     135      $x1      $y4     0.0
node     136      $x2      $y4     0.0
node     137      $x3      $y4     0.0
node     138     $x32      $y4     0.0
node     139     $x34      $y4     0.0
node     1310    $x36      $y4     0.0
node     1311     $x4      $y4     0.0

puts "Boundary conditions"
#fix  $NodeTag      DX     DY     DZ     RX     RY     RZ
### RC Frame
fix      01          1      1      1      1      1      1
fix      02          1      1      1      1      1      1
fix      03          1      1      1      1      1      1
fix      04          1      1      1      1      1      1
fix      11          0      0      1      1      1      0
fix      12          0      0      1      1      1      0
fix      13          0      0      1      1      1      0
fix      14          0      0      1      1      1      0
fix      71          0      0      1      1      1      0
fix      73          0      0      1      1      1      0
fix      77          0      0      1      1      1      0
fix      79          0      0      1      1      1      0

### Base anchoring
fix    4112          1      1      1      1      1      0
fix    4116          1      1      1      1      1      0
fix    4312          1      1      1      1      1      0
```

```
fix    4316          1      1      1      1      1      0

### Damper SX
fix    4111          0      0      1      1      1      0
fix    4113          0      0      1      1      1      0
fix    4114          0      0      1      1      1      0
fix    4115          0      0      1      1      1      0
fix    4117          0      0      1      1      1      0

fix    4121          0      0      1      1      1      0
fix    4122          0      0      1      1      1      0
fix    4123          0      0      1      1      1      0
fix    4124          0      0      1      1      1      0
fix    4125          0      0      1      1      1      0
fix    4126          0      0      1      1      1      0
fix    4127          0      0      1      1      1      0

fix    4131          0      0      1      1      1      0
fix    4132          0      0      1      1      1      0
fix    4133          0      0      1      1      1      0
fix    4134          0      0      1      1      1      0
fix    4135          0      0      1      1      1      0
fix    4136          0      0      1      1      1      0
fix    4137          0      0      1      1      1      0

fix    4141          0      0      1      1      1      0
fix    4142          0      0      1      1      1      0
fix    4143          0      0      1      1      1      0
fix    4144          0      0      1      1      1      0
fix    4145          0      0      1      1      1      0
fix    4146          0      0      1      1      1      0
fix    4147          0      0      1      1      1      0

### Damper DX
fix    4311          0      0      1      1      1      0
fix    4313          0      0      1      1      1      0
fix    4314          0      0      1      1      1      0
fix    4315          0      0      1      1      1      0
fix    4317          0      0      1      1      1      0

fix    4321          0      0      1      1      1      0
fix    4322          0      0      1      1      1      0
fix    4323          0      0      1      1      1      0
fix    4324          0      0      1      1      1      0
fix    4325          0      0      1      1      1      0
fix    4326          0      0      1      1      1      0
fix    4327          0      0      1      1      1      0

fix    4331          0      0      1      1      1      0
fix    4332          0      0      1      1      1      0
fix    4333          0      0      1      1      1      0
fix    4334          0      0      1      1      1      0
fix    4335          0      0      1      1      1      0
fix    4336          0      0      1      1      1      0
fix    4337          0      0      1      1      1      0

fix    4341          0      0      1      1      1      0
fix    4342          0      0      1      1      1      0
fix    4343          0      0      1      1      1      0
fix    4344          0      0      1      1      1      0
fix    4345          0      0      1      1      1      0
fix    4346          0      0      1      1      1      0
fix    4347          0      0      1      1      1      0

### Anchor profile SX
fix    4151          0      0      1      1      1      0
fix    4152          0      0      1      1      1      0
fix    4153          0      0      1      1      1      0
fix    4154          0      0      1      1      1      0
fix    4155          0      0      1      1      1      0
fix    4156          0      0      1      1      1      0
fix    4157          0      0      1      1      1      0

fix    4161          0      0      1      1      1      0
fix    4162          0      0      1      1      1      0
fix    4163          0      0      1      1      1      0
fix    4164          0      0      1      1      1      0
fix    4165          0      0      1      1      1      0
fix    4166          0      0      1      1      1      0
fix    4167          0      0      1      1      1      0

fix    4171          0      0      1      1      1      0
fix    4172          0      0      1      1      1      0
fix    4173          0      0      1      1      1      0
fix    4174          0      0      1      1      1      0
```

```
fix    4175          0      0      1      1      1      0
fix    4176          0      0      1      1      1      0
fix    4177          0      0      1      1      1      0

### Anchor profile DX
fix    4351          0      0      1      1      1      0
fix    4352          0      0      1      1      1      0
fix    4353          0      0      1      1      1      0
fix    4354          0      0      1      1      1      0
fix    4355          0      0      1      1      1      0
fix    4356          0      0      1      1      1      0
fix    4357          0      0      1      1      1      0

fix    4361          0      0      1      1      1      0
fix    4362          0      0      1      1      1      0
fix    4363          0      0      1      1      1      0
fix    4364          0      0      1      1      1      0
fix    4365          0      0      1      1      1      0
fix    4366          0      0      1      1      1      0
fix    4367          0      0      1      1      1      0

fix    4371          0      0      1      1      1      0
fix    4372          0      0      1      1      1      0
fix    4373          0      0      1      1      1      0
fix    4374          0      0      1      1      1      0
fix    4375          0      0      1      1      1      0
fix    4376          0      0      1      1      1      0
fix    4377          0      0      1      1      1      0

### CLT panel
fix     101          0      0      1      1      1      0
fix     102          0      0      1      1      1      0
fix     103          0      0      1      1      1      0
fix     104          0      0      1      1      1      0
fix     105          0      0      1      1      1      0
fix     106          0      0      1      1      1      0
fix     107          0      0      1      1      1      0
fix     108          0      0      1      1      1      0
fix     109          0      0      1      1      1      0
fix     1010         0      0      1      1      1      0
fix     1011         0      0      1      1      1      0

fix     111          0      0      1      1      1      0
fix     112          0      0      1      1      1      0
fix     113          0      0      1      1      1      0
fix     114          0      0      1      1      1      0
fix     115          0      0      1      1      1      0
fix     116          0      0      1      1      1      0
fix     117          0      0      1      1      1      0
fix     118          0      0      1      1      1      0
fix     119          0      0      1      1      1      0
fix     1110         0      0      1      1      1      0
fix     1111         0      0      1      1      1      0

fix     121          0      0      1      1      1      0
fix     122          0      0      1      1      1      0
fix     123          0      0      1      1      1      0
fix     124          0      0      1      1      1      0
fix     125          0      0      1      1      1      0
fix     126          0      0      1      1      1      0
fix     127          0      0      1      1      1      0
fix     128          0      0      1      1      1      0
fix     129          0      0      1      1      1      0
fix     1210         0      0      1      1      1      0
fix     1211         0      0      1      1      1      0

fix     131          0      0      1      1      1      0
fix     132          0      0      1      1      1      0
fix     133          0      0      1      1      1      0
fix     134          0      0      1      1      1      0
fix     135          0      0      1      1      1      0
fix     136          0      0      1      1      1      0
fix     137          0      0      1      1      1      0
fix     138          0      0      1      1      1      0
fix     139          0      0      1      1      1      0
fix     1310         0      0      1      1      1      0
fix     1311         0      0      1      1      1      0

puts "Materials"
### RC frame
#uniaxialMaterial Concrete04 $Tag   $fc     $ec     $ecu    $Ec     <$ft $et>        <$beta>
#columns - concrete core
uniaxialMaterial Concrete04     1  -25000  -0.002  -0.0035  31500000  0  0             0.1;
#columns - concrete cover
uniaxialMaterial Concrete04     2  -25000  -0.002  -0.0035  31500000  0  0             0.1;
```

```
#beams - concrete core
uniaxialMaterial Concrete04     3  -25000  -0.002  -0.0035  31500000  0  0             0.1;
#beams - concrete cover
uniaxialMaterial Concrete04     4  -25000  -0.002  -0.0035  31500000  0  0             0.1;

#uniaxialMaterial Steel02    $Tag   $Fy     $Es          $b       $R0    $cR1    $cR2
# steel rebars
uniaxialMaterial  Steel02       5   380000  200000000    0.0066   20     0.925   0.15;

### CLT panel
#nDMaterial ElasticOrthotropic $Tag $Ex     $Ey       $Ez   $vxy $vyz $vzx  $Gxy   $Gyz $Gzx <$rho>
nDMaterial ElasticOrthotropic   6  4622000  6748000  370000  0.0  0.0  0.0  500000  0.0  0.0 4.1202;

##### DAMPER #####
### Steel profile
#uniaxialMaterial Elastic             $matTag      $E
uniaxialMaterial Elastic               7           210000000;

### Friction surface (Direction X)
#uniaxialMaterial Steel01             $matTag      $Fy         $E0            $b
uniaxialMaterial Steel01               8           4.2857      42800.57       0.00001;

### Friction surface (Direction Y)
#uniaxialMaterial ENT                 $matTag      $E
uniaxialMaterial ENT                   9           21000000000000;

### Pretensioned bolts (Direction Y)
#uniaxialMaterial Elastic             $matTag      $E             <$eta>
uniaxialMaterial Elastic               10          21000000000000   0.0;

### Screws
#uniaxialMaterial Elastic             $matTag      $E
uniaxialMaterial Elastic               11          59878;

### Anchor bolts (Direction X)
#uniaxialMaterial Elastic             $matTag       $E
uniaxialMaterial Elastic               12           21000000000000;

### Truss
#uniaxialMateria Elastic              $matTag       $E               <eta>       <Eneg>
uniaxialMaterial  Elastic              16           200000000000      0.0       0.00001

puts "Sections"
### CLT panel
#section PlateFiber                   $secTag      $matTag      $h
section PlateFiber                     1           6            0.1;

### Damper profiles
#section ElasticMembranePlateSection  $secTag      $E           $nu          $h
section ElasticMembranePlateSection    2           210000000    0.3       0.008;

### Columns 30X30
section Fiber                  3   {

#patch rect $matTag $numSubdivY $numSubdivZ      $yI       $zI       $yJ       $zJ
patch rect        1          48          1     -0.12     -0.12      0.12      0.12;  #core
patch rect        2          48          1     -0.15     -0.12     -0.12      0.12;  #cover //z, y<0
patch rect        2          48          1      0.12     -0.12      0.15      0.12;  #cover //z, y>0
patch rect        2           6          1     -0.15      0.12      0.15      0.15;  #cover //y, z>0
patch rect        2           6          1     -0.15     -0.15      0.15     -0.12;  #cover //y, z<0
#fiber        $yLoc       $zLoc          $A   $matTag
fiber           -0.12      0.12    0.000154         5
fiber           -0.12     -0.12    0.000154         5
fiber            0.12      0.12    0.000154         5
fiber            0.12     -0.12    0.000154         5
};

### Beam 30X50
section Fiber                  4   {
#patch rect $matTag $numSubdivY $numSubdivZ      $yI       $zI       $yJ       $zJ
patch rect        3          1          88     -0.12     -0.22      0.12      0.22;  #core
patch rect        4          1          88     -0.15     -0.22     -0.12      0.22;  #cover //z, y<0
patch rect        4          1          88      0.12     -0.22      0.15      0.22;  #cover //z, y>0
patch rect        4          1           6     -0.15      0.22      0.15      0.25;  #cover //y, z>0
patch rect        4          1           6     -0.15     -0.25      0.15     -0.22;  #cover //y, z<0
#fiber        $yLoc       $zLoc          $A   $matTag
fiber           -0.12      0.22    0.000154         5
fiber           -0.04      0.22    0.000154         5
fiber            0.04      0.22    0.000154         5
fiber            0.12      0.22    0.000154         5
fiber           -0.12     -0.22    0.000154         5
fiber           -0.04     -0.22    0.000154         5
fiber            0.00     -0.22    0.000154         5
fiber            0.04     -0.22    0.000154         5
fiber            0.12     -0.22    0.000154         5
```

```
};

puts "Elements"
geomTransf Linear 1   0 1 0
geomTransf Linear 2   0 0 -1

### Columns
#element beamWithHinges   $eleTag  $iNode $jNode  $secTagI  $Lpi $secTagJ $Lpj  $E        $A     $Iz       $Iy       $G
#$J  $transfTag <-mass $massDens> <-iter $maxIters $tol>
element beamWithHinges    80111     01     11     3         0.3    3    0.3    25200000   0.09   0.000675  0.000675  0.0001
0.0000001  2   -iter    150    1.0e-8
element beamWithHinges    80212     02     12     3         0.3    3    0.3    25200000   0.09   0.000675  0.000675  0.0001
0.0000001  2   -iter    150    1.0e-8
element beamWithHinges    80313     03     13     3         0.3    3    0.3    25200000   0.09   0.000675  0.000675  0.0001
0.0000001  2   -iter    150    1.0e-8
element beamWithHinges    80414     04     14     3         0.3    3    0.3    25200000   0.09   0.000675  0.000675  0.0001
0.0000001  2    -iter    150    1.0e-8

#### Beams - plastic part
#element nonlinearBeamColumn      $eleTag   $iNode $jNode  $numIntgrPts  $secTag  $transfTag <-mass $massDens> <-iter $maxIters $tol>
element nonlinearBeamColumn       91112     11     12       5     4    1    -iter    150    1.0e-8
element nonlinearBeamColumn       91271     12     71       3     4    1    -iter    150    1.0e-8
element nonlinearBeamColumn       97377     73     77       5     4    1    -iter    150    1.0e-8
element nonlinearBeamColumn       97913     79     13       3     4    1    -iter    150    1.0e-8
element nonlinearBeamColumn       91314     13     14       5     4    1    -iter    150    1.0e-8

#### Beams - elastic part
#element elasticBeamColumn        $eleTag   $iNode $jNode   $A    $E        $G        $J            $Iy         $Iz
$transfTag
element elasticBeamColumn         97173     71     73       0.15  25200000  0.0001    0.0000001     0.003125    0.001125       1
element elasticBeamColumn         97779     77     79       0.15  25200000  0.0001    0.0000001     0.003125    0.001125       1

######################################## PROFILES ##########################################
################################### PROFILES - DAMPER SX ###################################
### Profiles Web
#element ShellMITC4               $eleTag        $iNode   $jNode   $kNode   $lNode     $secTag
element ShellMITC4                 411121          4111     4112     4122     4121           2
element ShellMITC4                 411222          4112     4113     4123     4122           2
element ShellMITC4                 411323          4113     4114     4124     4123           2
element ShellMITC4                 411424          4114     4115     4125     4124           2
element ShellMITC4                 411525          4115     4116     4126     4125           2
element ShellMITC4                 411626          4116     4117     4127     4126           2

element ShellMITC4                 413141          4131     4132     4142     4141           2
element ShellMITC4                 413242          4132     4133     4143     4142           2
element ShellMITC4                 413343          4133     4134     4144     4143           2
element ShellMITC4                 413444          4134     4135     4145     4144           2
element ShellMITC4                 413545          4135     4136     4146     4145           2
element ShellMITC4                 413646          4136     4137     4147     4146           2

### Profiles Flanges
#element truss                    $eleTag        $iNode   $jNode              $A     $matTag
element truss                      512122          4121     4122         0.000904           7
element truss                      512223          4122     4123         0.000904           7
element truss                      512324          4123     4124         0.000904           7
element truss                      512425          4124     4125         0.000904           7
element truss                      512526          4125     4126         0.000904           7
element truss                      512627          4126     4127         0.000904           7
element truss                      513132          4131     4132         0.000904           7
element truss                      513233          4132     4133         0.000904           7
element truss                      513334          4133     4134         0.000904           7
element truss                      513435          4134     4135         0.000904           7
element truss                      513536          4135     4136         0.000904           7
element truss                      513637          4136     4137         0.000904           7
element truss                      514142          4141     4142         0.000904           7
element truss                      514243          4142     4143         0.000904           7
element truss                      514344          4143     4144         0.000904           7
element truss                      514445          4144     4145         0.000904           7
element truss                      514546          4145     4146         0.000904           7
element truss                      514647          4146     4147         0.000904           7


################################### PROFILES - DAMPER DX ###################################
#### Profiles Web
#element ShellMITC4               $eleTag        $iNode   $jNode   $kNode   $lNode     $secTag
element ShellMITC4                 431121          4311     4312     4322     4321           2
element ShellMITC4                 431222          4312     4313     4323     4322           2
element ShellMITC4                 431323          4313     4314     4324     4323           2
element ShellMITC4                 431424          4314     4315     4325     4324           2
element ShellMITC4                 431525          4315     4316     4326     4325           2
element ShellMITC4                 431626          4316     4317     4327     4326           2

element ShellMITC4                 433141          4331     4332     4342     4341           2
element ShellMITC4                 433242          4332     4333     4343     4342           2
element ShellMITC4                 433343          4333     4334     4344     4343           2
```

```
element ShellMITC4                433444          4334     4335     4345     4344           2
element ShellMITC4                433545          4335     4336     4346     4345           2
element ShellMITC4                433646          4336     4337     4347     4346           2

#### Profiles Flanges
#element truss                   $eleTag        $iNode   $jNode              $A      $matTag
element truss                     532122          4321     4322        0.000904           7
element truss                     532223          4322     4323        0.000904           7
element truss                     532324          4323     4324        0.000904           7
element truss                     532425          4324     4325        0.000904           7
element truss                     532526          4325     4326        0.000904           7
element truss                     532627          4326     4327        0.000904           7
element truss                     533132          4331     4332        0.000904           7
element truss                     533233          4332     4333        0.000904           7
element truss                     533334          4333     4334        0.000904           7
element truss                     533435          4334     4335        0.000904           7
element truss                     533536          4335     4336        0.000904           7
element truss                     533637          4336     4337        0.000904           7
element truss                     534142          4341     4342        0.000904           7
element truss                     534243          4342     4343        0.000904           7
element truss                     534344          4343     4344        0.000904           7
element truss                     534445          4344     4345        0.000904           7
element truss                     534546          4345     4346        0.000904           7
element truss                     534647          4346     4347        0.000904           7

################################### PROFILES - ANCHOR SX #######################################
#### Profiles Web
#element ShellMITC4               $eleTag        $iNode   $jNode   $kNode   $lNode     $secTag
element ShellMITC4                415161          4151     4152     4162     4161           2
element ShellMITC4                415262          4152     4153     4163     4162           2
element ShellMITC4                415363          4153     4154     4164     4163           2
element ShellMITC4                415464          4154     4155     4165     4164           2
element ShellMITC4                415565          4155     4156     4166     4165           2
element ShellMITC4                415666          4156     4157     4167     4166           2

element ShellMITC4                416171          4161     4162     4172     4171           2
element ShellMITC4                416272          4162     4163     4173     4172           2
element ShellMITC4                416373          4163     4164     4174     4173           2
element ShellMITC4                416474          4164     4165     4175     4174           2
element ShellMITC4                416575          4165     4166     4176     4175           2
element ShellMITC4                416676          4166     4167     4177     4176           2

### Profiles Flanges
#element truss                   $eleTag        $iNode   $jNode              $A      $matTag
element truss                     515152          4151     4152        0.000904           7
element truss                     515253          4152     4153        0.000904           7
element truss                     515354          4153     4154        0.000904           7
element truss                     515455          4154     4155        0.000904           7
element truss                     515556          4155     4156        0.000904           7
element truss                     515657          4156     4157        0.000904           7
element truss                     517172          4171     4172        0.000904           7
element truss                     517273          4172     4173        0.000904           7
element truss                     517374          4173     4174        0.000904           7
element truss                     517475          4174     4175        0.000904           7
element truss                     517576          4175     4176        0.000904           7
element truss                     517677          4176     4177        0.000904           7

################################### PROFILES - ANCHOR DX #######################################
#### Profiles Web
#element ShellMITC4               $eleTag        $iNode   $jNode   $kNode   $lNode     $secTag
element ShellMITC4                435161          4351     4352     4362     4361           2
element ShellMITC4                435262          4352     4353     4363     4362           2
element ShellMITC4                435363          4353     4354     4364     4363           2
element ShellMITC4                435464          4354     4355     4365     4364           2
element ShellMITC4                435565          4355     4356     4366     4365           2
element ShellMITC4                435666          4356     4357     4367     4366           2

element ShellMITC4                436171          4361     4362     4372     4371           2
element ShellMITC4                436272          4362     4363     4373     4372           2
element ShellMITC4                436373          4363     4364     4374     4373           2
element ShellMITC4                436474          4364     4365     4375     4374           2
element ShellMITC4                436575          4365     4366     4376     4375           2
element ShellMITC4                436676          4366     4367     4377     4376           2

### Profiles Flanges
#element truss                   $eleTag        $iNode   $jNode              $A      $matTag
element truss                     535152          4351     4352        0.000904           7
element truss                     535253          4352     4353        0.000904           7
element truss                     535354          4353     4354        0.000904           7
element truss                     535455          4354     4355        0.000904           7
element truss                     535556          4355     4356        0.000904           7
element truss                     535657          4356     4357        0.000904           7
element truss                     537172          4371     4372        0.000904           7
element truss                     537273          4372     4373        0.000904           7
element truss                     537374          4373     4374        0.000904           7
```

```
element truss                      537475          4374     4375         0.000904           7
element truss                      537576          4375     4376         0.000904           7
element truss                      537677          4376     4377         0.000904           7

######################################## CONNECTIONS ############################################

### Friction surfaces (Dampers)
#element zeroLength    $eleTag  $iNode $jNode -mat $matTags -dir $dirs <-orient $x1 $x2 $x3 $yp1 $yp2 $yp3>
element zeroLength     2101    4121    4131    -mat 8  9   -dir 1 2   -orient  1   0   0   0   1   0
element zeroLength     2102    4122    4132    -mat 8  9   -dir 1 2   -orient  1   0   0   0   1   0
element zeroLength     2103    4123    4133    -mat 8 10   -dir 1 2   -orient  1   0   0   0   1   0
element zeroLength     2104    4124    4134    -mat 8  9   -dir 1 2   -orient  1   0   0   0   1   0
element zeroLength     2105    4125    4135    -mat 8 10   -dir 1 2   -orient  1   0   0   0   1   0
element zeroLength     2106    4126    4136    -mat 8  9   -dir 1 2   -orient  1   0   0   0   1   0
element zeroLength     2107    4127    4137    -mat 8  9   -dir 1 2   -orient  1   0   0   0   1   0
element zeroLength     2301    4321    4331    -mat 8  9   -dir 1 2   -orient  1   0   0   0   1   0
element zeroLength     2302    4322    4332    -mat 8  9   -dir 1 2   -orient  1   0   0   0   1   0
element zeroLength     2303    4323    4333    -mat 8 10   -dir 1 2   -orient  1   0   0   0   1   0
element zeroLength     2304    4324    4334    -mat 8  9   -dir 1 2   -orient  1   0   0   0   1   0
element zeroLength     2305    4325    4335    -mat 8 10   -dir 1 2   -orient  1   0   0   0   1   0
element zeroLength     2306    4326    4336    -mat 8  9   -dir 1 2   -orient  1   0   0   0   1   0
element zeroLength     2307    4327    4337    -mat 8  9   -dir 1 2   -orient  1   0   0   0   1   0

#### Screws (Dampers)
#element twoNodeLink $eleTag $iNode $jNode -mat $matTags  -dir $dirs  <-orient <$x1 $x2 $x3> $y1 $y2 $y3>
element twoNodeLink   3101   4142   102   -mat 11 11 11  -dir 1 2 6  -orient  1   0   0   0   1   0
element twoNodeLink   3102   4144   103   -mat 11 11 11  -dir 1 2 6  -orient  1   0   0   0   1   0
element twoNodeLink   3103   4146   104   -mat 11 11 11  -dir 1 2 6  -orient  1   0   0   0   1   0
element twoNodeLink   3301   4342   108   -mat 11 11 11  -dir 1 2 6  -orient  1   0   0   0   1   0
element twoNodeLink   3302   4344   109   -mat 11 11 11  -dir 1 2 6  -orient  1   0   0   0   1   0
element twoNodeLink   3303   4346   1010  -mat 11 11 11  -dir 1 2 6  -orient  1   0   0   0   1   0

#### Screws (Anchor profiles)
#element twoNodeLink  $eleTag $iNode $jNode -mat $matTags  -dir $dirs  <-orient <$x1 $x2 $x3> $y1 $y2 $y3>
element twoNodeLink   3104   132    4152  -mat 11 11 11  -dir 1 2 6  -orient  1   0   0   0   1   0
element twoNodeLink   3105   133    4154  -mat 11 11 11  -dir 1 2 6  -orient  1   0   0   0   1   0
element twoNodeLink   3106   134    4156  -mat 11 11 11  -dir 1 2 6  -orient  1   0   0   0   1   0
element twoNodeLink   3304   138    4352  -mat 11 11 11  -dir 1 2 6  -orient  1   0   0   0   1   0
element twoNodeLink   3305   139    4354  -mat 11 11 11  -dir 1 2 6  -orient  1   0   0   0   1   0
element twoNodeLink   3306   1310   4356  -mat 11 11 11  -dir 1 2 6  -orient  1   0   0   0   1   0

#### Anchor bolts (Anchor profiles)
#element zeroLength   $eleTag $iNode $jNode -mat $matTags  -dir  $dirs   <-orient $x1 $x2 $x3 $yp1 $yp2 $yp3>
element zeroLength    7101   4162   71     -mat 12 12    -dir 1 2    -orient  1   0   0   0   1   0
element zeroLength    7103   4166   73     -mat 12 12    -dir 1 2    -orient  1   0   0   0   1   0
 element zeroLength   7301   4362   77     -mat 12 12    -dir 1 2    -orient  1   0   0   0   1   0
element zeroLength    7303   4366   79     -mat 12 12    -dir 1 2    -orient  1   0   0   0   1   0

######################################## CLT PANEL ##############################################

#element ShellMITC4               $eleTag         $iNode   $jNode    $kNode   $lNode    $secTag
element ShellMITC4                 10111           101      102       112      111          1
element ShellMITC4                 10212           102      103       113      112          1
element ShellMITC4                 10313           103      104       114      113          1
element ShellMITC4                 10414           104      105       115      114          1
element ShellMITC4                 10515           105      106       116      115          1
element ShellMITC4                 10616           106      107       117      116          1
element ShellMITC4                 10717           107      108       118      117          1
element ShellMITC4                 10818           108      109       119      118          1
element ShellMITC4                 10919           109     1010      1110      119          1
element ShellMITC4                1010110         1010     1011      1111     1110          1
element ShellMITC4                 11121           111      112       122      121          1
element ShellMITC4                 11222           112      113       123      122          1
element ShellMITC4                 11323           113      114       124      123          1
element ShellMITC4                 11424           114      115       125      124          1
element ShellMITC4                 11525           115      116       126      125          1
element ShellMITC4                 11626           116      117       127      126          1
element ShellMITC4                 11727           117      118       128      127          1
element ShellMITC4                 11828           118      119       129      128          1
element ShellMITC4                 11929           119     1110      1210      129          1
element ShellMITC4                1110210         1110     1111      1211     1210          1
element ShellMITC4                 12131           121      122       132      131          1
element ShellMITC4                 12232           122      123       133      132          1
element ShellMITC4                 12333           123      124       134      133          1
element ShellMITC4                 12434           124      125       135      134          1
element ShellMITC4                 12535           125      126       136      135          1
element ShellMITC4                 12636           126      127       137      136          1
element ShellMITC4                 12737           127      128       138      137          1
element ShellMITC4                 12838           128      129       139      138          1
element ShellMITC4                 12939           129     1210      1310      139          1
element ShellMITC4                1210310         1210     1211      1311     1310          1

######################################## INFILL #################################################
#uniaxialMaterial Hysteretic  $matTag  $s1p $e1p  $s2p $e2p <$s3p  $e3p>  $s1n  $e1n  $s2n  $e2n     <$s3n  $e3n>   $pinchX $pinchY
$damage1 $damage2 <$beta>
```

```
## Infill with high mechanical properties
uniaxialMaterial Hysteretic  14      .250891252943394   2.05614309474879E-07   .326158628826413   8.02430596112546E-07   6.52317257652825E-05   .0034219568988225   -250.891252943394                    -.00020561430947487   -326.158628826413   -.00080243059611254 6   -6.52317257652825                    -.0034219568988225   1.0   1.0    0.0    0.0   0.0
uniaxialMaterial Hysteretic  15       0.125445626       0.00000020561          0.163079314        0.00000080243          3.26159E-05   0.00342195690       -125.4456265                       -0.00020561431         -163.0793144        -0.00080243060         -3.261586288   -0.00342195690    1   1   0   0   0

#element truss                    $eleTag        $iNode    $jNode      $A      $matTag
element truss                           1            01        12       1           15
element truss                           2            02        11       1           15
element truss                           3            02        13       1           14
element truss                           4            03        12       1           14
element truss                           5            03        14       1           15
element truss                           6            04        13       1           15


#################################### TRUSS ############################################
#element truss                    $eleTag        $iNode    $jNode      $A      $matTag
element truss                           7            11        14       1           16


##############################################
#              Display the model
##############################################
recorder display "Model" 10 10 800 800 -wipe
prp 0 0 8
vup 0 1 0
vpn 0 0 1
display 1 3 10
##############################################


puts "Vertical Loads"
# Load pattern
pattern Plain   01 Linear {;
    #load        nodeTag      FX          FY      FZ      MX      MY      MZ
     load             11   0.00    -146.25   0.00   0.00   0.00   0.00;
     load             12   0.00    -292.5    0.00   0.00   0.00   0.00;
     load             13   0.00    -292.5    0.00   0.00   0.00   0.00;
     load             14   0.00    -146.25   0.00   0.00   0.00   0.00;
    #eleLoad   -ele    eleTag1  -type -beamUniform    Wy      Wz       <Wx>
     eleLoad   -ele      91112  -type -beamUniform    0.00   -26      0.00;
     eleLoad   -ele      91314  -type -beamUniform    0.00   -26      0.00;
     eleLoad   -ele      91271  -type -beamUniform    0.00   -26      0.00;
     eleLoad   -ele      97173  -type -beamUniform    0.00   -26      0.00;
     eleLoad   -ele      97377  -type -beamUniform    0.00   -26      0.00;
     eleLoad   -ele      97779  -type -beamUniform    0.00   -26      0.00;
     eleLoad   -ele      97913  -type -beamUniform    0.00   -26      0.00;
}


puts "Analysis"
#Analysis details
constraints Transformation
numberer RCM
system BandGeneral
test EnergyIncr 1.0e-8 100 0
algorithm KrylovNewton
#algorithm NewtonLineSearch
integrator LoadControl 0.1
analysis Static
analyze 10
loadConst -time 0.0

puts "Horizontal load"
# Load pattern
pattern Plain 02 Linear { ;
    #load       nodeTag     FX     FY     FZ     MX     MY     MZ
     load            11      1   0.00   0.00   0.00   0.00   0.00;
}

puts "Analysis"
#Analysis details
constraints Transformation
numberer RCM
system BandGeneral
test EnergyIncr 1.0e-8 100 0
algorithm Newton

foreach {numSteps stepSize} { 100 0.00016 200 -0.00016 300 0.00016 400 -0.00016 500 0.00016 600 -0.00016 700 0.00016 800 -0.00016 900 0.00016 1000 -0.00016 500 0.00016 } {
   integrator DisplacementControl 11  1 $stepSize
   analysis Static

```

```
  set Step 0
  while {$Step <  $numSteps } {
     set Step [expr $Step + 1]
     set ok 0
     set ok [analyze 1]
     if {$ok != 0} {
         puts "Trying KrylowNewton .."
         test NormDispIncr 9.0e-6 1000
         algorithm KrylovNewton
         set ok [analyze 1]

         test EnergyIncr 1.0e-8 100 0
         algorithm Newton
     }
     if {$ok != 0} {
         puts "Trying Newton with Initial Tangent .."
         test NormDispIncr 9.0e-6  1000  0
         algorithm Newton - initial
         set ok [analyze 1]

         test EnergyIncr 1.0e-8 100 0
         algorithm Newton
     }
     if {$ok != 0} {
         puts "Trying Broyden .."
         test NormDispIncr 9.0e-6 1000
         algorithm Broyden 8
         set ok [analyze 1]

         test EnergyIncr 1.0e-8 100 0
         algorithm Newton
     }
     if {$ok != 0} {
         puts "Trying NewtonWithLineSearch .."
         test NormDispIncr 9.0e-6 1000 0
         algorithm NewtonLineSearch .8
         set ok [analyze 1]

         test EnergyIncr 1.0e-8 100 0
         algorithm Newton
     }
     if {$ok != 0} {
         break
     }
  }
}
```